Geological Survey of Canada
Commission géologique du Canada

PAPER/ÉTUDE
89-1F

CURRENT RESEARCH PART F
NATIONAL AND GENERAL PROGRAMS

RECHERCHES EN COURS PARTIE F
PROGRAMMES NATIONAUX ET GÉNÉRAUX

Canada

1989

89-04657/

NOTICE TO LIBRARIANS AND INDEXERS

The Geological Survey's Current Research series contains many reports comparable in scope and subject matter to those appearing in scientific journals and other serials. Most contributions to Current Research include an abstract and bibliographic citation. It is hoped that these will assist you in cataloguing and indexing these reports and that this will result in a still wider dissemination of the results of the Geological Survey's research activities.

AVIS AUX BIBLIOTHÉCAIRES ET PRÉPARATEURS D'INDEX

La série Recherches en cours de la Commission géologique paraît une fois par année; elle contient plusieurs rapports dont la portée et la nature sont comparables à ceux qui paraissent dans les revues scientifiques et autres périodiques. La plupart des articles publiés dans Recherches en cours sont accompagnés d'un résumé et d'une bibliographie, ce qui vous permettra, nous l'espérons, de cataloguer et d'indexer ces rapports, d'ou une meilleure diffusion des résultats de recherche de la Commission géologique.

ERRATUM

Geological Survey of Canada, Paper 89-1F

Current Research Part F
National and General Programs

Commission géologique du Canada, Étude 89-1F

Recherches en cours partie F
Programmes nationaux et généraux

The following tables were omitted from the report by D.R. Boyle and D.C. Gregoire, entitled "$^{107}Ag/^{109}Ag$ ratios of minerals from various types of ore-forming environments using inductively coupled mass spectrometry", p. 23-26.

Table 1. $^{107}Ag/^{109}Ag$ ratios for mineral species from various ore deposit environments.

Sample No.	Mineral	Location	Deposit Type	$^{107}Ag/^{109}Ag$*
FR 83-008	galena	Soocana, Wawa, Ont.	hydrothermal vein	1.065 (.003)
A-74-27	chalcopyrite	Vermilion Mine, Ont.	layered intrusive (Ni,Cu)	1.068 (.008)
65344	covellite	Echo Bay Mine, N.W.T.	hydrothermal vein	1.069 (.007)
RF 65-42	galena	Mammoth, Wawa, Ont.	hydrothermal vein	1.069 (.003)
TQ 71-178	galena	Torbrit, Alice Arm, B.C.	barite-rich diatreme	1.069 (.007)
TQ 69-26	galena	Silver Bay, Camsell R., N.W.T.	hydrothermal vein	1.069 (.003)
SYA 82-76E	galena	Mount Pleasant, N.B.	hydrothermal vein/stockwork	1.069 (.002)
64052	native Au	Dominion Cr., Yukon	placer	1.070 (.003)
64055	native Au	Sulphur Cr., Yukon	placer	1.070 (.004)
64008	native Au	Highet Cr., Yukon	placer	1.070 (.005)
TQ 87-2	galena	Aquilar, Argentina	sediment-hosted sulphide	1.070 (.006)
LEA 78-554	galena	Tom Deposit, Yukon	sediment-hosted sulphide	1.070 (.003)
SP 1392B	galena	George Lake, Sask.	sandstone-hosted sulphide	1.070 (.003)
LEA 78-663	galena	Howards Pass, Yukon	sediment-hosted sulphide	1.071 (.006)
PP-10	galena	Pine Point, N.W.T.	carbonate-hosted sulphide	1.071 (.005)
TQ-82-S	galena	Nipissing Hill, Cobalt, Ont.	hydrothermal vein sulphide	1.071 (.005)
64 RFA-164	galena	Pamour, Timmins, Ont.	hydrothermal vein	1.071 (.001)
TQ 88-27	galena	Camflo, Que.	hydrothermal vein	1.071 (.002)
KQ 72-358	galena	Ross Mine, Holtyre, Ont.	hydrothermal vein	1.071 (.005)
SYA 83-11B	galena	Mount Pleasant, N.B.	hydrothermal vein/stockwork	1.071 (.002)
TQ 81-4	galena	MacLeod East, Wawa, Ont.	hydrothermal vein	1.071 (.004)
64113	native Au	Guysborough Co., N.S.	hydrothermal vein	1.072 (.002)
CO-1	native Ag	Cobalt, Ont.	hydrothermal vein	1.072 (.002)
TQ 71-264	galena	Turnback Lake, N.W.T.	volcanic massive sulphide	1.072 (.004)
TQ 72-67	galena	Buchans, Nfld	volcanic massive sulphide	1.072 (.004)
TQ 87-65	galena	Falun, Sweden	sediment-hosted sulphide	1.072 (.001)
TQ 88-28	galena	Robb Lake, B.C.	carbonate-hosted sulphide	1.072 (.003)
SP-2387	galena	Yava, N.S.	sandstone-hosted sulphide	1.072 (.004)
65487	native Ag	Reed Cr., Yukon	placer	1.073 (.004)
63685	native Ag	Cassiar District, B.C.	placer	1.073 (.004)
64018	native Au	Cariboo District, B.C.	placer	1.073 (.003)
64015	native Au	Cariboo District, B.C.	placer	1.073 (.005)
64050	native Au	Cassiar District, B.C.	placer	1.073 (.004)
64051	native Au	Cassiar District, B.C.	placer	1.073 (.004)
62035	native Au	Cassiar District, B.C.	placer	1.073 (.005)
63619	native Au	Kootenay District, B.C.	placer	1.073 (.005)
12015	native Ag	Broken Hill, Australia	sediment-hosted sulphide	1.073 (.005)
SP 4454	galena	Sullivan Mine, B.C.	sediment-hosted sulphide	1.073 (.004)
63 RF-12	galena	Mattagami Lake, Que.	volcanic massive sulphide	1.073 (.004)
LEA 78-646	galena	Howards Pass, Yukon	sediment-hosted sulphide	1.073 (.004)
TQ 84-176	galena	Gays River, N.S.	carbonate-hosted sulphide	1.073 (.003)
FR 79-331	galena	Sito West, Sask	sandstone-hosted sulphide	1.073 (.005)
TQ 71-306	galena	Terra, N.W.T.	hydrothermal vein	1.073 (.002)
64022	native Au	Cariboo District, B.C.	placer	1.074 (.004)
SP 4325-5	galena	Nanisivik, N.W.T.	carbonate-hosted sulphide	1.074 (.006)
SYA 83-35	galena	Mount Pleasant, N.B.	hydrothermal vein/stockwork	1.074 (.005)
63 RF-256	galena	Amulet C, Noranda, Que.	volcanic massive sulphide	1.074 (.003)
TQ 71-303	altaite	Mattagami Lake, Que.	volcanic massive sulphide	1.074 (.004)
LEA 78-525	galena	Tom Deposit, Yukon	sediment-hosted sulphide	1.074 (.001)
TQ 78-187	galena	Mistassini Lake, Que.	carbonate-hosted sulphide	1.074 (.003)
FR 79-354	galena	Kaz Lake, Sask.	sandstone-hosted sulphide	1.074 (.001)
TQ 78-10	galena	Muskox Intrusion, N.W.T.	ultrabasic layered complex	1.074 (.004)
64047	native Au	French Hill, Yukon	placer	1.075 (.005)

* numbers in brackets represent the analytical standard error measured as one standard deviation about the mean of 10 measurements.

Table 1 (cont'd)

Sample No.	Mineral	Location	Deposit Type	$^{107}Ag/^{109}Ag^*$
00418	native Au	Beauce Co., Que.	placer	1.075 (.003)
10179	galena	Worthington Mine, Sudbury, Ont.	hydrothermal breccia	1.075 (.001)
TQ 87-80	galena	Manitou-Barvue, Val d'Or, Que.	volcanic massive sulphide	1.075 (.005)
TQ 87-14	galena	Victory Lake, N.W.T.	volcanic massive sulphide	1.075 (001)
BH 115/7	galena	Ambaji, India	sediment-hosted sulphide	1.075 (.001)
BM-4	galena	Zawar, India	sediment-hosted sulphide	1.075 (.007)
GFA 83-523	galena	Artillery Lake, N.W.T.	carbonate-hosted sulphide	1.075 (.001)
TQ 66-19	galena	Echo Bay, N.W.T.	hydrothermal vein	1.075 (.001)
TQ 70-256	matildite	Terra, N.W.T.	hydrothermal vein	1.075 (.002)
TQ 86-15	galena	Mazowe Mine, Zimbabwe	hydrothermal vein	1.075 (.005)
TQ 86-65	galena	Langmuir Twp., Ont.	barite vein	1.075 (.002)
NBS REFERENCE STANDARD (silver nitrate)				1.0764 (.0002)
07179	native Au	Bonanza Cr., Yukon	placer	1.076 (.004)
00985	native Au	Beauce Co., Que.	placer	1.076 (.004)
65307	rammelsbergite	Echo Bay Mine, N.W.T.	hydrothermal vein	1.076 (.004)
63608	native Ag	Echo Bay Mine, N.W.T.	hydrothermal vein	1.076 (.006)
SP 3931	galena	Laisvall, Sweden	sandstone-hosted sulphide	1.076 (.003)
SP 3508	galena	Broken Hill, Australia	sediment-hosted sulphide	1.076 (.004)
TQ 74-551	galena	Kidd Creek, Ont.	volcanic massive sulphide	1.076 (.003)
RF 78-113	galena	Turnback Lake, N.W.T.	volcanic massive sulphide	1.076 (.005)
TQ 86-37B	galena	Indian Mountain Lake, N.W.T.	volcanic massive sulphide	1.076 (.002)
GFA 83-528	galena	Artillery Lake, N.W.T.	carbonate-hosted sulphide	1.076 (.001)
RFA 64-417	galena	Kerr Addison, Ont.	hydrothermal vein	1.076 (.002)
65 RF-10	galena	Botha Twp., Ont.	hydrothermal vein	1.076 (002)
TQ 78-190	galena	Copper Rand, Chibougamau, Que.	hydrothermal vein	1.076 (.004)
RF 66-579	galena	Opemiska, Que.	hydrothermal vein	1.076 (.003)
TQ 87-74	galena	Thor Lake	alkaline pegmatite	1.076 (.002)
SYA 82-26A	galena	Mt. Pleasant, N.B.	hydrothermal vein/stockwork	1.076 (.004)
63637	native Ag	Omineca District, B.C.	placer	1.077 (.005)
64059	native Au	Gold Run Cr., Yukon	placer	1.077 (.003)
12108	native Au	Beauce Co., Que.	placer	1.077 (.004)
63672	native Au	Kamloops District, B.C.	placer	1.077 (.005)
012106	native Au	N. Saskatchewan R., Sask.	placer	1.077 (.004)
64068	native Au	Cariboo District, B.C.	placer	1.077 (.002)
TQ 75-22	galena	Duck Lake, N.W.T.	volcanic massive sulphide	1.077 (.003)
62346	native Ag	El Bonanza Mine, N.W.T.	hydrothermal vein	1.077 (.009)
SP 4444	galena	Sullivan Mine, B.C.	sediment-hosted sulphide	1.077 (.002)
TQ 69-34	galena	Norex, Camsell R., N.W.T.	hydrothermal vein	1.077 (.003)
SYA 78-346	galena	Beiderman barite, Ont.	hydrothermal barite vein	1.077 (.002)
TQ 86-116	galena	Kaiser Celestite, N.S.	evaporite deposit	1.077 (.005)
63754	native Ag	Cassiar District, B.C.	placer	1.078 (.003)
64056	native Au	Seventeen Mile Cr., Yukon	placer	1.078 (.004)
01003	native Au	Beauce Co.	placer	1.078 (.004)
TQ 65-14	galena	Echo Bay, N.W.T.	hydrothermal vein	1.078 (.002)
FR 80-1000	galena	Fox R. Sill, Man.	mafic layered complex	1.078 (.005)
19706	native Ag	Burwash Cr., Yukon	placer	1.079 (.002)
64014	native Au	Cariboo District, B.C.	placer	1.079 (.004)
64027	native Au	Cariboo District, B.C.	placer	1.079 (.004)
12103	native Au	Omineca District, B.C.	placer	1.079 (.004)
62408	native Ag	Batopilas, Mexico	hydrothermal vein	1.079 (.007)
65369	skutterudite	Echo Bay Mine, N.W.T.	hydrothermal vein	1.079 (.004)
63723	argentite	Echo Bay Mine, N.W.T.	hydrothermal vein	1.079 (.006)
SP 3942A	galena	Rammelsberg, Germany	sediment-hosted sulphide	1.079 (.004)
12022	native Ag	Tsumeb Mine, Namibia	supergene; manto/vein	1.081 (.003)

Table 2. Repeat $^{107}Ag/^{109}Ag$ analyses for highest and lowest values in Table 1.

Sample	Initial Value	Repeat Value	Difference
FR 83-008	1.065 (.003)	1.069 (.007)	+ .004
A-74-27	1.068 (.008)	1.075 (.004)	+ .007
65344	1.069 (.007)	1.068 (.003)	-.001
RF 65-42	1.069 (.003)	1.074 (.005)	+ .005
65369	1.079 (.004)	1.081 (.004)	+ .002
63723	1.079 (.006)	1.083 (.006)	+ .004
SP 3942A	1.079 (.004)	1.079 (.004)	.000
12022	1.081 (.003)	1.079 (.005)	-.002

GEOLOGICAL SURVEY OF CANADA
COMMISSION GÉOLOGIQUE DU CANADA
PAPER/ÉTUDE 89-1F

CURRENT RESEARCH, PART F
NATIONAL AND GENERAL PROGRAMS

RECHERCHES EN COURS, PARTIE F
PROGRAMMES NATIONAUX ET GÉNÉRAUX

1989

Energy, Mines and Resources Canada

Énergie, Mines et Ressources Canada

© Minister of Supply and Services Canada 1989

Available in Canada through

authorized bookstore agents and other bookstores

or by mail from

Canadian Government Publishing Centre
Supply and Services Canada
Ottawa, Canada K1A 0S9

and from

Geological Survey of Canada offices:

601 Booth Street
Ottawa, Canada K1A 0E8

3303-33rd Street N.W
Calgary, Alberta T2L 2A7

100 West Pender Street
Vancouver, British Columbia V6B 1R8

A deposit copy of this publication is also available
for reference in public libraries across Canada

Cat. No. M44-89/1F
ISBN 0-660-54779-1

Cover description

Analytical method development in ion chromatography.
GSC 204789-A

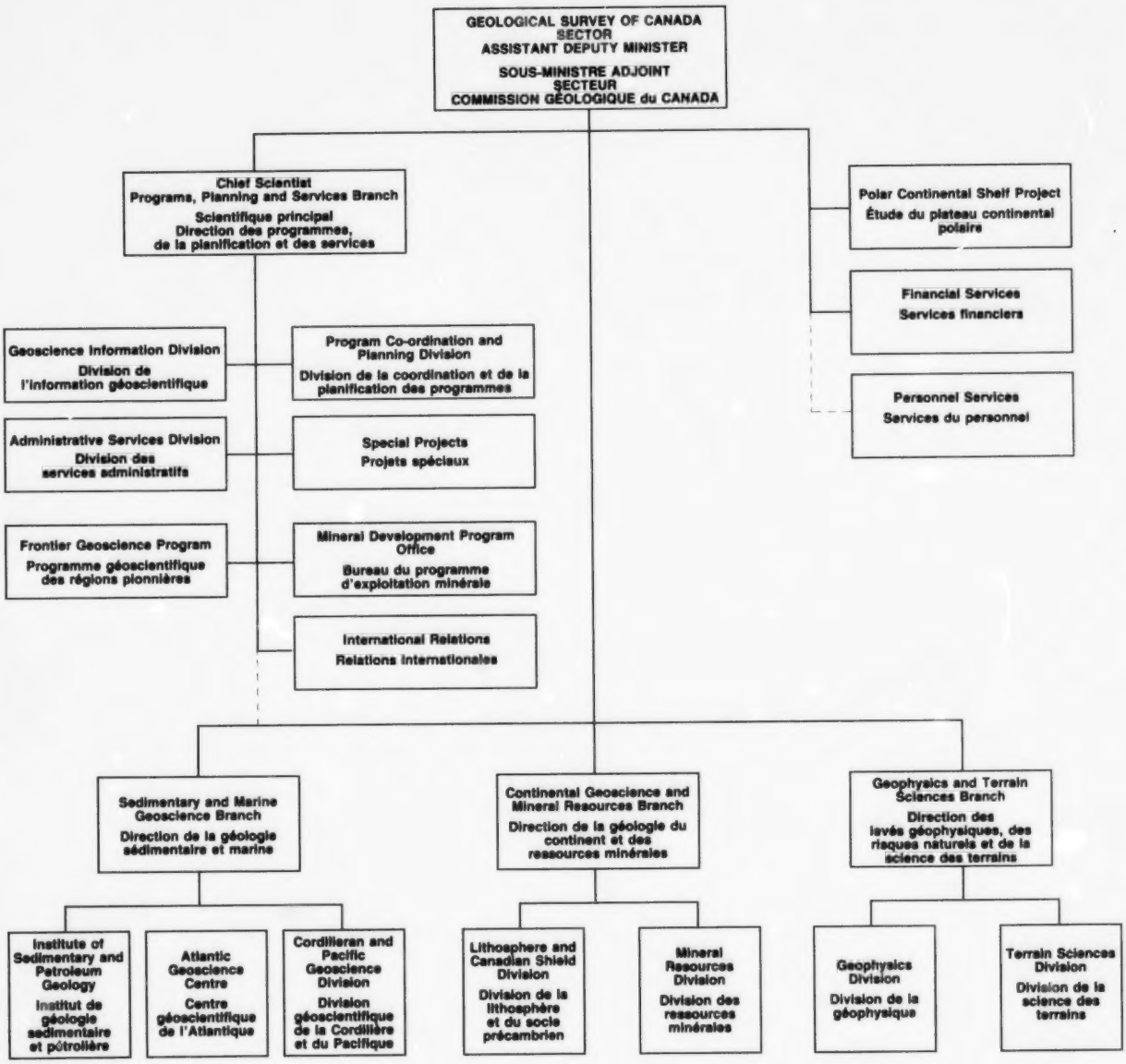
GEOLOGICAL SURVEY OF CANADA
SECTOR
ASSISTANT DEPUTY MINISTER
SOUS-MINISTRE ADJOINT
SECTEUR
COMMISSION GÉOLOGIQUE du CANADA
Chief Scientist
Programs, Planning and Services Branch
Scientifique principal
Direction des programmes,
de la planification et des services
Polar Continental Shelf Project
Étude du plateau continental polaire
Financial Services
Services financiers
Personnel Services
Services du personnel
Geoscience Information Division
Division de
l'information géoscientifique
Program Co-ordination and
Planning Division
Division de la coordination et de la
planification des programmes
Administrative Services Division
Division des
services administratifs
Special Projects
Projets spéciaux
Frontier Geoscience Program
Programme géoscientifique
des régions pionnières
Mineral Development Program
Office
Bureau du programme
d'exploitation minérale
International Relations
Relations internationales
Sedimentary and Marine
Geoscience Branch
Direction de la géologie
sédimentaire et marine
Continental Geoscience and
Mineral Resources Branch
Direction de la géologie du
continent et des
ressources minérales
Geophysics and Terrain
Sciences Branch
Direction des
levés géophysiques, des
risques naturels et de la
science des terrains
Institute of
Sedimentary and
Petroleum
Geology
Institut de
géologie
sédimentaire
et pétrolière
Atlantic
Geoscience
Centre
Centre
géoscientifique
de l'Atlantique
Cordilleran and
Pacific
Geoscience
Division
Division
géoscientifique
de la Cordillère
et du Pacifique
Lithosphere and
Canadian Shield
Division
Division de la
lithosphère
et du socle
précambrien
Mineral
Resources
Division
Division des
ressources
minérales
Geophysics
Division
Division de la
géophysique
Terrain Sciences
Division
Division de la
science des
terrains

Separates

A limited number of separates of the papers that appear in this volume are available by direct request to the individual authors. The addresses of the Geological Survey of Canada offices follow:

601 Booth Street,
OTTAWA, Ontario
K1A 0E8

Institute of Sedimentary and Petroleum Geology,
3303-33rd Street N.W.,
CALGARY, Alberta
T2L 2A7

Cordilleran and Pacific Geoscience Division,
100 West Pender Street,
VANCOUVER, B.C.
V6B 1R8

Pacific Geoscience Centre
P.O. Box 6000,
9860 Saanich Road
SIDNEY, B.C.
V8L 4B2

Atlantic Geoscience Centre
Bedford Institute of Oceanography,
P.O. Box 1006,
DARTMOUTH, N.S.
B2Y 4A2

Geological Survey of Canada
Institut national de la recherche scientifique
Complexe scientifique
2700, rue Einstein
C.P. 7500
Ste-Foy, Quebec
G1V 4C7

When no location accompanies an author's name in the title of a paper, the Ottawa address should be used.

Tirés à part

On peut obtenir un nombre limité de « tirés à part » des articles qui paraissent dans cette publication en s'adressant directement à chaque auteur. Les adresses des différents bureaux de la Commission géologique du Canada sont les suivantes:

601, rue Booth
OTTAWA, Ontario
K1A 0E8

Institut de géologie sédimentaire et pétrolière
3303-33rd St. N.W.,
CALGARY, Alberta
T2L 2A7

Division géoscientifique de la Cordillère et du Pacifique
100 West Pender Street,
VANCOUVER, Colombie-Britannique
V6B 1R8

Centre géoscientifique du Pacifique
B.P. 6000,
9860 Saanich Road
SIDNEY, Colombie-Britannique
V8L 4B2

Centre géoscientifique de l'Atlantique
Institut océanographique de Bedford
B.P. 1006
DARTMOUTH, Nouvelle-Écosse
B2Y 4A2

Commission géologique du Canada
Institut national de la recherche scientifique
Complexe scientifique
2700, rue Einstein
C.P. 7500
Ste-Foy, Québec
G1V 4C7

Lorsque l'adresse de l'auteur ne figure pas sous le titre d'un document, on doit alors utiliser l'adresse d'Ottawa.

CONTENTS

1 | J. BROOME and C. TURNER
Additions and improvements to microcomputer workstation software for potential field interpretation

5 | R.A. GIBB and J.B. BOYD
National gravity survey program, 1988-89

9 | A.C.L. LAROCQUE, I.R. JONASSON, and G.M. LECHEMINANT
Zonation of secondary minerals in hydrothermally altered seafloor lavas from the Galapagos Rift

17 | G.E.M. HALL and J.E. VAIVE
Comparison of the determination of sulphur in geological materials by pyrohydrolysis and ion chromatography with other production-oriented methods

23 | D.R. BOYLE and D.C. GREGOIRE
$^{107}Ag/^{109}Ag$ ratios of minerals from various types of ore-forming environments using inductively coupled mass spectrometry

27 | G.E.M. HALL and J.E. VAIVE
Effect of palladium as a matrix modifier in the determination of gold by graphite furnace atomic absorption spectrometry

31 | J.A. DRYSDALE, M. LAMONTAGNE, and R.B. HORNER
Canadian earthquakes, January 1987 to September 1988

37 | J. ADAMS
Turbidites off the Oregon-Washington margin record paleo-earthquakes on the Cascadia subduction zone

45 | P.W. BASHAM
A Paleozoic-Mesozoic rift framework for seismic hazard assessment in eastern North America

51 | D.J. TESKEY, E.E. READY, P.E. STONE, B. ELLIS, J. TOD, and R.A. GIBB
Aeromagnetic survey program of the Geological Survey of Canada, 1988-89

55 | D.C. MCGREGOR
Preservation of paleontological types

61 | K.G. NEAVE and S.E. PULLAN
Shallow seismic reflections using SV waves

Additions and improvements to microcomputer workstation software for potential field interpretation

J. Broome and C. Turner[1]
Lithosphere and Canadian Shield Division

Broome, J. and Turner, C., Additions and improvements to microcomputer workstation software for potential field interpretation; in Current Research, Part F, Geological Survey of Canada, Paper 89-1F, p. 1-4, 1989.

Abstract

The IBM-compatible microcomputer workstation, in use at the Geological Survey of Canada (GSC) for potential field interpretation and supported by published GSC software, has proved popular both within and outside the GSC. In response to suggestions from users, features have been modified and added to improve the utility of the software. Colour hard copies of images and models can now be generated and profile data for modelling can be interactively extracted from images. New utility programs are included with the modelling program which allow calculation of the magnetic field inclination and declination values from geographic co-ordinates, and plotting of scaled profile data.

Résumé

Le poste de travail sur micro-ordinateur compatible IBM actuellement utilisé par la Commission géologique du Canada (CGC) pour l'interprétation du champ de potentiel et qui exploite le logiciel publié par la CGC s'est avéré populaire tant à la CGC qu'à l'extérieur. En réponse à des suggestions des utilisateurs, des caractéristiques ont été modifiées et des éléments ont été ajoutés afin d'améliorer l'utilité du logiciel. Il est maintenant possible de produire de manière interactive à partir d'images des copies en couleurs sur papier et des données provenant de profils aux fins de modélisation. Le programme de modélisation comprend de nouveaux programmes utilitaires qui permettent de calculer les valeurs de l'inclinaison et de la déclinaison magnétiques à partir des coordonnées géographiques ainsi que de tracer les données de profils mises à l'échelle.

[1] Faculty of Mathematics, University of Waterloo, Waterloo, Ontario.

INTRODUCTION

Interpretation of potential field data often involves qualitative analysis of gridded data followed by more detailed quantitative analysis of the data using 2−, $2^1/_2$− or 3-dimensional modelling. The microcomputer workstation (Fig. 1) and software developed at the GSC (Broome, 1986, 1987, 1988) allow both types of interpretation to be conducted easily and quickly. The software written for this workstation has evolved in response to the needs of the author and suggestions from other users. The software now allows colour hard copies to be generated from both image and model displays, and profile data extraction from the image display. Other changes, including the addition of improved error messages, make the program easier to use.

Both the image display program, DISPLAY, and the modelling program, MAGRAV2, utilize a graphics tablet to simplify program control and cursor positioning. IBM-compatible mirocomputers using faster 80286 and 80386 microprocessors and improved compilers have increased program execution speed. However, faster execution speed causes problems with cursor response time from the graphics tablet leading to duplicate point entry and control problems. To accommodate variations in the performance of the different microcomputers and different user preferneces the graphics tablet response speed can now be set by the user.

Error messages and cursor control on the monochrome monitor have been improved in all programs by utilizing standard ANSI escape sequences recognized by the MS-DOS "ANSI.SYS" device driver.

IMAGING SOFTWARE

This revision of the geophysical imaging software open file (Broome, 1987), incorporates a number of new features. Each of the four programs has been improved.

DISPLAY

Program DISPLAY allows interactive display and colour manipulation of geophysical data in image form. DISPLAY has been modified to allow colour hard copy production on Tektronix 4696 colour ink-jet plotters. Although the plotter's colour palette is smaller than that available on the colour monitor, user-selected 2×2 or 3×3 dithering allows 64 or 1024 colours, respectively, to be generated from the 4 ink colours available with the plotter. Plot size is 22 cm square for 2×2 dithering or 33 cm square for 3×3 dithering. The plot is generated in two sections when 3×3 dithering is selected. Subroutine TEKPNT, which drives the Tektronix ink-jet plotter, must be compiled using Microsoft FORTRAN version 3.31 or 4.1. Versions 4.0 and 4.01 of the compiler have an error which causes the routine to fail.

Profile data, for modelling using MAGRAV2, may now be extracted interactively by selecting profile endpoints with the graphics tablet cursor. Since modelling requires that the

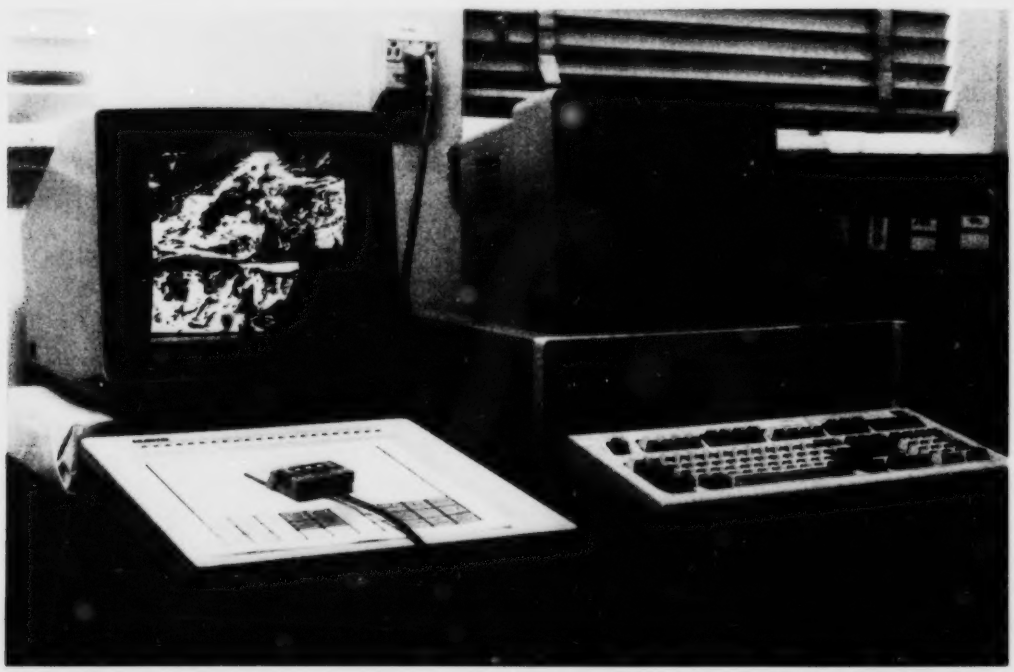

Figure 1. This photograph shows a complete workstation incorporating a IBM-PC/AT, 30 megabyte hard disc, 2 floppy discs, graphics tablet and monochrome and colour monitors. A grey-tone intensity image, generated from magnetic field data, is displayed on the colour monitor.

data accuracy be greater than that available from 8-bit image files, data is read from the 16-bit data file corresponding to the image file being displayed. The sampling interval along the profile may be entered directly or indirectly by specifying the number of points between the profile endpoints. Profile data values are stored in a profile file for direct entry to MAGRAV2. The profile extraction option may be selected either from the graphics tablet or from the main menu. On the graphics tablet, the profile extraction option is located on the bottom option row of the template adjacent to "lighten palette".

IMAGE

Program IMAGE is used to quantize gridded data to produce shaded-relief images and intensity images. Grey-tone hard copy generation on Epson FX-100, FX-186 or compatible dot-matrix printers is also supported. The new version of IMAGE incorporates both improved error messages and cursor control on the text monitor.

VAXPC

Program VAXPC has been changed to allow generation of reduced-resolution image or data grids. Reducing the resolution allows faster downloading and generation of images from large original grids without loss of detail in the image display. For example, every fourth grid cell can be extracted from an original grid of 2000×2000 cells to produce a 500×500 pixel image file. The resulting reduced-resolution image is almost identical to the 2000×2000 pixel image since display resolution is limited by hardware to 512×484 pixels. The 500×500 pixel image file could be downloaded and displayed in one quarter of the time required to process and display a 2000×2000 pixel image file.

SHADE

Program SHADE allows interactive modification of illumination direction on a colour or grey-tone shaded-relief image display. In previous versions, illumination inclination was specified first and then the illumination declination could be interactively changed in 12.5° increments to rotate the illumination around the compass. The new version of the program allows both the illumination inclination and declination to be changed in 12.5° increments without a processing delay.

In addition, SHADE now allows pan and zoom of the shaded-relief image. Zoom in or out is initiated using function keys "F1" and "F2". The image may then be panned using the cursor keys. Error reporting and cursor control on the text monitor have also been improved.

MAGRAV2

MAGRAV2, the interactive $2^1/_2$-dimensional magnetic and gravity data modelling program (Broome, 1986, 1988), has undergone many changes since it was originally published in August 1986. Version 1.5, the current release, incorporates a number of new functions which increase the user's control over the modelling process. Two new text mode command options, two graphics tablet options and numerous small improvements have also been added.

SAVE command

SAVE allows the model display to be saved as a Halo-format ("*.pic") image file together with a matching Halo-format ("*.pal") palette file. Halo-format files can be read by program DISPLAY to produce colour hard copy on a Tektronix 4696 colour ink-jet plotter. Halo compatible image manipulation software such as "Dr. Halo" and "Image-Pro", available from Media Cybernetics, can also be used to annotate or edit the saved image file before printing.

CONF command

Option CONF allows the number of program steps saved in the recovery file to be changed and the graphics tablet response time to be modified. The size of the recovery file is controlled by the number of saved program steps. Users without hard disks may choose to set the number of recovery steps to zero to avoid delays after each model modification caused by the slow response of floppy disks.

The wide execution speed range of IBM-compatible microcomputers caused problems with graphics tablet response time. The original program was designed with delays appropriate for a workstation using a slow 8088 microprocessor. On faster microcomputers using Intel 80286 and 80386 microprocessors, delays are reduced resulting in duplicate point entry from the graphics tablet. In the new version of MAGRAV2, the user can set the graphics tablet response, using option CONF, to suit his hardware and personal preference.

OFFSET tablet option

The graphics tablet "offset" option has been modified to allow the user to manually define the plotting offset between calculated and observed anomalies. When the offset option is called from the graphics tablet, the user must select automatic (the existing method) or manual offset determination. Manual offset determination allows the user to pick a point along the profile at which the calculated and observed data are set to the same level for plotting purposes. This option is particularly useful for controlled removal of regional level shifts during gravity modelling.

Improved automatic model optimization

Both automatic model optimization options have been improved to allow the user to identify a subsection of the profile to be fitted. For automatic point movement, the user is first asked to identify the point to be moved and then prompted to select the start and end points of the profile segment to be fitted. A new graphics tablet option has been added to the template called "Body contrast". This new option is located on the graphics tablet template between "body anomaly" and "delete point". The "body contrast"

option allows the user to optimize the density or magnetization contrast of a single body to fit a specified section of the profile. The improved offset and automatic optimization options give the user greater control of the modelling process. Specific parts of the model can now be modified more easily to fit selected sections of the observed anomaly.

Other changes

The original version of MAGRAV2 did not permit the user to locate a body point at a specific depth or lateral position using the graphics tablet cursor. With the new version the co-ordinates of the cursor crosshair location are continuously displayed in units of kilometers on the text monitor during cursor movement. This feature allows the user to locate body vertices at precise depths and lateral positions.

Version 1.5 of MAGRAV2 now allows up to 15 bodies to be defined with a maximum of 25 body points allowing more complex models to be generated. This change makes models files written by previous versions of the program incompatible with the new program. A utility program, called MODCVT, is provided to convert models files written by all previous versions of MAGRAV2 to the format used by version 1.5. Without this utility existing models must be manually entered into the new version of the program.

DECINC

A new program, called DECINC, is included in "Open File 1334 (Broome, 1985)". DECINC calculates the magnetic field declination and inclination values required for magnetic modelling at the profile location. DECINC prompts the user for geographic co-ordinates, altitude above sea level and time, then calculates International Geomagnetic Reference Field (IGRF) declination and inclination values (Cain et al., 1967; Peddie, 1982). IGRF values are calculated by a subroutine written by G. Haines of the GSC. The IGRF is a quantitative description of the Earth's main magnetic field defined by a series of solid internal spherical harmonics up to and including the 8th degree and order. Source code for the program is provided, as well as coefficients files for IGRF 1970 and IGRF 1985. Coefficients files for the Definitive Geomagnetic Reference Field (DGRF) for 1970, 1975 and 1980 are also included.

Although IGRF declination and inclination values may not exactly match measured values they are sufficiently accurate for most modelling applications. The five magnetic field models produce slightly different declination and inclination values but the differences are generally not significant for modelling.

PROPLT

PROPLT allows profile files, created manually or written by program DISPLAY, to be plotted on Epson FX series dot-matrix printers. Both horizontal and vertical scale are user-selectable allowing profile plots to be generated at a scale matching existing geological maps. The position of each profile point is marked on the baseline and a line grid is overlain on the profile to facilitate anomaly measurement. Source code for PROPLT is included in "Open File 1334 (Broome, 1985)".

ORDERING INFORMATION

The imaging programs DISPLAY, SHADE, VAXPC and IMAGE are available as GSC Open File 1581 (Broome, 1987) at a cost of $18. MAGRAV2 is packaged as GSC Open File 1334 (Broome, 1986) at a cost of $30. Both include a user's guide and sample data files. The purchase price includes surface mail postage. To avoid delivery delays, it is recommended that overseas customers request airmail delivery. Please contact the Publications Office to determine the extra cost of arimail delivery:

Publications Office
Geological Survey of Canada,
601 Booth St., Ottawa, Ont.
Canada, K1A 0E8.

Owners of older versions of the two software packages can obtain revised source code files by returning their original open file diskette, in an appropriate mailer, to John Broome at the Geological Survey of Canada.

REFERENCES

Broome, J.
1986: MAGRAV2: An interactive magnetics and gravity modelling program for IBM-compatible microcomputers; Geological Survey of Canada, Open File 1334, 21 p.
1987: Geophysical imaging software for IBM-compatible microcomputers; Geological Survey of Canada, Open File 581, 47 p.
1988: An IBM-compatible microcomputer workstation for geophysical imaging and interpretation; Computers and Geosciences, v. 14, pp. 659-666.

Cain, J.C., Hendricks, S.J., Langel, R.A., Hudson, W.V.
1967: A proposal model for the International Geomagnetic Reference Field-1965; Journal of Geomagnetism and Geoelectricity, v. 19, p. 335-355.

Peddie, N.W.
1982: International Geomagnetic Reference Field: the Third Generation; Journal of Geomagnetism and Geoelectricity, v. 34, p. 309-326.

National gravity survey program, 1988-89

R.A. Gibb and J.B. Boyd
Geophysics Division

Gibb, R.A. and Boyd, J.B., National gravity survey program, 1988-89; in Current Research, Part F, Geological Survey of Canada, Paper 89-1F, p. 5-8, 1989.

Abstract

In 1988, seven gravity surveys were completed under the national gravity survey program; two were reconnaissance surveys located in the high Arctic and in central British Columbia, five were local surveys over targets located in British Columbia, N.W.T., Quebec and Labrador (2). More than 1700 new gravity stations were added to the national gravity data base as a result of these surveys.

Résumé

En 1988, sept levés gravimétriques ont été complétés dans le cadre du programme national de levés gravimétriques: deux d'entre eux étaient des levés de reconnaissance dans l'extrême Arctique et en Colombie-Britannique et les cinq autres, des levés de cibles locales en Colombie-Britannique, dans les T.N.-O., au Québec et au Labrador (2). L'exécution de ces levés a permis d'ajouter plus de 1700 stations gravimétriques à la base nationale de données gravimétriques.

INTRODUCTION

Completion of the regional gravity survey of Canada's landmass and offshore areas by the year 2005 is a major objective of the GSC's gravity program (Gibb and Thomas, 1976). Major areas that remain to be surveyed include parts of the Cordillera of northern British Columbia and Yukon Territory, parts of the Arctic Islands and Arctic Channels and parts of the Arctic Ocean (Fig. 1). These regions all pose special problems with respect to horizontal and vertical positioning of gravity stations and logistic difficulties of terrain, ice and climate.

Gravity surveys completed in 1988-89 are numbered 1 to 7 in Figure 1 and are summarized below. Figure 2 is an index map showing the location of GSC Open File gravity maps.

COMMITTEE BAY (AREA 1, FIG. 1)

A gravity and bathymetry survey of Committee Bay, Gulf of Boothia was completed by the Geophysics Division in March 1988 in co-operation with the Canadian Hydrographic Service, Department of Fisheries and Oceans and the Polar Continental Shelf Project. Approximately 700 gravity and bathymetry stations were established from the frozen surface of the bay at a 6 to 10 km grid spacing. This survey completes a four year co-operative program to complete the reconnaissance gravity and bathymetry coverage of the Gulf of Boothia.

CENTRAL BRITISH COLUMBIA (AREA 2, FIG. 1)

A regional gravity survey of part of central British Columbia was completed in the summer of 1988 by the Pacific Geoscience Centre, Cordilleran and Pacific Geoscience Division. The survey covered approximately two and one half 1:250 000 map areas. About 450 new gravity stations were observed at a grid spacing of 10 to 12 km. Positions of the gravity stations were established by the Geodetic Survey of Canada, using their Litton Inertial Survey System.

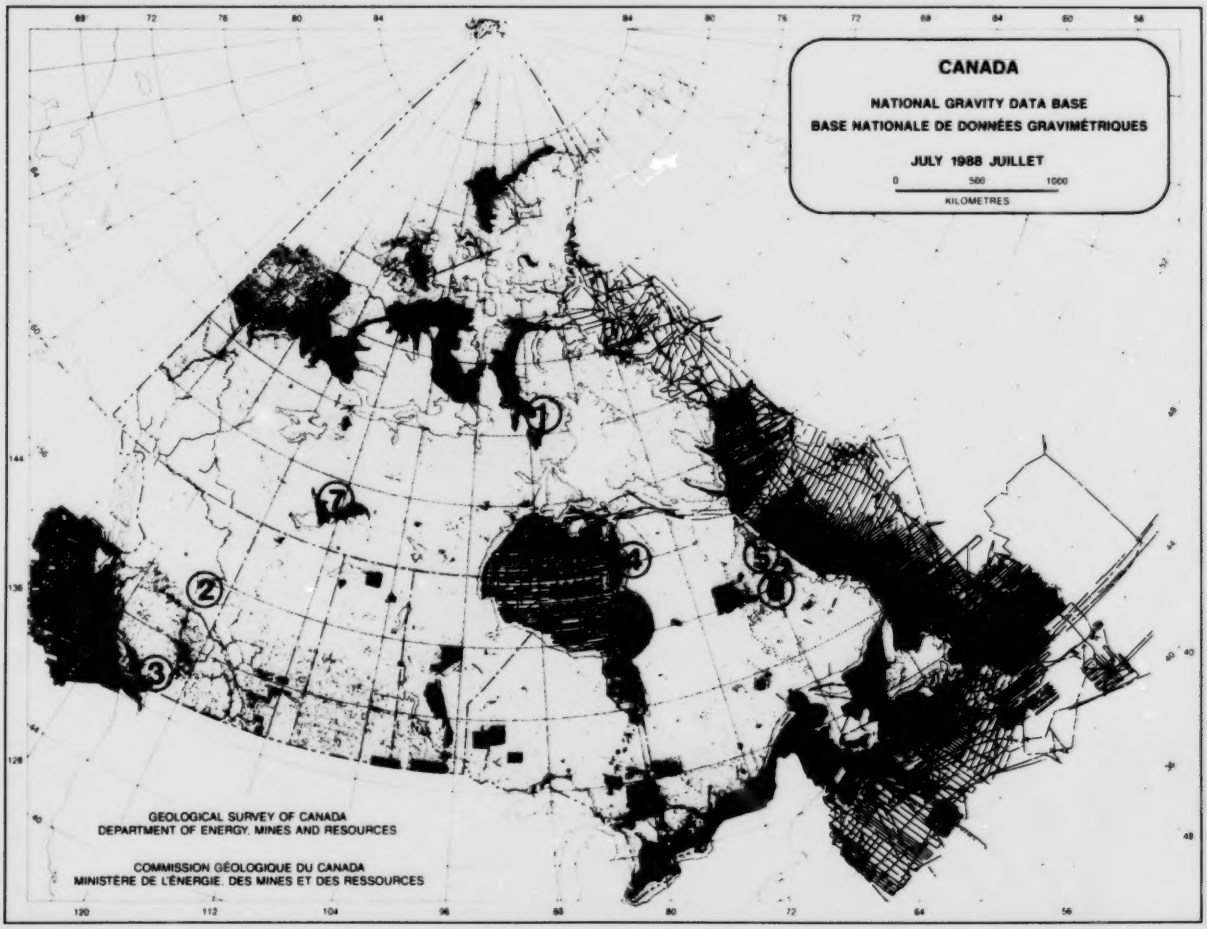

Figure 1. Distribution of gravity stations in Canada. Numbers refer to gravity surveys completed in 1988-89.

SOUTHWESTERN BRITISH COLUMBIA (AREA 3, FIG. 1)

A gravity survey along twelve Lithoprobe seismic lines was completed in southwestern British Columbia by the Geophysics Division in response to a request from the Lithosphere and Canadian Shield Division. More than 500 gravity stations at intervals of 2 km were observed along the seismic lines. The data will be analyzed in conjunction with the seismic reults.

UNGAVA, NORTHERN QUEBEC (AREA 4, FIG. 1)

A north-south gravity profile adjacent to the Hudson Bay coast was completed across the Cape Smith Foldbelt by the Geophysics Division in response to a request from the Lithosphere and Canadian Shield Division. Approximately 130 stations were observed at intervals of 2 km. This profile complements a similar profile observed in 1985 across the eastern part of the foldbelt.

NORTHERN LABRADOR (AREA 5, FIG. 1)

An east-west gravity profile across the Churchill-Nain structural province boundary was completed by the Geophysics Division in response to a request from the Lithosphere and Canadian Shield Division. Ninety new gravity stations were observed at intervals of 2 km. The profile was planned to investigate a series of thin thrust sheets that locally overlie the boundary.

LAC BRISSON/STRANGE LAKE, LABRADOR (AREA 6, FIG. 1)

A local gravity survey (37 stations) requested by the Mineral Resources Division was completed over the Lac Brisson/Strange Lake alkalic complex in Labrador. This survey formed part of a larger project to study the resource assessment of western Labrador under the Canada-Newfoundland Mineral Development Agreement.

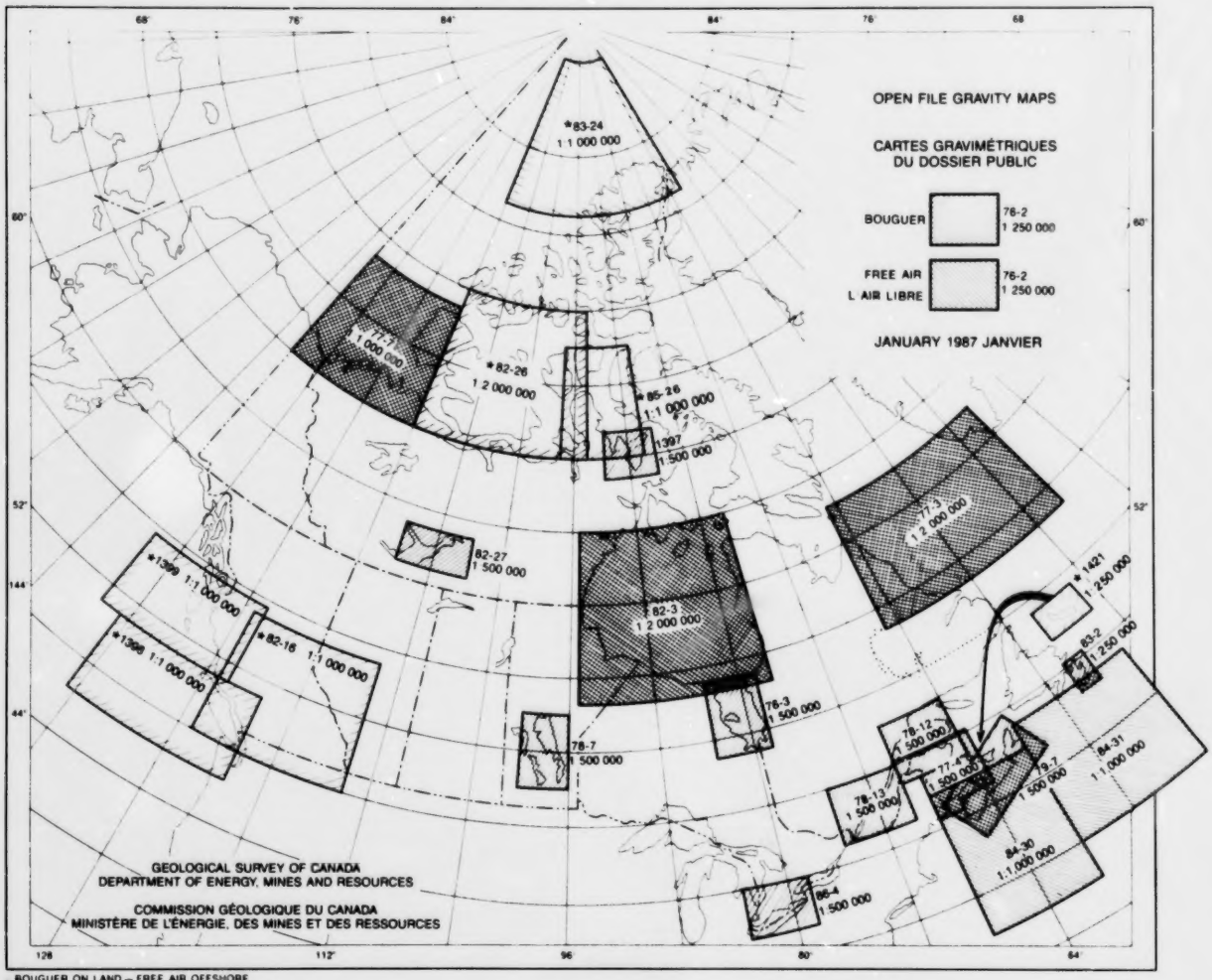

Figure 2. Index to open file gravity maps.

BLACHFORD LAKE, N.W.T. (AREA 7, FIG. 1)

A local gravity survey (90 stations) requested by the Mineral Resources Division was completed over the Blachford Lake alkalic complex, N.W.T. This survey contributed to a study of the relationship between the structure and composition of the complex and the Be-Y deposit contained within the intrusion.

GRAVITY DATA BASE AND GRAVITY MAPS

All GSC gravity data are maintained in the National Gravity Data Base of the Geophysical Data Centre (McConnell, 1976). It currently contains about 600 000 data points. The Geophysical Data Centre provides a variety of gravity data products to users both inside and outside the GSC. The major products include anomaly and control station data in the form of plots, tapes or listings; digital terrain data; open file-, manuscript- and applicon-type maps; contour overlays; derived maps; gridded gravity values; calibration line data; earth tide values; and computer programs.

Five new gravity maps of Canada (scale 1:10 000 000) were published in 1988 in the Geophysical Atlas Series. The maps portray observed gravity values, Bouguer anomalies, free air anomalies, isostatic anomalies and the horizontal gradient of the Bouguer anomaly, and include explanatory marginal notes. The first gravity map in the National Earth Science Series (NESS) (scale 1:1 000 000) has been published. Seventeen more NESS maps are in the final stages of preparation.

REFERENCES

Gibb, R.A. and Thomas, M.D.
1976: Gravity mapping in Canada; in Geophysics in the Americas, ed. J.G. Tanner and M.R. Dence, Publications of the Earth Physics Branch, Ottawa, v. 46(3), p. 48-57.

McConnell, R.K.
1976 The management of the Canadian national gravity data base; in Geophysics in the Americas, ed. J.G. Tanner and M.R. Dence, Publications of the Earth Physics Branch, Ottawa, v. 46(3), p. 107-112.

Zonation of secondary minerals in hydrothermally altered seafloor lavas from the Galapagos Rift

Adrienne C. L. Larocque[1], Ian R. Jonasson, and Gina M. LeCheminant
Mineral Resources Division

Larocque, A.C.L., Jonasson, I.R., and LeCheminant, G.M., Zonation of secondary minerals in hyrothermally altered seafloor lavas from the Galapagos Rift; in Current Research, Part F, Geological Survey of Canada, Paper 89-1F, p. 9-15, 1989.

Abstract

An extinct hydrothermal system that formed a massive Cu-Zn sulphide deposit is exposed on a horst block in the eastern Galapagos Rift. Samples collected from the hydrothermal alteration and stockwork zone exhibit pronounced compositional and textural zonation of secondary minerals. A basaltic andesite hyaloclastite bed consists of shards composed of micron- to millimetre-scale bands of chlorite, cristobalite, and smectite. Altered pillow fragments from a glassy Fe-Ti basalt flow contain chlorite, kaolinite, quartz, and illite-smectite, and exhibit zonation of primary quench textures. Differences in protolith composition and original permeability of the samples may have contributed to the differences in composition, type, and scale of alteration.

Résumé

Un système hydrothermal éteint qui a entraîné la formation d'un gisement de sulfures massifs cuprozincifères est mis à nu sur un massif soulevé dans la partie est du fossé d'effondrement des Galapagos. Des échantillons prélevés dans la zone d'altération hydrothermale et de fissures minéralisées présentent une zonation marquée de la composition et de la texture des minéraux accessoires. Une couche d'andésite basaltique hyaloclastique est formée d'éclats composés de bandes de chlorite, de cristobalite et de smectite dont la faille varie de l'ordre du micron au millimètre. Des fragments en coussins altérés d'une coulée de basalte vitreuse contenant Fe et Ti renferment de la chlorite, de la kaolinite, du quartz et de l'illite et smectite, et présentent une zonation de textures de trempe primaires. Des différences au niveau de la composition de la roche-mère et de la perméabilité originelle des échantillons peuvent avoir contribué à produire les différences observées au niveau du type et du degré d'altération ainsi qu'au niveau de la composition des roches altérées.

[1] Department of Geology, University of Western Ontario, London, Ontario, N6A 5B7

INTRODUCTION

A combination of tectonic activity and physical weathering has exposed a fossil massive Cu-Zn sulphide deposit and contiguous stockwork zone in the Galapagos Rift at 0°45′N; 85°50.5′W (Fig. 1). This occurrence was discovered during a series of dives of the DSRV ALVIN in 1980-1981 and 1985. The finding is significant because it facilitates the study of sulphide mineralization and attendant hydrothermal alteration unobscured by tectonic and metamorphic overprinting. A complete description and discussion of the mineralogy and geochemistry of the lavas, sulphide mounds, and alteration zone may be found in Embley et al. (1988). The purpose of this paper is to describe in detail and contrast the mineralogical and textural alteration of two typical samples of altered lava collected during the 1985 ALVIN dive series.

BACKGROUND/GEOLOGICAL SETTING

The extinct hydrothermal system is exposed on the sides of an east-trending horst along the axial ridge of the eastern Galapagos Rift. The horst block has a vertical throw of 50 to 80 m, and separates older pillowed volcanic rocks (Fe-Ti basalt to andesite) to the south from younger ones (n-MORB) to the north. Large Cu-Zn sulphide mounds, now separated by faulting, occur at the base of the southern horst face and on top of the horst. Altered volcanic rocks consist of glassy pillowed basalt and basaltic andesite interbedded with lobate and sheeted Fe-Ti basalt and ferrobasalt flows, as well as andesitic hyaloclastite beds (Embley, 1986; Embley et al., 1988). These highly altered and brecciated rocks are exposed extensively in vertical section on the north wall of the horst and to a lesser extent on the south wall. Sheeted and lobate flows are closely fractured and altered mainly along flow planes, whereas hyaloclastite beds are more pervasively altered due to high original permeability. According to Embley et al. (1988), the Galapagos Rift alteration zone is most analogous to stockwork zones associated with massive sulphide deposits in Cyprus (Lydon and Galley, 1986) and Oman (Collinson, 1986).

Analytical Procedures

The samples in this study exhibit textural and mineralogical zonation of sulphide and other secondary minerals. The mineralogical compositions of the bulk samples were determined using X-ray diffraction (XRD) techniques. Petro-

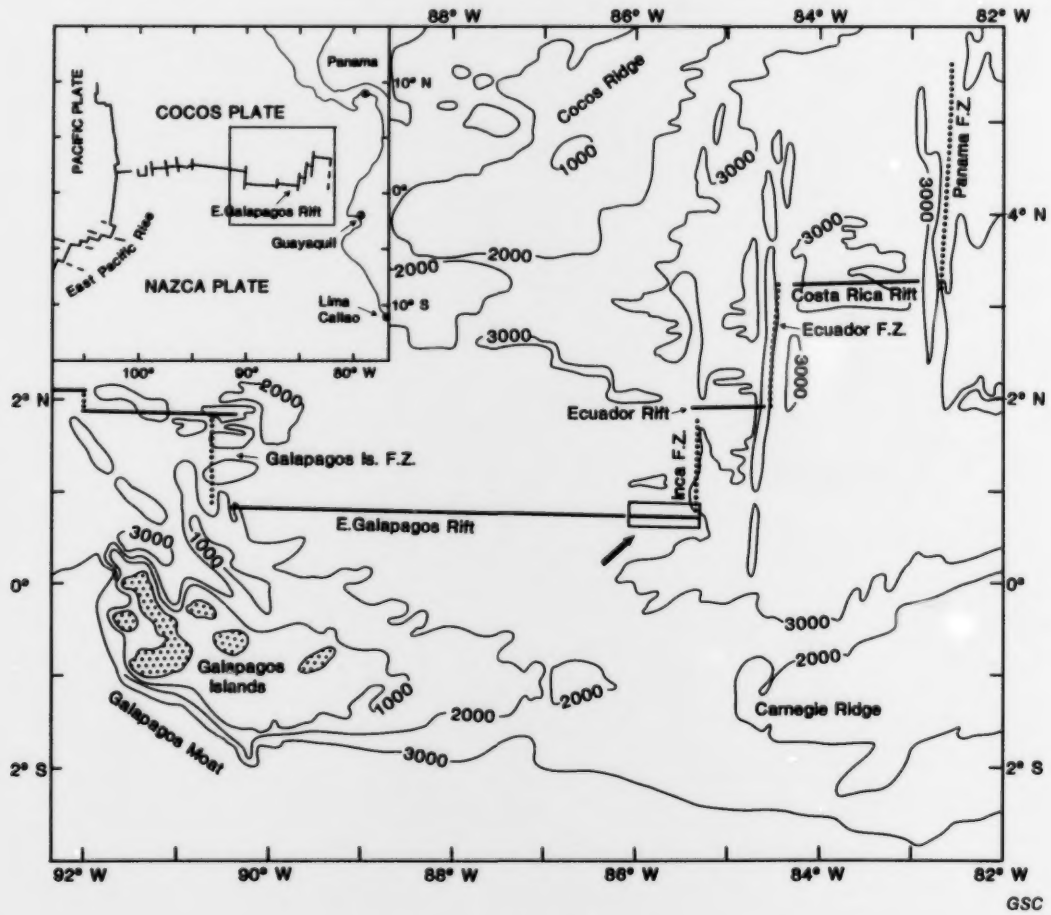

Figure 1. Location map of study area.

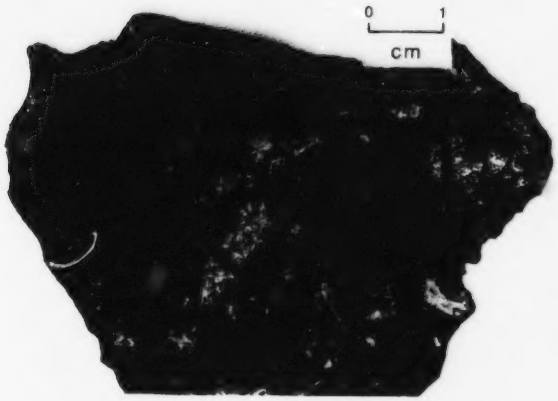

Figure 2. Sample 1654-5: altered basaltic andesite hyaloclastite. Shards exhibit micron- to millimetre-scale concentric zonation of secondary clay minerals.

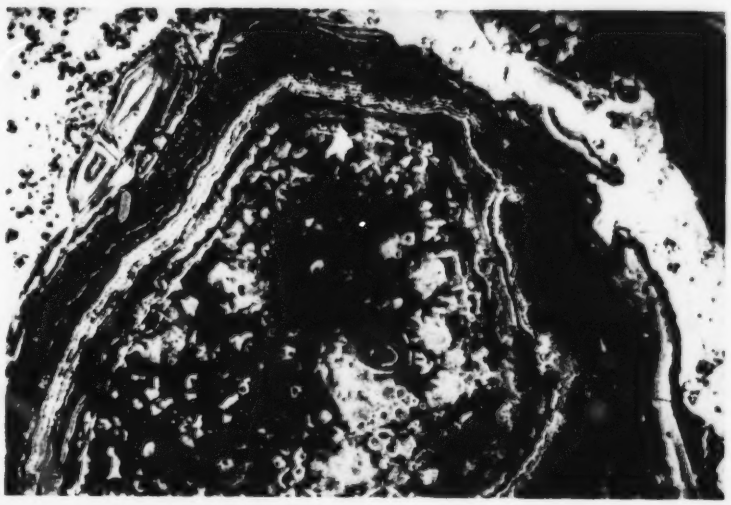

Figure 3. Photomicrograph of zoned shard in altered hyaloclastite cemented by sphalerite, pyrite, and cristobalite. Concentric zones consist mainly of chlorite and cristobalite, with some smectite. Interior of shard contains sulphides and silica. Transmitted light. Width of photo is 2.6 cm. Sample 1654-5.

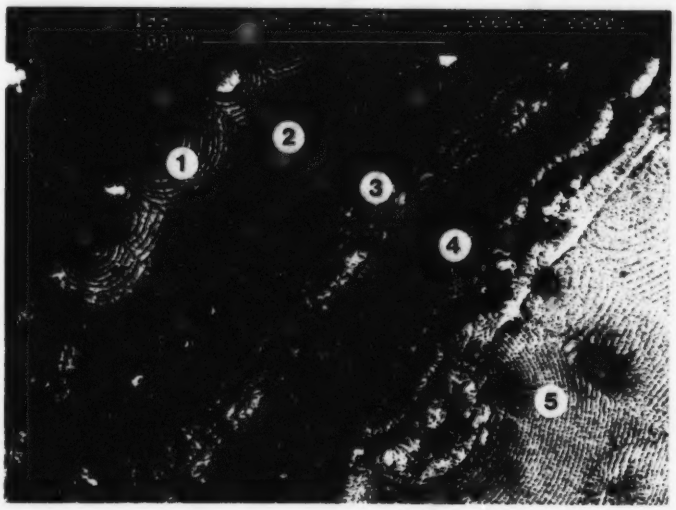

Figure 4. SEM backscatter electron image of zonation in altered shard. Zone 1: spheroidal chlorite with Ti-enriched microbanding; Zone 2: mixture of silica and chlorite; Zone 3: bands of radial chlorite separated by thin granular layers of Fe-rich material; Zone 4: massive mixture of silica, chlorite, and Fe-rich material; Zone 5: spheroidal chlorite with Ti-enriched microbanding. Core of shard is toward right of photo. Sample 1654-5.

graphic examination of polished thin sections permitted identification of individual mineral species within some zones. However, the material in other zones was commonly too fine grained to identify petrographically. Therefore, bulk mineralogical data were combined with detailed geochemical data (electron microprobe and SEM-EDS) to determine the minerals in these materials.

Sample Description

Sample **ALV-GR-1654-5** is a basaltic andesite hyaloclastite taken from a highly altered portion of the stringer zone. It comprises angular shards up to 1.5 cm in diameter, cemented by sphalerite, pyrite, and silica (Fig. 2). Some shards contain cavities and hollows which also have been filled by sulphide-silica cement (Fig. 3). The shards exhibit micron- to millimetre-scale concentric banding of secondary minerals that display spheroidal, radial habit and granular, massive textures (Fig. 4). In addition to sphalerite and pyrite, XRD analysis of the bulk sample indicates the presence of chlorite, cristobalite, and minor smectite or chlorite-smectite.

Most shards contain the same sharply bounded zoned sequences of minerals or mineral mixtures. The outermost zones of the shards are characterized by bands of brownish-green spheroidal material up to 100 μm wide (Zone 1, Fig. 4). Microprobe analyses indicate that the spheroids consist of radial Fe-rich chlorite (Table 1). There is optical continuity of chlorite crystals through regularly-spaced dark micron-thick microbands (Fig. 4). SEM analyses suggest that these bands are more Ti-rich and Fe-poor compared to intervening light bands. Inward, Zone 2 consists of mixtures of cristobalite and chlorite and ranges in width from 50 to 300 μm. Zone 3 is characterized by bands of pale green fibrous radial chlorite up to 25 μm thick, alternating with <5 μm-thick granular Fe-Ti-rich bands. Zone 4 consists of massive mixtures of silica, chlorite, and Fe-oxide(?), and ranges in width from 100 to 300 μm. The cores of these shards usually contain brownish-green spheroids of chlorite with Ti-rich microbands (Zone 5, Fig. 4). Small aggregates of fine grained apatite occur along the outer margins of Zone 5 in some cores. Microprobe analyses indicate higher proportions of Na in Zones 3 and 4 than in others, suggesting that smectite occurs as a mixture with other minerals, possibly as a mixed-layer chlorite-smectite. This example of altered hyaloclastite exhibits mineralogical and textural characteristics similar to altered hyaloclastites from Iceland (Geptner et al., 1987).

Samples **ALV-GR-1655-1A** and **1B** are highly altered pillows from a glassy Fe-Ti basalt flow. Zonation of secon-

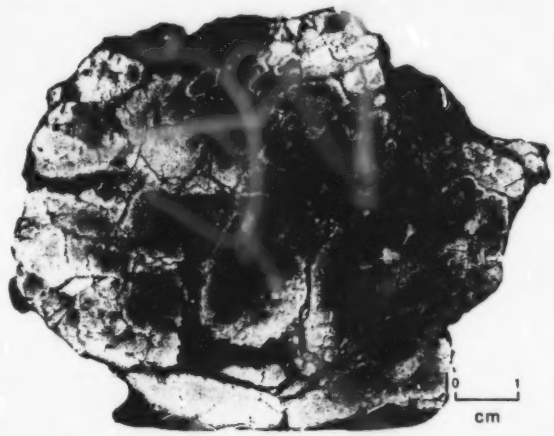

Figure 5. Sample 1655-1B: altered pillow from glassy Fe-Ti basalt flow: (1) rectorite rims along spheroidal margins of glass (Zone 1); (2) dominantly chlorite-kaolinite mixture (Zone 2); (3) chlorite cavity filling; (4) fractures filled with pyrite-quartz-chlorite; (5) altered rectorite halo adjacent to fracture.

Table 1. Electron microprobe analyses of fresh and altered glasses

	1661-9 Andesite	1651-4 Fe-Ti Basalt	1654-5 Altered Hyaloclastite[1]					1655-1 Altered Flow[2]
			Zone 1	Zone 2	Zone 3	Zone 4	Zone 5	
Na_2O	.98	.65	.98	.70	1.25	1.30	.47	1.57
MgO	1.99	5.31	4.20	1.84	4.41	4.89	4.95	11.50
Al_2O_3	11.88	12.34	14.97	4.15	15.30	15.37	17.10	18.36
SiO_2	58.34	52.22	25.51	77.95	31.56	26.35	26.56	31.05
K_2O	.39	.22	.07	.29	.22	.17	.00	.80
CaO	7.11	9.86	.11	.20	.10	.11	.01	.10
TiO_2	1.78	2.36	7.13	3.41	.27	3.49	1.97	.03
Cr_2O_3	.00	.07	.12	.07	.05	.00	.01	.00
MnO	.21	.24	.09	.05	.21	.10	.14	.06
FeO	14.84	15.64	33.35	7.27	34.88	32.72	36.77	24.99
TOTAL	97.52	98.91	86.53	95.93	88.25	84.50	87.98	88.46

[1] Analyses from Zones in Figure 4.
[2] Analysis from spherulite in Figure 8.

dary minerals is on a millimetre-scale, and is controlled by spherulitic and microlitic quench textures within the original glassy lava. The spherulitic outer margins of the glass pillow top (Zone 1) are characterized by thin (<2 mm), white rims altered to illite-smectite (var. rectorite) (Fig. 5). Inward, in Zone 2, the altered microlitic glass is pale brownish green and mottled, with translucent feathery networks (Fig. 6) and opaque needle-like crystals (Fig. 7) in an aphanitic matrix. XRD analyses indicate a mixture of chlorite, kaolinite, minor quartz, and minor rectorite. Microprobe analyses indicating Fe-chlorite composition (Table 1) were obtained on clusters of spherulites in Zone 2 (Fig. 7 and 8). Probe analyses of other areas were less conclusive. SEM-EDS data indicate very high Fe and high Mg in the feathery networks, suggesting that they also consist of chlorite, probably as pseudomorphs after skeletal pyroxenes (Embley et al., 1988). The opaque needle-like grains are up to 1 mm in length, are Ti-rich, and may be rutile pseudomorphs of titanomagnetite, as commonly observed in fresh Fe-Ti basalt on the Galapagos Rift (Embley et al., 1988). SEM backscatter photos show a bright (i.e. high average atomic number) halo surrounding a brighter core in these needles, suggesting that the core is more Fe-rich (i.e. composed of titanomagnetite) and the halo depleted in Fe (i.e. composed of rutile). Very fine grained disseminated pyrite is present throughout the altered glass.

Cavities subjacent to spherulites in the pillow margins are probably pipe vesicles now filled with Fe-rich chlorite, and are separated from the rectorite rims by 100 μm-thick layers of euhedral pyrite. Net-like fractures up to 8 mm wide cut the altered glass and filled cavities, and are partly to completely filled with euhedral pyrite up to 2 mm in diameter, as well as minor chlorite and quartz. The fractures are bounded on both sides by alteration haloes up to several millimetres wide composed of rectorite (area 5, Fig. 5). The original feathery networks are poorly preserved within these intensively altered zones, especially near the veinlets (Fig. 9)

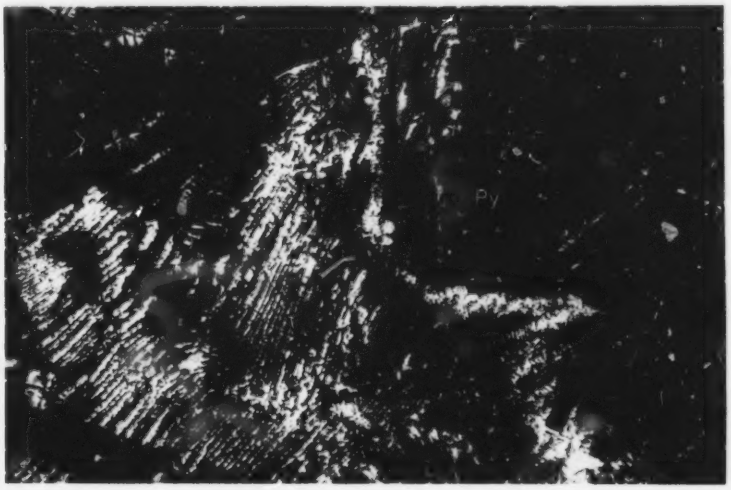

Figure 6. Photomicrograph of feathery microlite networks. Transmitted light, crossed nicols. Width of photo is 1.4 cm. Sample 1655-1B.

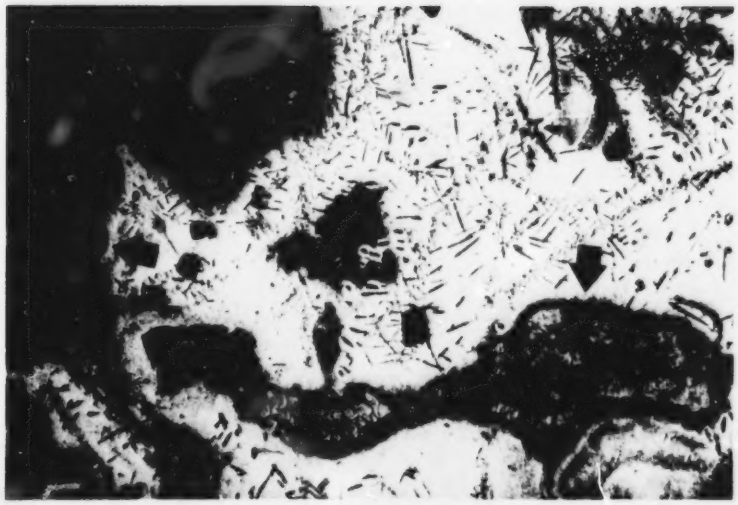

Figure 7. Photomicrograph of Ti-rich chlorite needles, and clusters of chlorite spherulites (arrows) in an aphanitic matrix. Transmitted light. Width of photo is 1.4 cm. Sample 1655-1A.

DISCUSSION

The compositional and textural characteristics of the two samples are contrasted and summarized in Table 2. An important difference is in the assemblages of alteration minerals. The hyaloclastite contains pyrite, sphalerite, and cristobalite in the matrix, and Fe-rich chlorite, cristobalite, and minor smectite in the shards. In contrast, the altered pillows contain pyrite, quartz, Fe-rich chlorite, and rectorite. The differences in composition of the protoliths (basaltic andesite versus Fe-Ti basalt respectively) may account, in part, for these differences. However, the presence of two polymorphs of silica suggests that the two samples could have been altered by fluids of different temperature and composition. Alternatively, cristobalite may have formed in the later stages of the evolution of the hydrothermal system. Either of these processes may have affected the inversion rate of cristobalite to quartz.

Although both samples exhibit marked textural and mineralogical zonation, the style and scale of zonation is

Table 2. Summary of compositional and textural characteristics

Sample #	1654-5-2	1655-1
Description	hyaloclastite	glassy flow
Protolith composition	basaltic andesite	Fe-Ti basalt
Mineralogy	pyrite, sphalerite, cristobalite, Fe-chlorit eminor smectite	pyrite, quartz, Fe-chlorite, rectorite
Type of zonation	bands of minerals or mixtures concentricto shard margins	preserved banding of quench textures
Scale of zonation	10^2 μm	mm
Mechanism of alteration	precipitation in open space	pseudomorphic replacement

Figure 8. Enlarged view of Fe-rich chlorite spherulite. Width of photo is 1.4 mm. Sample 1655-1A.

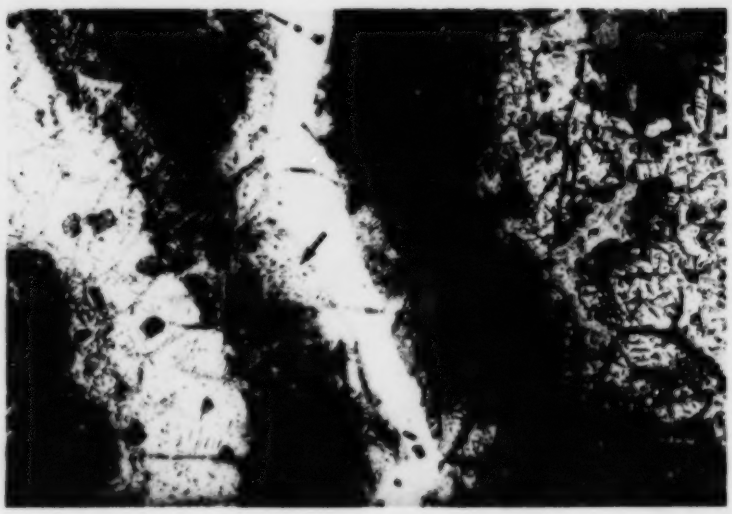

Figure 9. Photomicrograph of alteration halo bounding empty fracture. Feathery networks have been completely altered near the fracture (arrow). Width of photo is 2.6 cm. Sample 1655-1B.

quite different. In the hyaloclastite, mineral banding is of the order of hundreds of microns. The spheroidal and radial habits of some secondary minerals imply that they grew inward into fluid-filled cavities. This is supported by the existence of hollowed shards that remained unfilled. These are interpreted to be primary gas or fluid cavities in the shards. Concentric chemical zonation of Fe and Ti in chlorite and its microcrystalline optical continuity through those zones suggests a pulsation of altering fluids. The rhythmic spacing of microbands (5-10 μm apart) in the spheroids suggests regular episodic variation in fluid composition. In contrast, zonation in the altered pillows is on a broader scale of several millimetres, and perhaps was controlled by permeability differences in banding related to rapid chilling, and devitrification and fracturing of glassy pillow tops. These bands are now preserved by differential pseudomorphic alteration. Therefore, the quenched glass textures, at least in part, determined the type and distribution of alteration minerals.

The reasons for the mineralogical differences between these two altered samples remain unclear. They may be the result of differences in original permeability, protolith composition, fluid composition, and or fluid temperature. The hyaloclastite had a high initial porosity and permeability, facilitating movement of hydrothermal fluid through the rock. However, it is likely that fluid migration in the cryptocrystalline pillows was by diffusion along grain boundaries and microfractures. It is evident that some further fracturing, alteration, and deposition of coarse grained sulphides occurred after much of the sample had already been altered (Fig. 9). Embley et al. (1988) noted that multiple crack-seal veins were common in closely fractured and altered lobate and pillow flows.

ACKNOWLEDGMENTS

The manuscript benefited greatly from critical review by J.M. Franklin. D.A. Walker and M. Villeneuve carried out SEM analyses. We wish to acknowledge the fact that samples studied were collected on the ALVIN/ATLANTIS II expedition to Galapagos Ridge in 1985. Chief Scientist was R.W. Embley of NOAA/PMEL/MRRD, Hatfield Marine Science Center, Newport, Oregon.

REFERENCES

Collinson, T.B.
1986: Hydrothermal mineralization and basalt alteration in stockwork zones of the Bayda and Lasail massive sulphide deposits, Oman Ophiolite; M.A. thesis, University of California, Santa Barbara, California.

Embley, R.W.
1986: Galapagos hydrothermal alteration zone found; EOS, v. 67, no. 22, p. 497.

Embley, R.W., Jonasson, I.R., Perfit, M.R., Franklin, J. M., Tivey, M.A., Malahoff, A., Smith, M.F., and Francis, T.J.G.
1988: Submersible investigation of an extinct hydrothermal system on the Galapagos Ridge: sulphide mounds, stockwork zone, and differentiated lavas; Canadian Mineralogist, v. 26, p. 517-539.

Geptner, A.R., Kristmannsdottir, H., and Selezneva, M.A.
1987: Secondary minerals of basaltoids altered by hydrothermal brine on the Reykjanes Peninsula (Iceland): Lithology and Mineral Resources, v. 22, no. 2, p. 128-141.

Lydon, J.W. and Galley, A.
1986: The chemical and mineralogical zonation of Mathiati alteration pipe, Cyprus, and genetic significance; in Metallogeny of Basic and Ultrabasic Rocks, ed. M.J. Gallagher, R.A. Ixer, C.R. Neary, and H.M. Prichard. Institute of Mining and Metallurgy, London, U.K., p. 49-68.

Comparison of the determination of sulphur in geological materials by pyrohydrolysis and ion chromatography with other production-oriented methods

G.E.M. Hall and J.E. Vaive
Mineral Resources Division

Hall, G.E.M. and Vaive, J.E., Comparison of the determination of sulphur in geological materials by pyrohydrolysis and ion chromatography with other production-oriented methods; in Current Research, Part F, Geological Survey of Canada, Paper 89-1F, p. 17-21, 1989.

Abstract

The determination of S by pyrohydrolysis and ion chromatography in a wide variety of sample matrices is compared to the two other production — oriented methods which have been used at the Geological Survey of Canada: inductive heating/iodimetric titration and resistive heating/infra-red spectrometry. Results compare extremely well for the three methods from 0.1-30% S for all samples studied (rocks and sediments) with the exception of those high in F (>0.2%) and Cl (>1%). This group of samples are subject to interference by these halides in the latter two methods, while the ion chromatographic technique is actually amenable to the concurrent determination of F and Cl with S. With the instrumentation described, the productivity (80 samples per day) of the method based upon infra-red spectrometry is about twice that of the other two methods while the determination limit of 5 ppm S by ion chromatography is superior to the other two methods.

Résumé

L'évaluation du S par hydropyrolyse et chromatographie des ions dans une grande variété d'échantillons de matrices est comparée à deux autres méthodes orientées vers la production qui ont été utilisées à la Commission géologique du Canada: chauffage inductif/titration iodométrique et chauffage résistif/spectrométrie infrarouge. Les résultats des trois méthodes concordent extrêmement bien à partir de 0,1-30% S pour tous les échantillons étudiés (roches et sédiments) sauf ceux riches en F (>0,2%) et en Cl (>1%). Ce groupe d'échantillons est sujet à l'interférence de ces halogénures dans les deux dernières méthodes, tandis que la chromatographie des ions convient en fait au dosage concourant de F et de Cl avec S. Avec l'instrumentation décrite, la productivité (80 échantillons par jour) de la méthode basée sur la spectrométrie infrarouge est environ deux fois supérieure à celle des deux autres méthodes, tandis que le seuil de détection de 5 ppm S par chromatographie des ions est supérieur à celui des deux autres méthodes.

INTRODUCTION

The analysis of geological materials for S, as well as F and Cl, by pyrohydrolysis/ion chromatography was first described by the authors in 1986 (Hall et al., 1986) and since then in excess of 10 000 samples have been analyzed in this laboratory at the Geological Survey of Canada (GSC). Other production-oriented methods to determine S which have gained widespread acceptance are based upon wavelength-dispersive X-ray fluorescence and sample combustion (by high frequency inductive or resistive heating) with measurement of the SO_2 produced by iodimetric titration or infra-red spectrometry. This paper compares the performance of this method, based upon ion chromatography and conductimetric detection, with those that have been in routine use at the GSC, namely detection by iodimetric titration (Bouvier et al., 1972) and by infra-red spectrometry. Detection of S by infra-red spectrometry replaced iodimetric titration at the GSC in 1986. In order to accommodate the analysis of large numbers of samples of widely varying S content, the conditions employed in the latter two methods have not been optimized with the intent of obtaining the lowest possible detection limit; rather, a compromise has been made between high productivity and the ultimate refinement of the method. Procedural modifications have been carried out in the ion chromatographic technique in order to improve precision and detection capability below 50 ppm of S in response to a request for accurate Se:S ratios at low concentrations of these elements (Eckstrand et al., 1989).

PYROHYDROLYSIS/ION CHROMATOGRAPHIC MEASUREMENT OF SULPHUR

A complete description of the method and associated instrumentation can be found elsewhere (Hall et al., 1986). Briefly, S is extracted from the sample in the gaseous forms, SO_2 and SO_3, by heating in moist O_2 at 1050°C in the presence of the accelerator, V_2O_5. The gases, evolved during a 15 minute period, are swept by the flow of O_2 into a receiver solution of 0.003M $NaHCO_3$-0.0024M Na_2CO_3 containing 250 ppm H_2O_2 (to oxidize any SO_3^{2-} to SO_4^{2-}). These solutions are analyzed directly using the Dionex Model 12 fully automated ion chromatograph with conductimetric detection of the SO_4^{2-} peak occurring at about 8.2 minutes into the chromatogram. This is a particularly "clean" region of the chromatogram (unlike the F and Cl peak positions); moreover, an effective and efficient separation of the analyte from its matrix has been accomplished by gaseous evolution (cf. sample fusion with Na_2O_2 described by Stallings et al., 1988). Calibration is made against a series of standards (spiked V_2O_5 of 600-mg weight) taken through the procedure; response is found to be linear up to a S content of about 10 % in a 100-mg sample weight. Samples containing greater than 10 % S are reanalyzed at a lower weight.

An example of the precision obtained by this method is given by the in-house control, a quartz-feldspar porphyry, which has been analyzed regularly. A total of 353 separate analyses resulted in a mean value of 4643 ppm S with a standard deviation (SD) of 199 ppm (relative standard deviation, RSD: 4.2 %). Further data on reproducibility are shown in Table 1; results are given for 10 analyses each of lake and stream sediment control samples soon to be released under the Canadian Certified Reference Materials Project (CCRMP). It is apparent that the precision, ranging from 0.9 to 5.0 % RSD, is dependent on the representativeness of the 100-mg sample weight for S, and not mainly on the concentration level. Duplicate analyses of 103 rock, soil and sediment samples, ranging in S content from about 50 ppm to 6.2 %, are shown graphically in Figure 1. By plotting the difference (or standard deviation) against the mean for these results, according to the method of Thompson and Howarth (1976), we arrive at the relationships between precision and concentration shown in Table 2.

While the value of the constant (4.2, 1.8, 154 in Table 2) depends largely on the size of group chosen within a concentration range (e.g. group of 7, 9, or 11 points), the value of the coefficient ranges only from 0.014 to 0.025. Hence, a reliable estimate of the precision over this wide concentration range can be made at between 1.5 and 3.0 % RSD, naturally being dependent upon sample homogeneity. The samples used in this study were of widely varying matrix, from high F-bearing granites to marine sediments, relatively organic-rich soils and lake sediments, and sulphides.

For routine work, a determination limit of 50 ppm S is achieved using a 100-mg sample weight. By increasing the sample weight to 200 mg, decreasing the collection volume of the eluent from 50 to 25 mL, and increasing the sample injection size from 100 to 500?L, a determination limit (2.5 times the detection limit) of 5 ppm is obtained. The purity of the accelerator, V_2O_5, is critical to low level analysis and changes from one batch to another must be carefully monitored. Ten analyses of "blank" V_2O_5 (600 mg) charges resulted in a mean S content of 24.2 ppm with a standard deviation of 0.6 ppm. Hence, the detection limit, defined as three times the standard deviation of the blank carried through the entire procedure, is approximately 2 ppm. The accuracy of the method at S concentrations below 100 ppm is difficult to assess owing to the lack of recommended values for standard reference materials. The analysis, in triplicate, of the CCRMP sample SCH-1, a hematite of S content 0.007 ± 0.001 % (recommended;

Table 1. Determination of S in lake (LKSD-) and stream (STSD-) sediment reference materials by pyrohydrolysis/ion chromatography. Number of analyses per sample: 10.

Sample	Mean S, ppm	SD, ppm	RSD, %
LKSD-1	17454	168	0.96
-2	1948	71	3.62
-3	1973	30	1.50
-4	10588	534	5.05
STSD-1	2533	50	1.97
-2	702	23	3.23
-3	1957	19	0.98
-4	1203	28	2.35

Steger, 1986) gave a value of 0.0065 ± 0.0005 %. The standard deviation obtained by three analyses of a quartz latite containing 10.0 ppm S was very low, at 0.8 ppm S. Results for three analyses of the Japanese granodiorite, JG-1a, gave 10.6 ± 0.5 ppm S. This compares favourably with the recommended value of 11.3 ppm S in JG-1, the original sample collected from the same location (Govindaraju, 1984).

COMPARISON WITH INDUCTIVE HEATING/IODIMETRIC TITRATION

This method, employing the LECO automatic titrator and combustion apparatus, is based upon the evolution of SO_2 by inductive heating of the sample and its subsequent reaction with free I_2 in solution. A mixture of HCl, KI and starch solution is placed in the titration vessel and a small amount of standard KIO_3 solution is added to produce free I_2, indicated by the typical blue colour obtained with starch (reaction 1).

$$KIO_3 + 5KI + 6HCl \rightarrow 6KCl + 3I_2 + 3H_2O \quad (1)$$

The SO_2 released during combustion reacts with free I_2 to form HI (reaction 2), eliminating the blue colour.

$$SO_2 + I_2 + 2H_2O \rightarrow H_2SO_4 + 2HI \quad (2)$$

Automatic addition of KIO_3 solution restores the I_2 to its original concentration; this volume is proportional to the S content of the sample, assuming a constant ratio of SO_2:SO_3 in the evolution. Results are usually reported to 0.01 % S with standard deviations in the order of 0.02 to 0.04 %.

Kiss (1986) has reported severe interferences when applying this method to chloride-bearing materials such as marine muds and saline sediments. The free Cl_2 liberated during combustion was thought to interfere via three

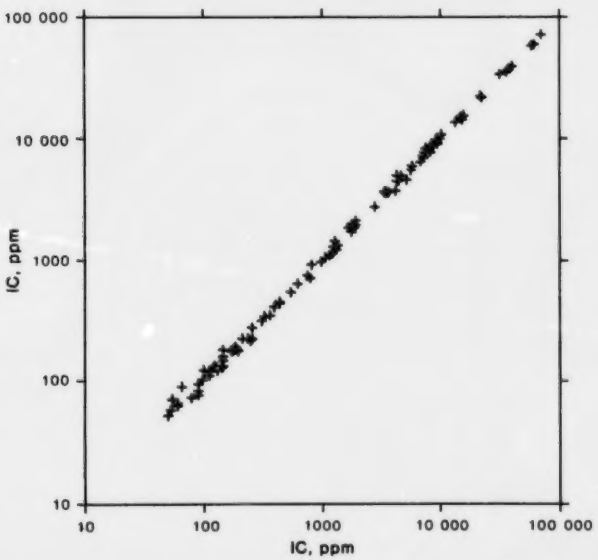

Figure 1. Duplicate analyses of 103 samples for S by pyrohydrolysis/ion chromatography (IC).

Table 2. Relationship between standard deviation (SD) and concentration (C) of S at various concentrations ranges in analysis by pyrohydrolysis/ion chromatography.

Concentration (C) range, ppm of S	Number of duplicates	SD[a], ppm
50-1000	49	4.2 + 0.01C
1001-10 000	38	1.8 + 0.022C
10 001-100 000	16	154 + 0.0176C
50-100 000	103	14 + 0.0184C

[a] As computed according to Thompson and Howarth (1976)

mechanisms: (1) immediate oxidation of SO_2 to SO_3 in the induction furnace at 1500°C and above; (2) gas-phase oxidation of SO_2 during transfer to the titration vessel; and (3) liberation of I_2 in the titration vessel by the remaining Cl_2. A thorough investigation of means by which to either suppress the formation of Cl_2 during heating or to remove Cl_2 in transit to the titration cell was carried out. The composition of the accelerators (Cu, Fe, V_2O_5, Sn) was altered and various solid-state absorbents (Sb lumps, Cu) were tested; none of these remedies proved to be satisfactory for the analysis of sediments containing greater than 2 % Cl. The introduction of a procedure to desalinate the sample, by carrying out a Soxhlet extraction with anhydrous methanol, was found to be most effective, as evidenced by the result of 0.400 ± 0.005 % S in the marine mud, MAG-1.

Prior separation of halide has not been practical for large-scale analyses at the GSC and, hence, results by the iodimetric method were degraded in the presence of significant amounts of Cl in the sample. This is seen in Table 3 where results by the two methods are compared for deep-sea sediments collected from the Juan de Fuca Ridge. Agreement is good when the concentration of Cl is below 0.3 % but severe suppression is evident in the S data by iodimetric titration at Cl concentrations of 2-5 %. The problem is less severe at high S concentrations (sample 4A, Table 3). A memory effect of Cl_2 in the system was also thought to contribute to the erratic data. Chlorine does not interfere in the ion chromatographic technique; indeed, it is determined from the same solution at a retention time of 2.1 minutes in the chromatogram. For samples of low Cl content (<0.2 %), the methods compare well. Results for duplicate samples, totalling 127, from the two data bases were chosen at random and compared (Fig. 2). In this concentration range, from 100 ppm to 4 % S, the Spearman rank coefficient was computed to be 0.972. The "noisy" region clearly lies around the detection limit of the iodimetric technique, at 0.01-0.04 % S (Fig. 2).

COMPARISON WITH RESISTIVE HEATING/ INFRA-RED SPECTROMETRY

This method, employing the LECO SC-32 micro-processor controlled infra-red (IR) analyzer, is based on the absorption of IR radiation, at a specific wavelength (filter selec-

tion), by the SO_2 liberated from a sample combusted at about 1400°C. The routine procedure employed at the GSC involves the use of a 500-mg sample weight mixed with 1.0 g of V_2O_5 as accelerator; the SO_2 generated is swept into the IR cell in a stream of O_2. Water vapour is removed by drying tubes containing magnesium perchlorate, thus preventing erroneously high readings. Terashima (1979) has found it advisable to dry samples containing greater than 4 % H_2O in an oven at 140°C prior to analysis.

Again, results were extracted at random from the two data bases for samples analyzed by both methods (infra-red spectrometry, IR and ion chromatography, IC) and are plotted in Figure 3. Values below the detection limit of 100 ppm S by IR were set to 50 ppm. Agreement between the two methods over this wide concentration range of 100 ppm to 30 % S is remarkable, bearing in mind the different matrices and different sample weights taken (100 and 500 mg). For the 190 points, the Spearman rank coefficient was computed to be 0.981. This suite of samples had F contents of less than 0.2 %. An interference was detected in the IR technique for a group of samples containing 0.3-2.0 % F. The F, evolved as a gas during combustion, acted as a mask to the IR detector and the absorption due to SO_2 could not be differentiated. Detection limits are comparable for the two methods as an alternative instrument, the LECO SC-132, may be used for greater sensitivity (Terashima, 1979; Bower et al., 1986). However, productivity for S using the IR technique is at least double that using IC. While F and Cl may be determined concurrently with S in the IC technique, C may be determined with S in the IR technique with certain models of instrumentation.

Table 3. Results of analyses of deep-sea sediment samples for S by pyrohydrolysis/ion chromatography (IC) and inductive/iodimetric titration (TIT).

Sample	Cl, %	S by IC, %	S by TIT, %
1A	4.38	0.29	0.10
2A	4.07	0.27	0.13
3A	2.77	1.38	0.87
4A	3.24	22.8	21.8
5A	3.36	0.24	0.10
6A	1.91	0.13	0.02
7A	2.36	0.72	0.56
8A	2.62	0.17	0.02
9A	3.07	0.22	0.05
10A	4.84	0.37	0.05
11A	3.31	0.25	0.02
12A	4.38	0.35	0.08
13A	3.70	0.31	0.05
6B	0.21	0.04	0.04
7B	0.19	0.55	0.55
8B	0.32	0.07	0.07

CONCLUSIONS

The determination of S by pyrohydrolysis/ion chromatography offers an advantage over methods based upon iodimetric titration and infra-red spectrometry in that samples high in F (>0.2 %) and Cl (>1 %) concentration can be analyzed without interference. Indeed, these elements can be concurrently determined with S. However, for samples containing less F and Cl, the results by all three methods agree very well over a broad range of S concentration (0.1-30 %); no

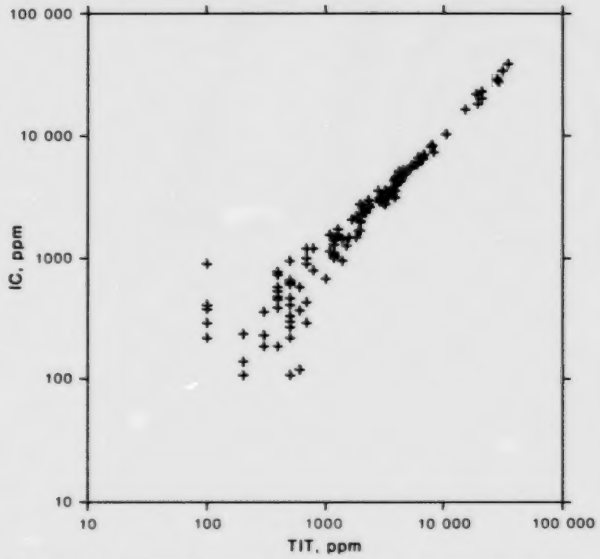

Figure 2. Comparison of results for S by pyrohydrolysis/ion chromatography (IC) and inductive/iodimetric titration (TIT) in 127 duplicate samples.

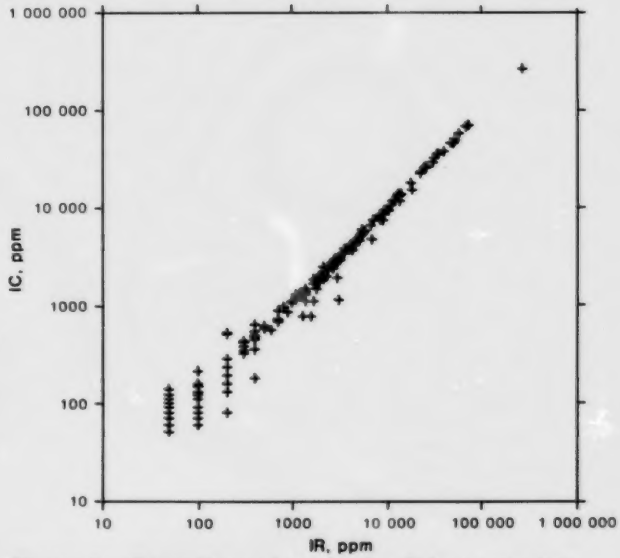

Figure 3. Comparison of results for S by pyrohydrolysis/ion chromatography (IC) and combustion/infra-red spectrometry (IR) in 190 duplicate samples.

evidence of bias was detected in the two sets of data examined. Below 1000 ppm S, analyses by ion chromatography are more closely matched to those by infra-red spectrometry than the less sensitive titrimetric method described here. The best productivity (80 samples per day) was obtained by employing infra-red spectrometry, also capable of concurrently determining C in the sample. The efficiency (40 samples per day) of the ion chromatographic method could be improved by increasing the number of furnaces (2) used for pyrohydrolysis.

Modifications to the procedure in the ion chromatographic method have decreased the determination limit to 5 ppm for a 200-mg sample weight. Precision, while apparently sample dependent, can be expected to be in the range 2-4 % RSD. In view of the features of each method, the analyses are divided into two groups at the GSC: those requiring the best possible detection limit and those likely to contain significant amounts of F and/or Cl are carried out by ion chromatography, while the majority of analyses are carried out by the less sensitive but more productive infra-red spectrometric technique.

ACKNOWLEDGMENTS

We thank the Analytical Chemistry Section for access to the data bases for S by the TIT and IR techniques, particularly Peter Belanger. We are also grateful to Nimal De Silva for constructive comments in his review of this manuscript.

REFERENCES

Bouvier, J.L., Sen Gupta, J.G., and Abbey, S.
1972: Use of an "automatic sulphur titrator" in rock and mineral analysis: determination of sulphur, total carbon, carbonate and ferrous iron; Geological Survey of Canada, Paper 72-31, 22 p.

Bower, N.W., Gladney, E.S., and Ferenbaugh, R.W.
1986: Critical comparison of X-ray fluorescence and combustion-infrared methods for the determination of sulphur in biological matrices; Analyst, v. III, p. 105-106.

Eckstrand, O.R., Grinenko, L., Krouse, H.R., Paktunc, A.D., Schwann, P., and Scoates, R.F.J.
1989: Preliminary data on sulphur isotopes and Se/S ratios, and the source of sulphur in magmatic sulphides from the Fox River sill, Molson dykes and Thompson nickel deposits, northern Manitoba; in Current Research, Part C, Geological Survey of Canada, Paper 89-1C.

Govindaraju, K.
1984: 1984 compilation of working values and sample description for 170 international reference samples of mainly silicate rocks and minerals; Geostandards Newsletter, v. 8, Special Issue, p. 14, Appendix 1.

Hall, G.E.M., MacLaurin, A.I., and Vaive, J.
1986: The analysis of geological materials for fluorine, chlorine and sulphur using pyrohydrolysis and ion chromatography; Journal of Geochemical Exploration, v. 26, p. 177-186.

Kiss, E.
1986: Elimination of major molecular chlorine interference in the iodimetric determination of sulphur in saline sediments; Analytical Chimica Acta, v. 182, p. 33-45.

Stallings, E.A., Cardalaria, L.M., and Gladney, E.S.
1988: Investigation of a fusion technique for the determination of total sulphur in geological samples by ion chromatography; Analytical Chemistry, v. 60, p. 1246-1248.

Steger, H.F.
1986: Certified reference materials; CANMET, Paper CM84-14E, Energy, Mines and Resources, Canada, p. 9.

Terashima, S.
1979: Determination of total carbon and sulphur in forty-two geochemical reference samples by combustion and infrared spectrometry; Geostandards Newsletter, v. 3, p. 195-198.

Thompson, M. and Howarth, R.J.
1976: Duplicate analysis in geochemical practice. Part 1. Theoretical approach and estimation of analytical reproducibility; Analyst, v. 101, p. 690-698.

$^{107}Ag/^{109}Ag$ ratios of minerals from various types of ore-forming environments using inductively coupled mass spectrometry

D.R. Boyle and D.C. Gregoire
Mineral Resources Division

Boyle, D.R. and Gregoire, D.C., $^{107}Ag/^{109}Ag$ ratios of minerals from various types of ore-forming environments using inductively coupled mass spectrometry; in Current Research, Part F, Geological Survey of Canada, Paper 89-1F, p. 23-26, 1989.

Abstract

$^{107}Ag/^{109}Ag$ ratios have been determined for 106 mineral specimens from a wide variety of mineral deposits using inductively coupled plasma mass spectrometry (ICP-MS) and a number of sample preparation techniques. Isotopic shifts in the silver ratio from a defined norm may occur: a) as the result of physicochemical processes during leaching, mobilization and depositional events involved in hydrothermal, magmatic and weathering regimes; b) from slow neutron bombardment via neutron capture reactions; or, c) through the decay of ^{107}Pd to form ^{107}Ag.

Shifts in the silver isotopic ratio relative to an NBS Reference Standard do occur but such shifts are very small and more detailed deposit studies and further refinement of the analytical technique are required in order to make more definitive interpretations.

Résumé

On a évalué les rapports $^{107}Ag/^{109}$ Ag pour 106 spécimens de minéraux provenant d'une grande variété de gisements minéraux par spectométrie de masse en plasma à couplage inductif (ICP-MS) et par certaines techniques de préparation des échantillons. Des écarts isotopiques par rapport à une norme définie peuvent se produire dans le rapport des isotopes d'argent: a) à cause de processus physicochimiques qui se manifestent pendant la lixiviation, la mobilisation et la sédimentation dans les régimes hydrothermiques, magmatiques et d'altération, b) à cause d'un bombardement par des neutrons lents lors de réactions de capture neutronique ou c) à cause de la désintégration du ^{107} Pd en ^{107} Ag.

Il se produit des écarts de rapport isotopique de l'argent par rapport à une norme de référence NBS, mais ces écarts sont très faibles et il faudrait approfondir l'étude des gisements et améliorer la technique analytique pour en arriver à des interprétations plus définitives.

INTRODUCTION

Recent studies of the isotopic abundance of $^{107}Ag/^{109}Ag$ in meteorites have shown significant excesses of ^{107}Ag with concomitant increases in $^{107}Ag/^{109}Ag$ of up to 212 % of the average terrestrial abundance (Kaiser and Wasserburg, 1983; Chen and Wasserburg, 1984; Wasserburg, 1985). These same authors have found large variations in the $^{107}Ag/^{109}Ag$ ratio of coexisting sulphide, metal and silicate phases of various types of meteorites. Terrestrial abundance data for $^{107}Ag/^{109}Ag$ is very scant. Hess et al. (1957) reported no variation in $^{107}Ag/^{109}Ag$ in four samples of native silver and one meteorite sample but their precision was only about 2 % of the isotope ratio. Data of Shields et al. (1960) for several samples of native silver show a statistically significant variation in the ratio of one sample from Cobalt, Ontario. Later work by Shields et al. (1962) for 13 native silver and 11 silver minerals from various areas showed a variation from 1.0734 to 1.0783. This variation was not considered to be statistically significant, and the authors give a pooled average terrestrial value for $^{107}Ag/^{109}Ag$ of 1.07597. In view of the recently measured highly anomalous shifts in $^{107}Ag/^{109}Ag$ for many types of meteorites and the uncertainties still present as to whether terrestrial shifts in the ratio exist, the present analytical research employing inductively coupled plasma mass spectrometry (ICP-MS) was initiated using a large number of silver-bearing minerals from a variety of geological environments. The purpose of the study was two-fold; firstly, to see if a statistically significant overall variation in the $^{107}Ag/^{109}Ag$ ratio exists for the samples analyzed and secondly, whether there are any variations that can be related to the different mineralizing processes.

EXPERIMENTAL PROCEDURE

Dissolution of sample material and separation of silver for silver isotope measurements was accomplished using several procedures depending on the composition of the sample. For samples low in silver, it was necessary to effect a partial separation of silver from matrix elements in order to allow for a preconcentration of silver in the final solution, as well as to avoid analyte signal suppression and possible matrix induced mass discrimination effects due to the presence of concomitant elements in solution. Where silver occurred in very high concentrations, only simple dilution of sample solutions was required to obtain satisfactory results.

Galena and sphalerite

One hundred milligrams of sulphide-containing material were treated with 5 mL of 12 M hydrochloric acid and warmed on a hot plate until the evolution of hydrogen sulphide ceased. One millilitre of 200 ppm NaCl solution was added and the sample solution was evaporated to dryness. The quantity of lead in solution was reduced by rinsing the solid residue with several 5 mL aliquots of distilled water. Precipitated silver (as chloride) was separated from the solid residue with 2 mL of 6 M ammonium hydroxide solution. The resulting solution was evaporated to dryness and the residue dissolved in 1 mL of 2 M nitric acid.

Gold

Ten to fifty milligram samples of gold were dissolved in 5 mL of aqua regia. Sample solutions were evaporated to dryness and redissolved in 5 mL of 1 M nitric acid. Ten microlitres of this solution were diluted to 100 mL with 2 M nitric acid.

Native silver and silver-bearing minerals

One hundred milligrams of sample were dissolved in 5 mL of 3 M nitric acid. Samples containing resistant minerals were first treated with hydrofluoric acid, followed by aqua regia. Following evaporation to dryness, silver was separated from major matrix components using the procedure as described for sulphides. Ten to one hundred microlitres of the sample solution were diluted with 2 M nitric acid for measurement of silver isotopes.

Mass spectrometry

Silver isotope ratios were measured using a Perkin-Elmer/Sciex Model 250 ICP-MS. Sample solutions were nebulized directly into the argon plasma using a Meinhard concentric glass nebulizer. A sample uptake rate of 1 mL per minute was maintained by the use of a peristaltic pump.

Ion count rates for each of the silver isotopes were obtained by sequentially measuring the signal intensity for each isotope for a period of 0.4 seconds. The average value obtained for ten measurement cycles was used to calculate an initial isotope ratio. The average of ten such isotope ratio determinations was used to calculate the reported silver isotope ratio. The standard error given in Tables 1 and 2 are the standard deviations of these measurements. Silver isotope ratios were determined with a precision of 0.3 %.

Before analysis by ICP-MS, sample and reference solutions were diluted with 2 M nitric acid to give an ion count rate of approximately 100 000 c/s. Correction for instrumental mass discrimination was done using National Bureau of Standards Reference Material #978a (silver nitrate of certified isotopic composition 1.0764 ± 0.0002). The isotope ratio of the standard reference solution was measured before and after each sample solution to minimize any drift in instrumental mass discrimination.

RESULTS AND DISCUSSION

One hundred and six $^{107}Ag/^{109}Ag$ analyses for a variety of mineral types from various mineral deposit environments are shown in Table 1. The values vary from a low of 1.065 to a high of 1.081; a spread of 0.016. The average standard error for this set of data is $\pm$ 0.004 and even if the two standard deviation error limit is taken it cannot account for the variations shown in Table 1. Repeat analyses of the four highest and four lowest ratios are presented in Table 2. Differences between initial and repeat values are random and are generally within analytical precision for this method; all values remain significantly below or above the NBS Reference Standard analyzed before and after each

sample. The precision of the method as indicated above is 0.3 %; values greater than the standard error limits on the NBS Reference Standard of 1.073 and 1.079 can be considered as anomalous. Only one value of supergene native silver from the Tsumeb mine in Namibia (1.081) is above the upper error limit on the standard. However a considerable number of samples display ratios below the 1.073 lower limit. The deposit types for these samples are not significantly different from those displaying ratios greater than 1.073. The mechanisms which give rise to low ratios are not, therefore, peculiar to sedimentary, hydrothermal or volcanogenic ore deposit environments in general but instead appear to be related to regional ore-forming processes or perhaps in some cases to specific chemical reactions within a particular deposit environment. Of particular note in this respect are the samples from the Echo Bay deposit in the Northwest Territories. This deposit displays $^{107}Ag/^{109}Ag$ ratios of 1.069, 1.075, 1.076, 1.076, 1.078, 1.079 and 1.079 for covellite, galena, rammelsbergite, native silver, galena, skutterudite and argentite, respectively; i.e. spanning almost the full range of observed ratios.

The percentage positive and negative spread from the reference standard for the ratio data in Table 1 is +0.42 % to -1.06 %. These are not large deviations compared to those observed for meteorites (2-212 %; Kaiser and Wasserburg, 1983). It should be noted that deviations in the $^{107}Ag/^{109}Ag$ ratio in meteorites relative to the average terrestrial abundance are all positive indicating ^{107}Ag excesses. Three processes may give rise to shifts in the $^{107}Ag/^{109}Ag$ from an average norm value (i.e. average terrestrial abundance or some standard). These are: a) pysicochemical processes during the leaching, mobilization and depositional events involved in hydrothermal, magmatic and weathering regimes, b) slow neutron bombardment via the neutron capture reaction $^{109}Ag(n, \gamma)\ ^{110m}Ag$. c) decay of ^{107}Pd to form ^{107}Ag. The decay of presently extinct ^{107}Pd in the solar system is believed to be the cause of high positive ratios in many types of meteorites (Reedy, 1980; Wasserburg, 1985). Of particular note in this respect is the fact that there is often large variations in the $^{107}Ag/^{109}Ag$ ratios for the sulphide, metal and silicate phases of meteorites (Wasserburg, 1985). Often there is a strong positive correlation between Ag and Pd in the various mineral phases of meteorites (Chen and Wasserburg, 1984). We have not as yet investigated the $^{107}Ag/^{109}Ag$ ratio of ore deposits rich in Pd or those (e.g. Sudbury) suspected to result from meteorite impact to see if terrestrial shifts related to ^{107}Pd decay can be found. Of the various types of meteorites, iron-nickel meteorites show the largest shifts (^{107}Ag excesses) in the $^{107}Ag/^{109}Ag$ ratio (Wasserburg, 1985). A significant positive shift in $^{107}Ag/^{109}Ag$ ratios of Sudbury irruptive ores or host rocks and a strong positive correlation between such ratios and Pd abundances may support a meteorite impact origin for the Sudbury complex. Such research would require a large number of analyses to identify those minerals or intrusive phases most influenced by meteorite composition. The assumption must also be made that any meteorite that did impact on the Sudbury area influenced the composition of the ores and host rocks and also exhibited a significant positive shift in its silver isotope ratio.

The silver isotope ratios of minerals within uraniferous deposits such as the Echo Bay mine mentioned above may be affected by slow neutron bombardment reactions for which there are several neutron sources, namely various (α, n) reactions involving alpha particles from uranium and its decay products and various light elements such as F, Li, B and Be. Neutrons are also generated during the spontaneous fission of uranium. Loss et al. (1984) showed that for the Oklo natural reactor system in Gabon a significant amount of fission-produced Ag has migrated from the reactor zones. Determinations of fission yields for the isotopes of silver produced by neutron bombardment in uraniferous deposits are severely hampered by the fact that Ag possesses only two isotopes, both of which are the end members of the 107 and 109 isobaric fission chains, thus making it impossible to correct for the natural Ag component. The ratio shifts noted in Table 1 for the Echo Bay samples may represent the combined effects of slow neutron fission and physicochemical fractionation processes. Clearly, more research will be required to verify this.

Native gold and silver samples, largely from placer deposits, were analyzed for $^{107}Ag/^{109}Ag$ since they offer a relatively pure chemical media free of possible matrix effects that might affect mass discrimination with the technique used. From the data in Table 1 it can be seen that the $^{107}Ag/^{109}Ag$ ratios of placer native Au and Ag vary from 1.070 to 1.079. Of note is the fact that, with one exception, all of the placer Au and Ag samples from the Cassiar gold camp of British Columbia display a uniform silver ratio of 1.073. Samples from other gold camps in British Columbia and Yukon show a wide variation in their silver isotopic content both within and between camps.

CONCLUSIONS AND PROPOSALS FOR FURTHER RESEARCH

The data presented in Table 1 indicate that shifts in the terrestrial abundance of $^{107}Ag/^{109}Ag$ do occur but that such shifts are very small, and more detailed deposit studies and refinements in the analytical technique are required in order to make definitive interpretations.

The analytical technique might be improved by:

1. Selective extraction and preconcentration of silver using solvent extraction procedures resulting in solutions free of interfering concomitant elements (e.g. lead). This could also improve the counting statistics of the measured ratio. This improvement is probably not needed for native silver or gold samples but would be very useful in the measurement of silver ratios of rocks and coexisting minerals having low silver contents.
2. The instrumental mass discrimination correction factor could be determined using a linear regression analysis of data obtained from a series of artificial solutions of different silver isotope ratios whose values would bracket the isotope ratio of the reference material. At present this factor is determined using a single reference analyzed before and after each sample solution.
3. Improvement of analytical precision to within the 0.1

to 0.2 % range might be accomplished by the measurement of sample isotope ratios at least five times during different analysis sessions (days) together with a large number of measurements (10) of each sample within each session.

Detailed studies of a particular ore deposit environment should involve the analysis of as many coexisting minerals and host rock types as possible. It is hoped that after improving the analytical technique, giving the best possible precision, that further detailed studies may shed more light on the possible usefulness of $^{107}Ag/^{109}Ag$ systematics in ore genesis, especially as regards extraterrestrial meteorite impact theories.

ACKNOWLEDGMENTS

The authors would like to thank R. Phillips and S. Livingstone for their able assistance with analytical procedures and A.G. Ansell, Head National Mineral Collection, for supplying us with some of the necessary minerals. The authors would especially like to thank R.I. Thorpe of the Mineral Resources Division for allowing them to analyze his extensive suite of galena samples from many Canadian and foreign mineral deposits. Critical reviews of this work by I. R. Jonasson and W.D. Goodfellow, both of the Mineral Resources Division, are greatly appreciated.

REFERENCES

Chen, J.H. and Wasserburg, G.J.
1984: The origin of excess ^{107}Ag in Gibeon (IVA) and other iron meteorites; Proceeding of the 15th Lunar and Planetary Sci. Conference, Houston, Texas, Abstract, p. 144-145.

Hess, D.C., Marshall, R.R., and Urey, H.C.
1957: Surface ionization of silver: silver in meteorites; Science, v. 126, p. 1291-1293.

Kaiser, T. and Wasserburg, G.J.
1983: The isotopic composition and concentration of Ag in iron meteorites and the origin of exotic silver; Geochimica et Cosmochimica Acta, v. 47, p. 43-58.

Loss, R.D., Rosman, K.J.R., and de Laeter, J.R.
1984: Transport of symmetric mass region fission products at the Oklo natural reactors; Earth and Planetary Science Letters, v. 68, p. 240-248.

Reedy, R.C.
1980: Silver isotopic anomalies in iron meteorites: cosmic ray productionand other possible sources; Geochimica et Cosmochimica Acta, Supplement 14, Meteorite and Regolith Studies, v. 2, p. 1169-1178.

Shields, W.R., Craig, D.N., and Dibeler, V.H.
1960: Absolute isotopic abundance ratio and the atomic weight of silver; Journal of the American Society, v. 82, p. 5033-5036.

Shields, W.R., Garner, E.L., and Dibeler, V.H.
1962: Absolute isotopic abundance of terrestrial silver; Journal of Research, National Bureau of Standards-A. Physics and Chemistry, v. 66A, no. 1, p. 1-3.

Wasserburg, G.J.
1985: Short-lived nuclei in the early solar system; in Protostars and Planets II, Space Science Series Volume II, University of Arizona Press, p. 703-737.

Effect of palladium as a matrix modifier in the determination of gold by graphite furnace atomic absorption spectrometry

G.E.M. Hall and J.E. Vaive
Mineral Resources Division

Hall, G.E.M. and Vaive, J.E., Effect of palladium as a matrix modifier in the determination of gold by graphite furnace atomic absorption spectrometry; in Current Research, Part F, Geological Survey of Canada, Paper 89-1F, p. 27-30, 1989.

Abstract

The benefits of adding palladium as a matrix modifier in the analysis of MIBK (4-methyl-2-pentanone) extracts for gold by graphite furnace atomic absorption spectrometry are described. Palladium is added as its iodo-complex in MIBK and successfully fulfils two functions. A much higher charring temperature (1150°C) can be employed without loss of Au and a two-fold enhancement in sensitivity is observed for MIBK phases which have been separated from acidic media containing nitric acid. Additionally, much improved linearity is obtained at the low concentration region of the calibration curve. This is particularly advantageous for the low-level detection of Au in samples of unashed vegetation. The mechanism of modification probably lies in the form of a thermally-stable Pd-Au intermetallic compound, Pd being in the reduced form in the presence of MIBK during the heating programme.

Résumé

On décrit les avantages de l'addition de palladium pour modifier une matrice dans le dosage de l'or dans des extraits de MIBK (4-méthyl–2-pentanone) par spectrométrie d'absorption atomique en four graphite. Du palladium est ajouté comme iodo-complexe dans le MIBK et remplit efficacement deux fonctions. Une température de carbonisation beaucoup plus élevée (1150°C) peut être employée sans perte d'Au, et la sensibilité est doublée par les phases du MIBK qui ont été séparées des milieux acides contenant de l'acide nitrique. En outre, la courbe d'étalonnage est beaucoup plus linéaire dans la région des faibles concentrations. Cela est particulièrement avantageux pour la détection des faibles concentrations d'or dans des échantillons de végétation sans cendre. Le mécanisme de modification est probablement lié à un composé intermétallique de Pd et Au thermiquement stable, le palladium étant la forme réduite en présence de MIBK pendant le programme de chauffage.

INTRODUCTION

Gold is often extracted from an acidic medium into MIBK (4-methyl-2-pentanone) prior to analysis by GFAAS (graphite furnace atomic absorption spectrometry) in order to eliminate interferences and to provide pre-concentration (Hall, 1979). Iron, which is also extracted, can cause significant background absorption at high concentrations and is removed by backwashing the organic phase with 0.1-0.5 M HCl. A method in common use to analyze rocks, soils and sediments for Au consists of an acid or cyanide attack (aqua regia, HBr-Br_2, alkaline CN^-), followed by extraction of Au into MIBK (or DIBK, diisobutylketone) and measurement by GFAAS (Brooks et al., 1981; Benedetti et al., 1987; Fletcher and Horsky, 1988; Terashima, 1988).

The technique used at the Geological Survey of Canada (GSC) laboratory to analyze geological materials for Au (Hall and Bonham-Carter, 1988) has involved the removal of HNO_3, used in the decomposition, by evaporation with HCl prior to extraction into MIBK. Traces of HNO_3, dissolved in MIBK, were found to suppress the absorption signal of Au; this has also been reported by Brajter and Slonawska (1987). In the course of developing a method to determine Au and Tl simultaneously in dried vegetation, it was evident that a trace amount of HNO_3 was being carried over into the organic phase from the leach solution and was creating an undesirable suppression of the Au signal. Evaporation with HCl to get rid of HNO_3 was not feasible due to the possible loss of other analytes such as Tl through volatilization of the chloride, and hence other means were sought to overcome the detrimental effect of HNO_3. The use of palladium and other metallic salts as a matrix modifier in GFAAS has been reviewed by Ni and Shan (1987). Recently, a mixture of palladium nitrate and magnesium nitrate has been proposed as a modifier of wide applicability (Welz et al., 1988). This would serve to allow the use of a sufficiently high pyrolysis or charring temperature to prevolatilize potential interferents and to delay analyte vaporization until conditions within the graphite furnace were nearly isothermal. We have successfully employed Pd in the determination of Tl, not only to allow a higher charring temperature in the thermal program but also to increase the sensitivity (Hall et al., 1987). Hence, we decided to test its effectiveness in the determination of Au. To our knowledge, this is the first reported application of Pd as a matrix modifier for Au in an organic medium.

EXPERIMENTAL

The instrumentation used for analysis was the Perkin-Elmer Model 5000 AA spectrometer equipped with the HGA-500 graphite furnace and AS-1 autosampler. The operating conditions are given in Table 1. The argon interrupt mode during atomization was used thoughout. Pyrolytically-coated graphite tubes were employed and absorbances were read as peak heights. All chemicals were reagent-grade; deionized distilled water was used thoughout.

As Au was in an organic medium for analysis, Pd was also extracted into MIBK as its iodo-complex (Diamantatos, 1981). A 10-mL volume of 6 M HCl, containing 60 mg of KI and 100 μL of a 5 % $PdCl_2$ solution, was shaken for 5 minutes with 6 mL of MIBK (saturated with 6 M HCl). The MIBK layer was separated and diluted with solvent to result in a final concentration of 150 μg mL^{-1} of Pd. A 5 μL aliquot of this modifier solution was added automatically following the 30 μL aliquot of analyte in MIBK. Effectively, the Pd is in excess of Au in the highest calibration standard (250 pg) by a factor of about 3000.

Table 1. Operating conditions used in the determination of Au by GFAAS.

Wavelength :		242.8 nm	
Slit width :		0.7 nm	
Lamp current :		14 mA	
Argon Flow rate:		300 mL min^{-1}	
Sample volume :		30 μL	
Modifier volume:		5 μL	
Stage	**Temperature/°C**	**Ramp time/s**	**Hold/s**
Dry	120	100	20
Char	300–1500	10	10
Atomize	2400	0	5

The decomposition procedure designed for dried vegetation (leaves, twigs, needles, etc.) is as follows. Ten mL of fuming HNO_3 are added to a sample of 0.5-1.0 g weight and the mixture is refluxed for several hours. Three mL of HF are added, the volume reduced to about 2 mL and 25 μL of Br_2 added. After warming to remove excess Br_2, 10 mL of HCl are added and allowed to stand for 10 minutes. This solution is again warmed, and about 5 mL of H_20 are added and transferred to a calibrated plastic test tube. The volume is made up to 30 mL with H_20 and allowed to stand (to expel gases such as nitrosyl chloride) prior to transfer to a separatory funnel. Extraction with 2.5 mL of pre-equilibrated MIBK is performed (5 minutes) followed by backwashing with 10 mL of 0.1 M HCl. The MIBK phase is then pipetted with the autosampler onto the graphite tube and analyzed against standards also in MIBK. Test solutions were made by spiking 10 mL aliquots of fuming HNO_3 with nanogram quantities of Au and carrying out the decomposition and extraction procedures. These were employed to investigate the effect of the Pd modifier while varying the charring temperature from 300°C to 1500°C. Calibration curves with and without added Pd were also compared using standards taken through the procedure for rocks where Au is extracted from a 4M HCl solution devoid of trace HNO_3.

RESULTS AND DISCUSSION

The beneficial effect of Pd on the absorbance signal of Au is shown in Figure 1, where variation in charring temperature is plotted against the peak absorbance for 180 pg of Au (30 μL of 6 μg L^{-1} Au in MIBK). It is evident that, in the absence of Pd, Au is beginning to be lost in the charring stage at 700-800°C, whereas, in the presence of Pd, this

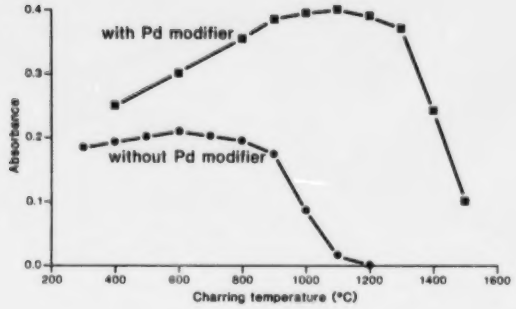

Figure 1. Effect of charring temperature on the absorbance of 180 pg Au in MIBK with and without Pd modifier.

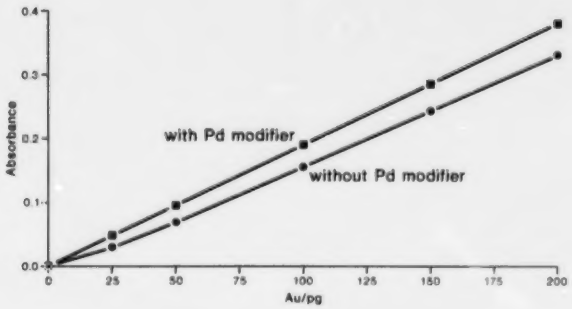

Figure 2. Calibration curves for Au extracted into MIBK from 4M HCl alone: without Pd modifier, charring temperature of 450°C; with Pd modifier, charring temperature of 1150°C.

does not occur until 1200-1300°C. Hence, it becomes possible to volatilize much more of the matrix prior to atomization of Au when Pd in MIBK is used as a modifier. Furthermore, the maximum absorbance signal for Au in the presence of Pd is about twice that in its absence. This doubling of the peak height becomes particularly advantageous in analyzing small sample weights of dried vegetation where a low detection limit is required. We have found that the trace amount of HNO_3 present in the MIBK allows the use of a 600-700°C charring temperature before Au is lost; 450°C is the maximum charring temperature permissible when Au has been extracted from 4M HCl solution alone. The sensitivity obtained when analyzing the MIBK solution containing trace amounts of HNO_3 in the presence of the Pd modifier is approximately equal to that obtained for the 4M HCl - extracted solutions with Pd. Only a slight enhancement is shown by the presence of Pd for MIBK solutions extracted from 4M HCl, as shown in Figure 2. An increase in absorbance of about 14 % is seen for the 200 pg Au standard solution when Pd is used and the charring tempearture is increased from 450°C to 1150°C. Furthermore, linearity is much improved as it is evident that the curvature toward the y-axis at low levels of Au is negated.

Voth-Beach and Shrader (1987) postulate that Pd must be in its reduced form on the graphite surface in order for it to act effectively in delaying the atomization of analytes; ascorbic acid has been used for this purpose. Styris and Prell (1988) have studied the stabilization characteristics of Pd on Se and As by the molecular beam sampling technique. They propose that formation of a palladium-analyte compound inhibits the early loss of analyte as oxides, hydroxides, and dimers. Work by Hinds et al., (1988) concerning the effectiveness of Pd modification (with and without Mg) in the analysis of soil slurries by GFAAS for Pb serves to reinforce the belief that delay of analyte vaporization is due to the formation of analyte-Pd bonding. The apparently beneficial effect of organic matter in the soil slurries supports previous evidence that Pd acts in its reduced form. In this study, the matrix of the organic solvent, MIBK, would serve to effect reduction of Pd during the heating program. Brajter and Slonawska (1987) have reported significant suppression by Pd on Au at ratios greater than 200:1 (Pd:Au) and recommended separation of analyte from the Pd matrix by ion exchange. In their study, palladium was not in a favourable medium for reduction in the acidic media under investigation.

In conclusion, it has been demonstrated that the benefit derived from matrix modification with Pd in MIBK in the determination of Au by GFAAS is two-fold. First, it delays vaporization of Au, thus allowing a charring temperature of about 1200°C to eliminate concomitants. Second, it produces an enhancement in the absorption signal of Au and negates the suppression effect created by trace amounts of HNO_3 present in the analyte matrix with improved linearity of response. Future studies will investigate the ability of Pd to reduce the interferences on Au in an aqueous medium due to a) Cu (reported by Hall et al., in press) and b) the major elements Na, K, Ca, and Mg (reported by Slavin, 1984).

REFERENCES

Benedetti, M.F., De Kersabiec, A.M., and Boulegue, J.
1987: Determination of gold in twenty geochemical reference samples by flameless atomic absorption spectrometry; Geostandards Newsletter, v. 11, p. 127-129.

Brajter, K. and Slonawska, K.
1987: Determination of gold in the presence of platinum and palladium by electrothermal atomisation atomic absorption spectrometry; Journal of Analytical Atomic Spectrometry, v. 2, p. 167-170.

Brooks, R.R., Holzbecher, J., Ryan, D.E., and Zhang, H.F.
1981: A rapid method for the determination of gold and silver in sulphide ores and rocks; Atomic Spectroscopy, v. 2, p. 151-154.

Diamantatos, A.
1981: A solvent-extraction scheme for the determination of platinum, palladium, rhodium, iridium and gold in platiniferous materials; Analytica Chimica Acta, v. 131, p. 53-62.

Fletcher, K. and Horsky, S.
1988: Determination of gold by cyanidation and graphite furnace atomic absorption spectroscopy; Journal of Geochemical Exploration, v. 30, p. 29-34.

Hall, G.E.M. and Bonham-Carter, G.F.
1988: Review of methods to determine gold, platinum and palladium in production-oriented laboratories, with application of a statistical procedure to test for bias; Journal of Geochemical Exploration, (v. 30, p. 255-286).

Hall, G.E.M., de Silva, K.N., Pelchat, J.C., and Vaive, J.E.
1987: Advances in analytical methods based on atomic absorption spectrometry in the Geochemistry Laboratories of the Geological Survey of Canada; in Current Research, Part A, Geological Survey of Canada, Paper 87-1A, p. 477-484.

Hall, G.E.M., Pelchat, J.C., and Dunn, C.E.
—: The determination of Au, Pd and Pt in ashed vegetation by ICP-mass spectrometry and graphite furnace atomic absorption spectrometry; Journal of Geochemical Exploration, (in press).

Hall, S.H.
1979: A rapid method for gold extraction using MIBK; Atomic Absorption Newletter, v. 18, p. 126-127.

Hinds, M.W., Katyal, M., and Jackson, K.W.
1988: Effectiveness of palladium plus magnesium as a matrix modifier for the determination of lead in solutions and soil slurries by electrothermal atomisation atomic absorption spectrometry; Journal of Analytical Atomic Spectrometry, v. 3, p. 83-87.

Ni, Z. and Shan, X.-Q.
1987: The reduction and elimination of matrix interferences in graphite furnace atomic absorption spectrometry; Spectrochimica Acta, v. 42B, p. 937-949.

Slavin, W.
1984: Graphite Furnace AAS: A Source Book, Perkin-Elmer Corporation, CT, U.S.A., p. 105.

Styris, D.L. and Prell, L.J.
1988: Investigation of palladium-induced stabilization in GFAAS; paper presented at the 35th Canadian Spectroscopy Conference, Ottawa, Ontario, Program with Abstracts, p. 22.

Terashima, S.
1988: Determination of gold in sixty geochemical reference samples by flameless atomic absorption spectrometry; Geostandards Newsletter, v. 12, p. 57-60.

Voth-Beach, L.M. and Shrader, D.E.
1987: Investigation of a reduced palladium chemical modifier for GFAAS; Journal of Analytical Atomic Spectrometry, v. 2, p. 45-50.

Welz, B., Schlemmer, G., and Mudakavi, J.R.
1988: Palladium nitrate-magnesium nitrate modifier for graphite furnace atomic absorption spectrometry. Part 2. Determination of arsenic, cadmium, copper, manganese, lead, antimony, selenium, and thallium in water; Journal of Analytical Atomic Spectrometry, v. 3, p. 695-701.

Canadian earthquakes, January 1987 to September 1988

Janet A. Drysdale, Maurice Lamontagne, and Robert B. Horner[1]
Geophysics Division

Drysdale, J.A., Lamontagne, M., and Horner, R.B., Canadian earthquakes, January 1987 to September 1989; in Current Research, Part F, Geological Survey of Canada, Paper 89-1F, p. 31-36, 1989.

Abstract

During 1987, approximately 1500 earthquakes were located in Canada and an additional 375 provisional epicentre locations were processed for 1988. Four hundred and forty-five earthquakes were greater than magnitude 3.0 and 18 were magnitude 5.0 or greater. Forty-seven earthquakes were reported felt in Canada.

The pattern of earthquake activity continued to be similar to that observed in previous years and to be concentrated in distinct areas. Of significance in northern Canada was a magnitude 5.4 earthquake that occurred on December 13, 1987 south of Resolute Bay in Barrow Strait. It was felt in Resolute Bay, in Polaris, and in Arctic Bay. The Nahanni, N.W.T. region experienced a third major earthquake since the first earthquake in October 1985, with a magnitude 6.0 event on March 25, 1988. An unprecedented sequence of earthquakes in the Gulf of Alaska started November 17, 1987 with a magnitude 6.9 earthquake, followed by a magnitude 7.6 earthquake on November 30, 1987 and numerous aftershocks. The larger events were felt throughout the southern Yukon and northern British Columbia. A magnitude 4.9 earthquake, centred in Illinois, on June 10, 1987, was felt widely in the United States and southwestern Ontario.

Résumé

En 1987, environ 1500 tremblements de terre furent localisés au Canada auxquels s'ajoutent 375 localisations provisoires pour 1988. Quatre cent quarante-cinq tremblements de terre étaient de magnitude supérieure à 3.0 et 18 de magnitude supérieure ou égale à 5.0. Quarante-sept furent rapportés ressentis au Canada.

La distribution de l'activité fut similaire à celle observée dans les années passées et fut concentrée dans des régions distinctes. Important, dans le Nord canadien, fut le séisme de magnitude 5.4 localisé au sud de Resolute Bay dans le détroit de Barrow. Il fut ressenti à Resolute Bay, Polaris et Arctic Bay. La région de la Nahanni dans les T.N.-O. a connu un troisième séisme majeur depuis le premier d'octobre 1985, lorsqu'un événement de magnitude 6.0 s'est produit le 25 mars 1988. Une série de séismes sans précédent a commencé dans le golfe d'Alaska le 17 novembre 1987 avec un séisme de magnitude 6.9, suivi, le 30 novembre 1987, par un séisme de magnitude 7.6 et par de nombreuses répliques. Les événements les plus forts furent largement ressentis dans le sud du Yukon et le nord de la C.-B.. Le 10 juin 1987, un séisme de magnitude 4.9, localisé en Illinois, fut largement ressenti aux États-Unis et dans le sud-ouest ontarien.

[1] Cordilleran and Pacific Geoscience Division, Sidney, B.C.

INTRODUCTION

This is the first report on Canadian seismicity to appear in Current Research. In this report the earthquake activity across the country during 1987 and the first 9 months of 1988 is summarized. The data are complete to the end of 1987 and preliminary epicentres in southern Canada have been processed for 1988. The activity in eastern Canada and the Arctic is described in more detail since earthquakes in western Canada, including the western Arctic are described more fully by Horner and Kolinsky (1989).

The Geological Survey of Canada operates the Canadian National Seismograph Network, which includes standard, regional, and telemetered stations (Fig. 1, 2, and 3). Approximately 97 stations, a six-station array near Charlevoix,Quebec, and a three-station array in the Sudbury Basin were operating in Canada during the report period (Munro et al., in press). The magnitude threshold of located earthquakes, a function of station spacing and distribution, is approximately 3.0 in Arctic Canada and 2.5 for southern Canada. Smaller earthquakes are located within the Vancouver Island-British Columbia lower mainland and the two special array areas.

Earthquakes in western Canada, including the Yukon and western Arctic, are analyzed by the Cordilleran and Pacific Geoscience Division (PGC) in Sidney, British Columbia. Eastern Canadian, and eastern Arctic earthquakes are analyzed by the Geophysics Division in Ottawa. The Geophysics Division compiles all the information collected, including that analyzed at PGC, into a national earthquake data base and produces and distributes various routine reports to interested agencies and people. The final descriptive publication is the biannual Canadian Earthquake Catalogue, which was an annual publication prior to 1985. A list of previous catalogues is included in the appendix of Canadian Earthquakes - 1984 (Drysdale and Horner, 1987). Within the context of global seismicity, the Canadian data, for events larger than magnitude 3.0, are supplied regularly to the International Seismological Centre in the United Kingdom for inclusion in its worldwide earthquake data base. Selected station data are routinely sent to the National Earthquake Information Center in Boulder, Colorado.

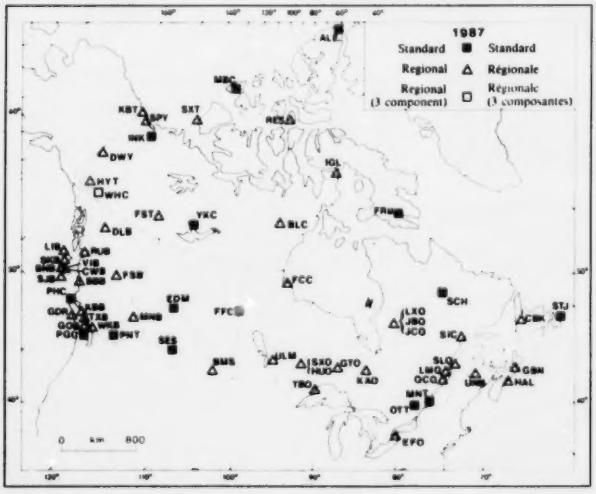

Figure 1. Canadian standard and regional seismograph stations operated during 1987. Station codes are indicated.

CANADIAN SEISMICITY JANUARY 1987-SEPTEMBER 1988

A total of 445 magnitude 3.0 or greater earthquakes were located in Canada or its environs during the period January 1987 to September 1988 (Fig. 4). One hundred and seven earthquakes were magnitude 4.0 or greater and 18 were over magnitude 5.0. The largest earthquake, magnitude 7.6, occurred on November 30, 1987 as part of the

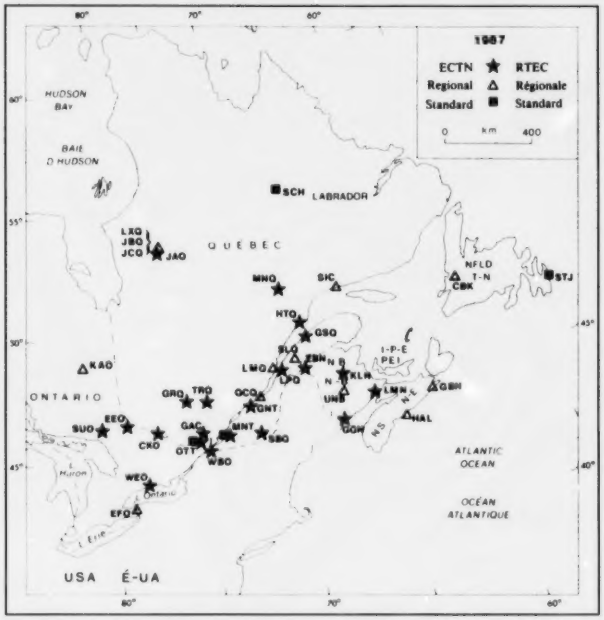

Figure 2. Eastern Canada Telemetered Network (ECTN) and other stations in eastern Canada operating during 1987. Station codes are indicated.

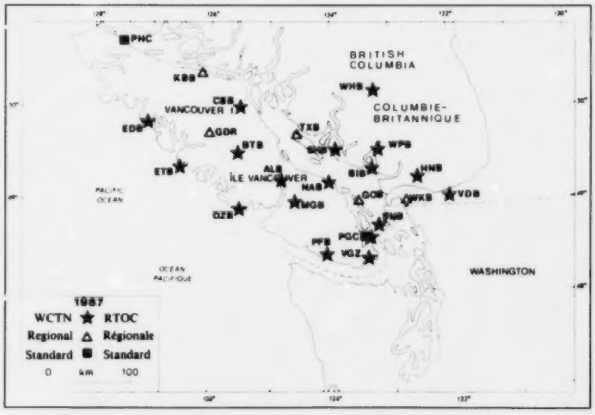

Figure 3. Western Canada Telemetered Network (WCTN) and other stations in southwestern British Columbia operating during 1987. Station codes are indicated.

unprecedented Gulf of Alaska swarm, which started November 17, 1987 with a magnitude 6.9 earthquake. In Canada the largest earthquake, magnitude 6.0, occurred on March 25, 1988, and was located in the Nahanni, N.W.T., aftershock zone. The Nahanni area has been continually active since the magnitude 6.6 October 5, 1985 and magnitude 6.9 December 23, 1985 Nahanni main shock earthquakes took place. Other notable earthquakes, magnitude 5.5 and 5.4, occurred in the Beaufort Sea on March 30, 1987, and in Barrow Strait south of Resolute on December 13, 1987, respectively.

Forty-seven earthquakes were reported felt in Canada during this report period. In western Canada, including the Yukon, 29 earthquakes were felt and 27 were felt in eastern Canada and the eastern Arctic. The large Gulf of Alaska event was felt maximum intensity V as far as Whitehorse, Yukon Territory. Six other earthquakes were felt in the Yukon during a 15 day period from November 14-30, 1987. This created many inquiries from the media and general public. The Nahanni earthquake, on March 25, 1988, was felt in a wide area including the Northwest Territories, Yukon Territory, northern British Columbia, and northern Alberta. The magnitude 5.4 earthquake that occurred on December 13, 1987 south of Resolute Bay, Northwest Territories was felt in Resolute Bay on Cornwallis Island, in Polaris on Little Cornwallis Island, and in Arctic Bay on Baffin Island. A magnitude 4.9 earthquake, on June 10, 1987, centred near Lawrenceville, Illinois was felt widely in the United States and in southern Ontario as far north as Owen Sound and east to Toronto.

EASTERN CANADA

Four hundred and forty-one earthquakes (all magnitudes) and 155 rockbursts were located in eastern Canada. The rockbursts and mine-related seismic events are discussed by Wetmiller et al. (1989). Forty-nine earthquakes were magnitude 3.0 or greater, only three of which were over magnitude 4.0. Twenty-seven earthquakes were felt, nine of which were less than magnitude 3.0.

Figure 5 shows that much of the activity is restricted primarily to several distinct seismic zones. However, several notable earthquakes were recorded during the 1987 period. The largest earthquake affecting eastern Canada was the magnitude 4.9 Illinois earthquake mentioned previously, which was felt throughout southwestern Ontario. It is south of the area plotted on Figure 5. Another notable Ontario event, although only magnitude 3.4, took place on July 23, 1987 at the western end of Lake Ontario. The tremor was felt in Toronto, Burlington, Stoney Creek, Guelph, St. Catharines, and Mississauga, Ontario. The last earthquake recorded from the same area occurred on January 12, 1986 and was magnitude 2.8.

In northwestern Ontario, four magnitude 2.9 to 3.6 earthquakes were detected west of James Bay in an area where previously there had been little seismic activity. Ten earthquakes were located north of Lake Superior, west of 80 degrees west longitude (see Fig. 5). These were thoroughly investigated and could not be attributed to any blasting or mining-related activities. They may indicate an extension of the historically active Western Quebec zone.

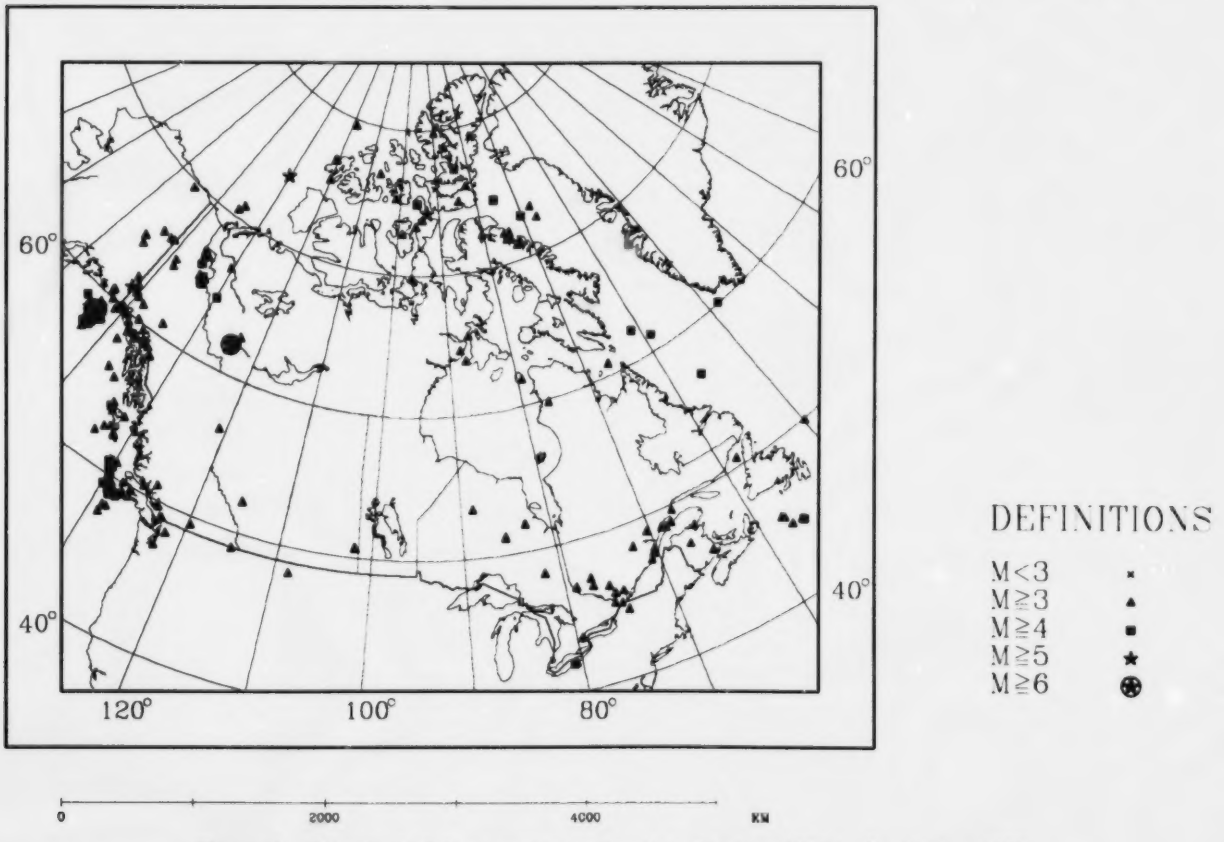

Figure 4. Magnitude 3.0 or greater earthquakes January 1987 to September 1988.

It should be noted that regional coverage for northern Ontario has improved in large measure due to the additional monitoring facilities provided by the Nuclear Fuel Waste Management Program, which started in 1982. Similarly, the three-station telemetered array in Sudbury, completed in 1987 as part of the Canada-Ontario-Industry Rockburst Project, has increased the detection capabilities, particularly with respect to mining-induced seismicity, in the Sudbury Basin.

A magnitude 3.7 earthquake occurred on October 23, 1987 near Kilmar, Quebec. It was felt to distances of about 50 km. In the Maritimes, two earthquakes were located in areas of previous low level and sporadic activity. The first, magnitude 3.8, occurred on January 28, 1988 in the Bay of Chaleur, between Quebec and New Brunswick, and the other, magnitude 3.6, occurred on April 24, 1988 near Moncton, New Brunswick. Both were felt locally and resulted in many inquiries from the public. On December 11, 1987 a magnitude 3.4 earthquake was the first event ever located in the Strait of Belle Isle between Newfoundland and eastern Quebec. Located offshore were six earthquakes on the Laurentian Slope, ranging in magnitude from 3.0 to 4.2.

The remaining seismic events occurred primarily in the recognized seismic areas of Western Quebec, Charlevoix, Quebec, Lower St. Lawrence, and Miramichi, New Brunswick.

ARCTIC CANADA

A total of 285 earthquakes in the Arctic (north of 60 degrees north latitude) have been located, again mainly in previously recognized active zones (Fig. 6). One hundred and thirty-two events were magnitude 3.0 or larger and five were greater than magnitude 5.0. Because of the wider station distribution, relatively few earthquakes less than magnitude 3.0 are routinely located.

The most significant northern event occurred on December 13, 1987 south of Resolute Bay in Barrow Strait near the northern end of Somerset Island. This earthquake was magnitude 5.4 and it was felt, as described earlier, in Resolute Bay on Cornwallis Island, in Polaris on Little Cornwallis Island, and in Arctic Bay on Baffin Island. There were many aftershocks in the following two months.

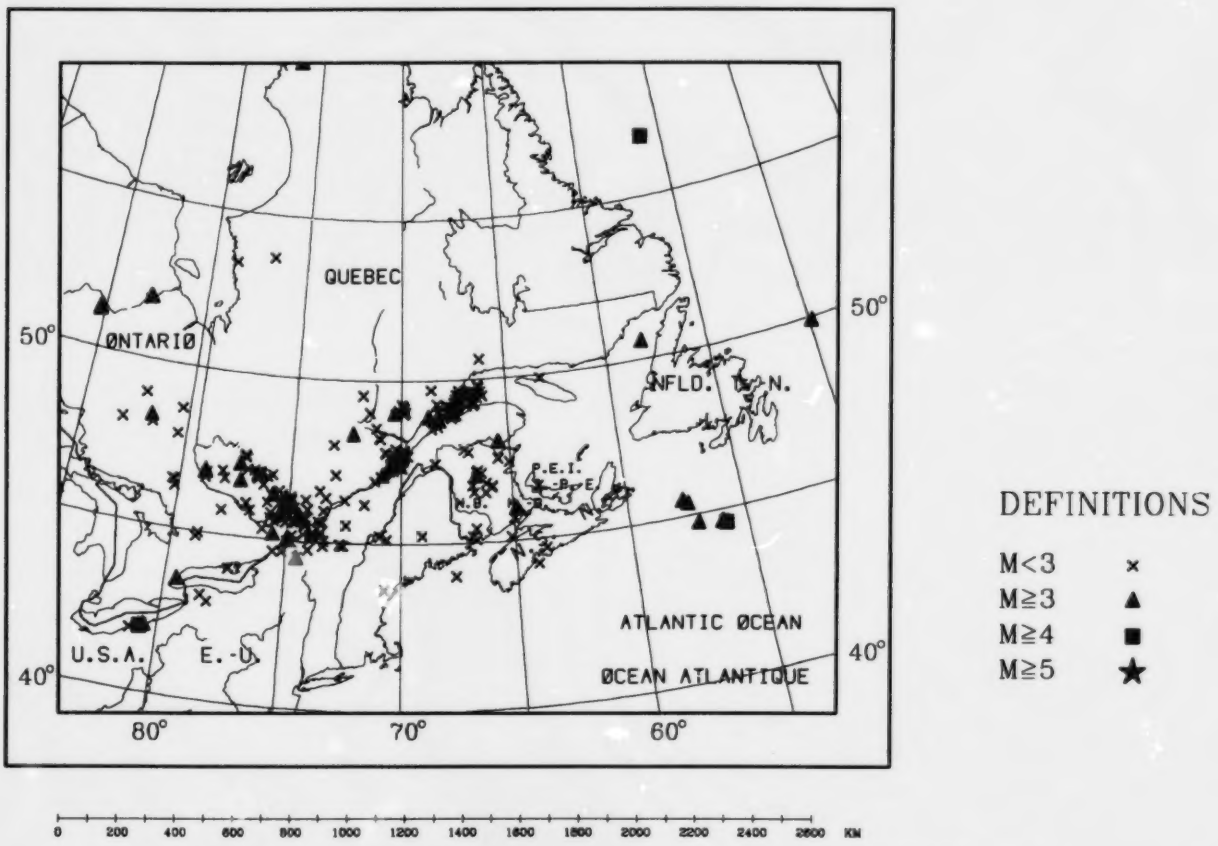

Figure 5. Earthquake epicentres in eastern Canada and adjacent regions of the United States, January 1987 to September 1988.

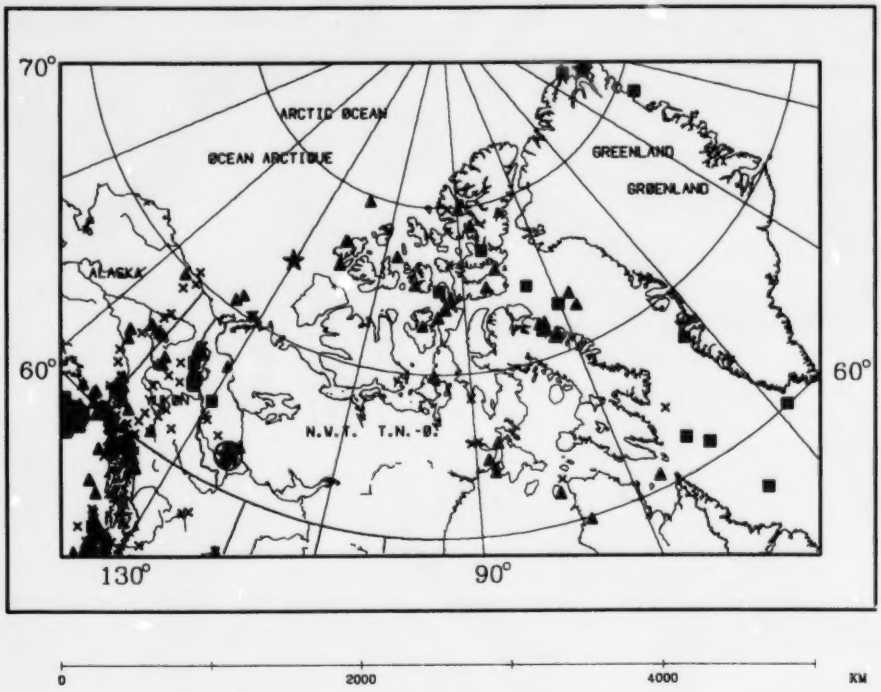

DEFINITIONS

M<3 ×
M≧3 ▲
M≧4 ■
M≧5 ★
M≧6 ⍟

Figure 6. Earthquake epicentres in Arctic Canada and adjacent regions, January 1987 to September 1988.

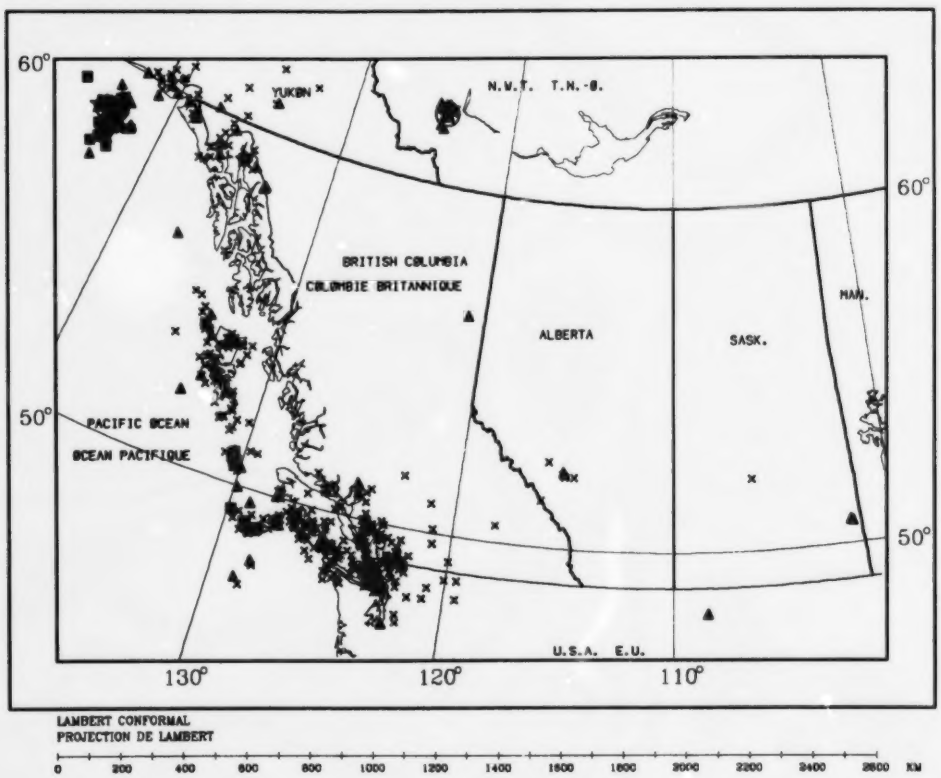

DEFINITIONS

M<3 ×
M≧3 ▲
M≧4 ■
M≧5 ★
M≧6 ⍟

Figure 7. Earthquake epicentres in western Canada and adjacent regions of the United States January 1987 to September 1988.

A magnitude 5.5 earthquake was located in the Beaufort Sea, but, because of the remoteness of the area, it was not felt. Three earthquakes were located on the northern coast of Greenland in an area of recurring activity. The largest, magnitude 5.5, occurred on July 11, 1987. A magnitude 4.6 earthquake (December 14, 1987), situated offshore in the Labrador Sea, was well recorded by the network, but was not felt onshore. Also of interest is the continuation of the aftershock sequence of the magnitude 6.6 October 5, 1985 and magnitude 6.9 December 23, 1985 Nahanni earthquakes in the Northwest Territories. The largest aftershock during 1987 occurred on January 10 and was magnitude 4.1; although a magnitude 6.0 earthquake on March 25, 1988 occured and was accompanied by another sequence of aftershocks. This sequence is described by Lamontagne et al. (1989).

There continued to be significant activity in the active St. Elias region of the southwest Yukon, the Richardson Mountains in the Northwest Territories, northern Baffin Island and northern Baffin Bay, and Wager Bay, Northwest Territories.

WESTERN CANADA

A detailed account of western seismicity including the Yukon and western Arctic for 1987-1988 is reported by Horner and Kolinsky (1989). South of 60 degrees north latitude, 965 earthquakes were located during 1987 and an additional 200 events have preliminary epicentres for 1988 (note: if the whole of western Canada including the Arctic is taken into account over 1200 earthquakes were located). There were a total of 258 earthquakes greater than magnitude 3.0 and 13 were magnitude 5.0 or greater.

The earthquakes were primarily concentrated along the Pacific margin and in particular the Queen Charlotte Islands, Vancouver Island, offshore of Vancouver Island, Puget Sound, and the southwestern British Columbia mainland (Fig. 7). There continued to be earthquakes near Rocky Mountain House, Alberta, which was probably related to the oil and gas works in the area and near the IMC potash mine in eastern Saskatchwan. One of the most widely felt earthquakes, magnitude 3.9, occurred April 8, 1987 near Salmon Inlet in the southern coast mountains. A magnitude 5.1 earthquake occurred west of Vancouver Island on May 26, 1988 and was felt only at Port McNeil.

SUMMARY

Approximately 1500 additional earthquakes have been added to the Canadian earthquake data base for 1987 and an additional 375 provisional locations for 1988. A large portion of the seismic activity has tended to be confined to distinct areas of continuous activity. These zones occur in a wide variety of geological terrains, revealing the potential for large damaging earthquakes in many different areas of Canada and demonstrating the need for continuing research into seismic hazards.

ACKNOWLEDGMENTS

Our colleagues F.M. Anglin, J.E. Adams, M.G. Cajka, R. Kolinsky, M. Plouffe, and R.J. Wetmiller all contribute to the analysis of the Canadian earthquakes. Valuable comments by J.E. Adams, M.G. Cajka, R.J. Wetmiller, and R. North on an earlier version of the manuscript are much appreciated.

REFERENCES

Drysdale, J.A. and Horner, R.B.
1987: Canadian Earthquakes - 1984; Geological Survey of Canada, Paper 87-19, Seismological Series Number 95, 44 p.

Horner, R.B., and Kolinsky, R.
1989: Earthquakes in western Canada in 1987, with preliminary results for 1988; Current Research, Part E, Geological Survey of Canada, Paper 89-1E.

Lamontagne, M., Horner R., Wetmiller, R.J., Monsees, D., and Vonk, A.
1989: Le séisme de mars 1988 de la rivière North Nahanni, T.N.-O., et ses répliques; Recherches en cours. Part E, Commission géologique du Canada, Étude 89-1E.

Munro, P.S., Halliday, R.J., Shannon, W.E., and Schieman, D.R.J.
1988: Canadian seismograph operations - 1987; Geological Survey of Canada, Paper 88-25, Seismological Series Number 99 (in press).

Wetmiller, R.J., Plouffe, M., Cajka, M.G., and Hasegawa, H.S.
1989: Investigation of natural and mining-related seismic activity in northern Ontario; Current Research, Part C, Geological Survey of Canada, Paper 89-1C.

Turbidites off the Oregon-Washington margin record paleo-earthquakes on the Cascadia subduction zone

John Adams
Geophysics Division

Adams, J., Turbidites off the Oregon-Washington margin record paleo-earthquakes on the Cascadia subduction zone; in Current Research, Part F, Geological Survey of Canada, Paper 89-1F, p. 37-43, 1989.

Abstract

Cores from the Cascadia deep-sea channel contain turbidites that can be correlated and dated by the first occurrence of volcanic glass from the Mount Mazama eruption. Turbidity currents in the tributaries occurred synchronously, and formed 13 turbidite deposits in the lower main channel since the Mazama eruption. In addition to the Cascadia Channel, 13 post-Mazama turbidites were deposited at three other places, representing 580 km of the Oregon-Washington margin. Pelagic intervals deposited between the turbidites suggest that in each place the turbidity currents occurred every 590 ± 170 a. The turbidity currents were triggered by 13 great Cascadia subduction zone earthquakes. The variability of turbidite timing is similar to that for great earthquake cycles. The thickness of the topmost pelagic layer suggests the last event was 300 ± 60 a ago, but this number may be a biased underestimate. It is, however, consistent with the youngest subsidence event found on the Washington coast. The turbidite data demonstrate that the near-term risk of a great earthquake on the Cascadia subduction zone is appreciable, and rising.

Résumé

Des carottes du chenal marin Cascadia contiennent des turbidites qui peuvent être corrélées et datées par la première manifestation de verre volcanique provenant de l'éruption du mont Mazama. Les courants de turbidité dans les tributaires étaient contemporains et ont formé 13 gisements de turbidites dans le cours inférieur du chenal principal après l'éruption de Mazama. En plus du chenal Cascadia, trois autres zones couvrant 580 km de la marge des états d'Orégon et Washington se sont révélées contenir 13 turbidites post-Mazama. Des intervalles pélagiques mis en place entre les turbidites semblent indiquer que des courants de turbidité se sont produits dans chaque zone à tous les 590 + 170 ans. Les courants de turbidité ont probablement été déclenchés par 13 grands séismes de la zone de subduction de Cascadia. La chronologie variable des turbidites est semblable à celle des grands cycles sismiques. L'épaisseur de la couche pélagique supérieure indique que l'événement le plus récent remonte à 300 + 60 ans, mais ce chiffre pourrait être une sous-estimation erronée. Il concorde toutefois avec l'événement de subsidence le plus récent observé sur la côte du Washington. Les données sur les turbidites montrent que les risques à court terme d'un séisme majeur dans la zone de subduction de Cascadia est assez considérable et croissant.

THE EARTHQUAKE PROBLEM IN THE PACIFIC NORTHWEST

About a dozen years ago (e.g. Riddihough and Hyndman, 1976), perceptions of the nature of the subduction zone beneath southern British Columbia, Washington, and Oregon began to change. Earlier work had established that the Juan de Fuca plate was converging toward North America. However the lack of seismicity on the plate interface lead some to consider that the subduction was occurring extremely slowly or had stopped.

More recent studies of the deformation front at the base of the slope (e.g. Barnard, 1978), of geodetic deformation rates on land (Ando and Balazs, 1979; Reilinger and Adams, 1982), and of onshore tectonic deformation such as warped terraces (Adams, 1984) have confirmed that the Oregon-Washington margin is being deformed at rates as rapid as those at other subduction zones. Heaton and Kanamori (1984) and Rogers (1988) address similarities between the Cascadia subduction zone and other zones worldwide and conclude that the subduction zone could generate earthquakes of magnitude 8.3+.

Earthquakes have been known to cause submarine turbidity currents since the classic work on the earthquake-generated 1929 "Grand Banks" turbidity current off Canada's eastern margin (Heezen and Ewing, 1952). Because very frequent turbidity currents — every few years off deltas such as the Magdalena and Congo — suggested that many turbidity currents were caused by sediment instability due to rapid sedimentation, the role of infrequent earthquakes was less easy to assess. The present paper shows that the turbidite record off Oregon provides strong evidence for earthquakes about every 600 a. Such conclusions are important for the current debate (Heaton and Hartzell, 1987) on the level of seismic hazard in the Pacific Northwest.

CORRELATION AND DATING OF THE TURBIDITES BY THE MAZAMA TEPHRA

At the present time, sediment from the Columbia River is carried north along the shelf and is deposited on the shelf and the edge of the slope (Fig. 1). The sediment accumulates on the slope until submarine failure occurs and it then sweeps down the channels as a density flow or turbidity current (Fig. 2). Griggs and Kulm (1970) show that each major turbidity current takes about two days to travel the 735 km length of the Cascadia Channel and carries about 525 $x10^6$ m^3 of sediment in a flow up to 17 km wide and 100 m high. The predominantly muddy sedimentation in the channel and the similarity of all the cores suggest that they represent a complete record of turbidity currents in the Holocene.

Because large turbidity currents travel down the length of the Cascadia Channel, turbidites along the length of the channel should correlate. A unique event in the last 10 000 a was the eruption of Mount Mazama at 6845 ± 50 radiocarbon aBP (Bacon, 1983). Though little if any of the airfall tephra fell as far west as the coastal ranges (Fig. 1), much fell in the catchment of the Columbia River and was washed into the sea and deposited on the shelf. When the shelf-edge deposit slumped, the turbidity current carried the tephra-rich sediment down into channels.

The tephra allows the first turbidite with abundant glass to be traced down the Cascadia Channel and allows calculation of the mean period between turbidity currents. The position of the Mazama in the three cores from the middle and lower Cascadia Channel supports Griggs' (1969) assertion that not only must the lowest turbidite containing Mazama correlate, but so must each of the 12 overlying turbidites (i.e. the 13 turbidites in the cores represent the same 13 turbidity currents), and is further supported by the similar pattern of bioturbation in the top eight layers (Griggs et al., 1969). Griggs and Kulm (1970) computed return periods of 410-510 a for turbidity currents in the Cascadia Channel.

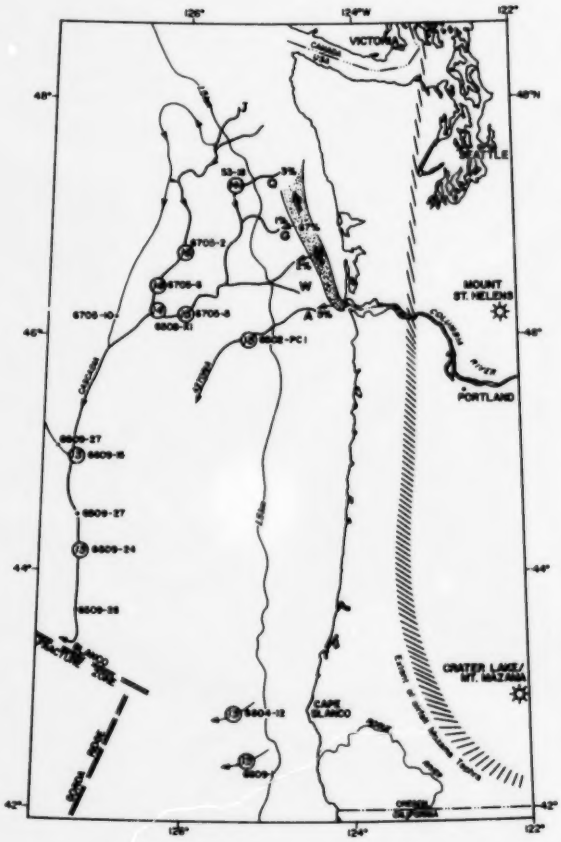

Figure 1. Map of the Oregon-Washington margin showing the extent of the airfall Mazama tephra (Fryxell, 1965), the pattern of sediment dispersal north from the Columbia River (with amounts of sediment as percentage of the river input after Sternberg, 1986), canyons on the Washington continental slope (J: Juan de Fuca, Q: Quinault, G: Grays, W: Willapa, and A: Astoria), submarine channels leading to the deep-sea floor, the location of cores mentioned (all from Oregon State University except core 53-18 which is University of Washington), and (within large circles) the number of post-Mazama turbidites as discussed in the text.

SYNCHRONOUS TURBIDITY CURRENTS FROM INDIVIDUAL TRIBUTARIES

Core 6508-K1 (see Fig. 1) lies in the Cascadia Channel downstream of the confluence of two main tributaries, the northern from the Juan de Fuca and nearby canyons and the southern from the Willapa, Grays, and Quinault canyons. In the northern tributary, core 6705-6 has 14 turbidites since the Mazama, the same as below the confluence. Farther upstream from core 6705-6, core 6705-2 contains 16 post-Mazama turbidites (according to Griggs and Kulm, 1970), and by inference two small turbidity currents did not flow down the channel as far as core 6705-6. In the Quinault Canyon, core 53-18 contains "at least 14" post-Mazama turbidites (Barnard, 1978, p. 111). Further downstream in the main Willapa Canyon, core 6705-5 has 15 turbidites since the Mazama; one explanation being that one small turbidity current did not flow downstream to the confluence and core 6508-K1.

The cores in the tributaries suggest that a few (2 or 3 out of a maximum of 16) small turbidity currents may have been generated that were smaller than the 13 turbidity currents in the lower channel and that did not travel as far. With this in mind, the remarkable inference can be made that pairs of turbidity currents were generated synchronously in the two tributaries. This arises because there have been 15 post-Mazama turbidites in the Willapa Channel and 14 turbidites in the northern channel, but only 14 turbidites below their confluence (where 29 might be expected if the flows had occurred independently). Therefore, turbidity currents were generated synchronously in two independent channels, and each pair of small currents merged to form one large turbidity current. That the number in the main channel is only 13 implies that **every** turbidity current in the two tributaries occurred synchronously, that is, synchronous occurrence is the rule rather than the exception.

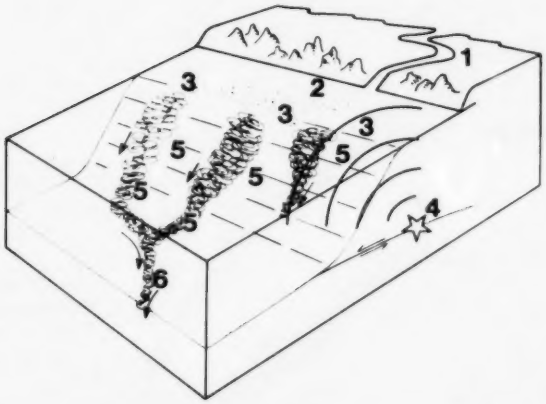

Figure 2. Perspective view showing schematically the genesis of turbidity currents in the Cascadia Channel. 1: sediment is carried down the Columbia River at about 21 million tonnes per year. 2: The sediment drifts north along the shelf. 3: Sediment accumulates at the top of the slope in the heads of deep-sea canyons. 4: A great thrust earthquake under the margin every 590 a causes strong shaking of the shelf and slope. 5: The shaking causes sediment liquefaction and slumping simultaneously at many places along the margin. The resultant massive under-sea debris flows mix with the water to become a series of turbidity currents travelling synchronously down the channels. 6: At junctions, the tributary turbidity currents coalesce to travel down the Cascadia Channel as one large turbidity current.

SPATIAL EXTENT OF THE 13 TURBIDITY CURRENTS SINCE THE MAZAMA ERUPTION, AND THEIR REGULAR OCCURRENCE

Figure 1 shows three other cores that lie outside the Cascadia Channel system but contain the Mazama turbidite, one from Astoria Canyon, and two from off Cape Blanco. The Astoria Canyon was a major conduit for sediment up until 7000 a ago. While the lower Astoria Fan has been almost inactive since about the time of the Mazama (Nelson, 1976), core 6502-PC1 shows that 13 thin (average thickness 130 mm) post-Mazama turbidity currents occurred in the upper channel. Apparently these small turbidity currents did not travel all the way down the Astoria Channel.

Both the core directly off Cape Blanco (6604-12) and the one off the Rogue River (6609-1) are remote from the Columbia River mouth, and heavy mineral analysis shows that at least since the Mazama eruption their sediment has come from the Klamath Mountains, inland and south of Cape Blanco (Duncan, 1968). Despite their remoteness from the Cascadia and Astoria Channel systems, each contains 13 post-Mazama turbidites.

It is at least 50 km from the Juan de Fuca to the Quinault Canyon, 100 km across the Quinault-Willapa canyon system, 30 km more to the Astoria Canyon, and then 350 km farther to Cape Blanco, then 50 km to the Rogue. From all five sites along the margin there have been 13 turbidity currents since the Mazama. The simplest explanation for the synchronous events in neighbouring tributaries, and the same numbers of events at sites 580 km apart, is a series of great earthquakes.

As noted by Griggs (1969) and Griggs and Kulm (1970), the turbidites in the Cascadia system have generally similar thicknesses and are separated by pelagic intervals also of generally constant thickness. The scatter of pelagic thicknesses for several cores can be seen conveniently by plotting cumulative pelagic thickness against turbidite sequence number (Fig. 3). The cumulative curves are remarkably linear, confirming that the 13 events affecting the margin were fairly regular in time.

MEAN INTERVAL BETWEEN THE EVENTS AND VARIABILITY OF THE MEAN

The Mazama eruption is well-dated by multiple Carbon-14 dates at 6845 $\pm$ 50 radiocarbon yrBP (Bacon, 1983), and provides a reliable date to compute the mean return period. The radiocarbon age is equivalent to 7420^{+159}_{-51} calibrated years before 1950 (at the 2σ confidence level using version 2.0 of the computer program of Stuiver and Reimer, 1986). The difference between the upper and lower errors is small

relative to the stochastic error discussed below, so adjusting for the 38 a since the 1950 reference date gives 7660 ± 100 calibrated years before 1988. The Mazama tephra was probably carried rapidly to the shelf-edge and was available for slumping almost immediately after eruption. When did the next turbidity current occur? For 13 turbidity currents the mean return period is about 600 a, so the next one would probably have been 300 ± 300 a later. Therefore, 7360 ± 400 a before 1988 is adopted as the age of the 13th turbidite.

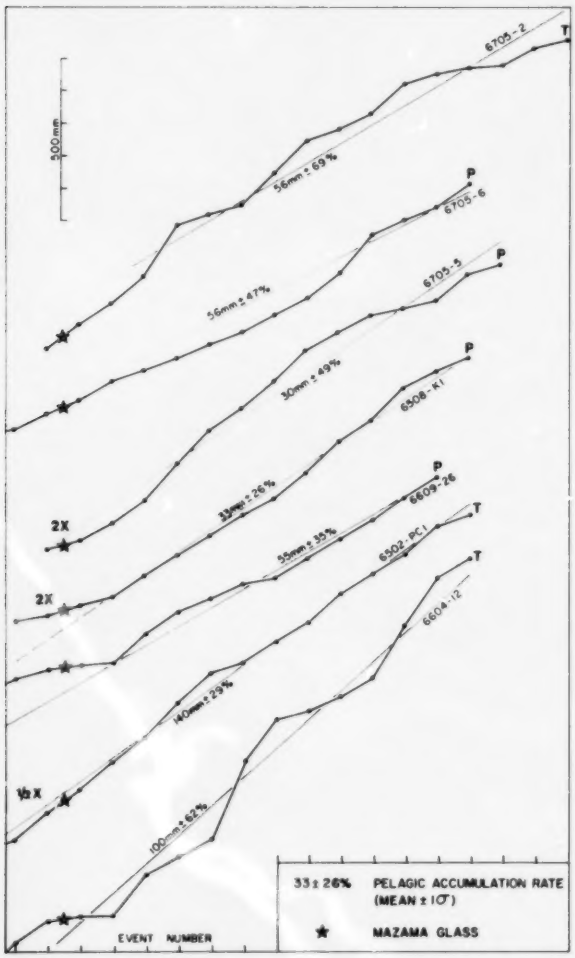

Figure 3. Cumulative pelagic sediment deposition versus turbidite number for seven cores from the Oregon-Washington margin. The plots are lined up on the turbidite containing the first Mazama glass. If the pelagic sediment has accumulated steadily, and if the turbidity currents occurred regularly, the plots for each core would be a straight line. The data (dots joined by heavy lines) show a good approximation to the expected relationship (light lines). Note that the vertical scale has been adjusted for three of the cores. The slope of the fitted line represents the mean pelagic sediment accumulation rate (millimetres per turbidity current), and the deviations of the data about the line gives information on the variability of turbidity current timing, here expressed as a percentage of the mean pelagic accumulation per event.

Since the 13th turbidite there have been 12 turbidites, 12 inter-turbidite intervals, and a period of time since the last turbidite. *A priori*, the length of the last period is not known so is taken as ½ ± ½ interval for a total of 12.5 ± 0.5 intervals. The mean time between turbidites is then 7360 ± 400 a / 12.5 ± 0.5 intervals or 590 ± 50 a. Not used in this analysis is the information that if the last turbidity current was earthquake-triggered, it must have occured more than 150 a ago, for there has been no great earthquake on the Cascadia subduction zone in historical times.

An independent check comes from core 6509-27 from which plant material in the eighth turbidite from the surface was dated at 4646 ± 190 radiocarbon aBP (Griggs et al., 1969), or about 5400 calibrated years before 1988, giving an interval of about 680 ± 100 a and by extrapolation beyond the base of the core, about 12 ± 1 turbidites since the Mazama, in good agreement with sedimentological correlations made on the basis of the degree of bioturbation, and the presence of 13 post-Mazama turbidites in the channel above and below the core.

The above error on the mean return period does not measure the variability of turbidity current timing, which can be estimated by examining the thickness variations of the pelagic intervals. The numbers against the plot for each core on Figure 3 represent the best-estimate mean pelagic accumulation per event and the standard deviation expressed as a percentage of the mean. Both accumulation rates and their variability are generally largest near shore, while the deeper cores are the most regular, ±26% for 6508-K1 (±20% if the extra, "14th" turbidite is the one following the Mazama turbidite) and ±36% for 6509-15 (not shown on Fig. 3). For a 590-a return period, this translates to a variability of about 170 a, and an implied standard error on the mean of 50 a.

DO THE TURBIDITES REPRESENT GREAT EARTHQUAKES, OR NOT?

Griggs and Kulm (1970) noted that if sediment were supplied by the Columbia River at a constant rate, it would accumulate in the canyon heads until there was enough to trigger collapse, whereupon the cycle would start again. Such a self-triggering system would tend to repeat itself, and would generate similar-sized turbidites in the channel system.

Of course, triggering by external events of a cyclic nature (such as great earthquakes) would also tend to displace similar masses of sediment and produce similar-sized turbidites. Perhaps the strongest argument against the self-triggering hypothesis is that similar numbers of events are found all along the margin; it would be highly improbable that every canyon had the same temporal response to the spatially-varying rates of sedimentation that occur along the margin. It is simpler to conclude that, while self-triggering might occur in the absence of an external trigger, the triggers occur more frequently than the time needed to reach the critical mass in every canyon, and so always short-circuit the endogenic slumping process.

For a similar reason, events local to one canyon head (e.g. a magnitude 6.5 earthquake within 50 km) do not provide a sufficient explanation for the data. Therefore the cause must be exogenic to the canyon heads and affect the Oregon-Washington margin as a whole. Three such external triggers with the required spatial extent are: tsunamis, wave-induced slumping during large storms, and great earthquakes on the Cascadia subduction zone.

The case for wave- or tsunami-induced slumping on such a large scale is poorly documented, and computations suggest that, for all but the steepest slopes, wave loading does not influence slope stability in water depths greater than 120 m (Moran and Hurlbut, 1987), i.e. shallower than most of the canyon heads. The most recent damaging tsunami on the Oregon-Washington coast (from the 1964 Alaska earthquake) did not trigger one of the 13 great turbidites in the Cascadia Channel. Furthermore, it seems unlikely that a coupling of storm or tsunami-triggers with the time-dependent stability changes in the canyon heads would give both long return periods and the same number of events all along the margin.

Earthquakes are an unusual natural phenomenon in that even for quite rare events the expected ground shaking increases dramatically as the probability level drops. Thus a great earthquake is so overwhelmingly large that it will trigger both marginally stable and stable canyon head deposits. Great earthquakes, should they occur on the Cascadia subduction zone, would probably have a long return period, and indeed return periods of several hundred to a thousand years have been estimated by Adams (1984) and Heaton and Hartzell (1986), based on the rate of geodetic strain accumulation. Plate-boundary earthquakes occur fairly regularly (a consequence of the steady build-up of strain due to plate movement and the constant physical parameters of the fault zone), and so tend to have a "characteristic" size. Very short intervals are excluded because insufficient strain is available to be released, and very long intervals are excluded because the strength of the fault zone limits the amount of strain that can be stored. For such characteristic earthquakes there is scale-independent variability in timing amounting to about $\pm 1/5$ of the mean return period (Nishenko and Buland, 1987), 120 a for a 590-a return period. This is close to the 20-30 % variability in pelagic thicknesses found in the cores (which includes not only variability due to the earthquake cycle but also that due to determining the thickness of the pelagic layers and then estimating the recurrence intervals).

Evidence that the 13 turbidity currents indeed represent earthquakes, is circumstantial and is likely to remain so for several years. Nevertheless, because a great thrust earthquake is an extremely large and relatively rare event, it should cause synchronous effects throughout the coastal Pacific Northwest. Such confirmatory effects would include: sudden coastal subsidence or uplift, landslides, sediment liquefaction and sand volcanoes, sediment slumping in large lakes, and submarine debris flows. Other less direct evidence would be: abnormal sedimentation events, deformed tree growth, abandonment of Indian settlements, secondary faulting on crustal faults, and perhaps triggered volcanic eruptions. A first step to providing onland evidence to confirm the interpretation of past great earthquakes has been made by Atwater (1987a,b) who has ascribed buried marsh deposits in Washington to sudden coseismic subsidences of the coast. His most recent work (Atwater, 1988) suggests 5 subsidence events and 1 shaking event in the last 3100 a. Corresponding evidence comes also from 8 (or possibly 9) buried soils in about 5000 a from coastal Washington (Hull, 1987), 7 buried marshes in about 3700 a from northern Oregon (Peterson et al., 1988), and 8 buried marshes in about 5000 a from southern Oregon (Nelson et al. in press). In each place the implied return period is about 520-620 a, in good agreement with the mean period between turbidity currents.

IMPLICATIONS FOR GREAT THRUST EARTHQUAKES ON THE CASCADIA SUBDUCTION ZONE

The occurrence of 13 great thrust earthquakes, their mean return period of 590 a, a variability of 170 a, and the 580 km extent of triggered turbidity currents and hence inferred strong ground motion, place some constraints on the slip, the rupture dimensions, magnitude, and style of rupture of the margin. Rogers (1988) has divided the Cascadia subduction zone into plausible segments. The Juan de Fuca plate extends 900 km from the Nootka Fault Zone off Vancouver Island to a boundary with the South Gorda plate off northern California. An alternative segmentation stops the Juan de Fuca plate at the Blanco Fracture Zone.

Subduction of the Juan de Fuca plate at 45 mm/a and the mean return period of 590 a gives 26 m for the average slip per earthquake. A 26 m slip for the 750 km long Juan de Fuca plate north of the Blanco Fracture Zone and a fault width of 100 km (Rogers, 1988) gives a maximum moment magnitude (M_w) of 9.1, which is in accord with the maximum size proposed by Rogers (1988). A variability of 26 % in event timing (derived from core 6508-K1) would lead to slip displacements of between 19 and 32 m, but a variability in magnitude of only ± 0.1 magnitude unit.

Would a rupture of the Juan de Fuca subduction zone stop at the Blanco Fracture Zone? Key evidence comes from core 6604-12, which lies on the extension of the fracture zone. This core — as does core 6609-1 to the south, on the subducting Gorda plate — contains 13 post-Mazama turbidites, presumed to represent great earthquakes on the Juan de Fuca subduction zone. If the Gorda plate had a history of independent subduction (e.g. in M_w 8.3 earthquakes; Rogers, 1988) core 6604-12 is close enough that additional turbidity currents might have been generated by earthquakes to both north and south. Therefore the presence of only 13 events in these two cores suggests that either every Juan de Fuca rupture extends past the Blanco Fracture Zone (i.e. a M_w 9.2 earthquake), or the earthquakes on the Gorda segment are synchronized with those on the Juan de Fuca (i.e. zipper effect in which an earthquake on one segment triggers earthquakes on adjacent segments in succession a few hours to years later).

WHEN WAS THE LAST EVENT?

The age of the last event can be estimated roughly from the thickness of the topmost pelagic sediment in the cores relative to the mean accumulation rate. From six cores (Table 1) an age of about 300 ± 60 a (before 1988) is estimated. This is consistant with the lack of a great earthquake in the 150-a historical record, but may be a biased underestimate if some sediment has been washed out from the top of each core. It is noteworthy that both the Astoria and the Blanco cores give similar (to within the poor resolution) ages to the four Cascadia cores, thereby showing that they did not occur at greatly different times (though this is not proof that they occurred at the same time).

A date for the last turbidite could also be derived from the amount of sediment that has accumulated in the submarine canyons since the sediment last slumped away, but estimates range from 100-400 a because the sediment accumulation rates are uncertain (Barnard, 1978, p. 111; Thorbjarnarson et al., 1986). The above rates generally support the inference that about 300 a or more have elapsed since the last event. Dates on the youngest buried marsh in southwest Washington suggest the last subsidence event occurred 300 years ago (Atwater et al., 1987), in agreement with the preceding analysis.

Working from the pelagic thicknesses in core 6508-K1 (chosen because its pelagic thicknesses are the most regular), assuming that no sediment has been eroded by the overlying turbidite, and adopting 300 a for the age of the last event, the following dates for the last five earthquakes are deduced (Table 2): 1690 AD, 1300 AD, 820 AD, 150 BC, and 770 BC. Although the slow accumulation rates of the hemipelagic sediment and the disturbance by the corer mean these dates may not be especially accurate (and in particular, the errors compound for the older dates), they should prove useful to other researchers seeking to match their onshore events to the record of great earthquakes provided by the turbidites.

Table 1. Age of the last turbidite from thickness of the topmost pelagic sediment

Core #	Pelagic thickness[a] (mm)	Accumulation rate[b] (mm/event)	Age of last turbidite (a)[c]
6705-2	23 ± 6	59	230 ± 60
6705-6	25 ± 3	51	290 ± 35
6509-26	17 ± 5	38	260 ± 75
6509-27	16 ± 3	28	335 ± 60
6502-PC1	70 ± 20	135	305 ± 90
6604-12	47 ± 10	100	275 ± 60
mean age			280 ± 60[d]

Notes [a] thickness (± possible error) in 1965/67
[b] from Figure 3 and similar plots
[c] relative to 1965/67; add 20 a to get years before 1988
[d] or 300 a before 1988. May be biased toward being too young because of washouts at top of core; see text.

Table 2. Age of the last 5 events in core 6508-K1

Pelagic (mm)	Turbidite (mm)	Δa[a]	Age[b] (a)	Date
?		300[c]		
	160+		300	1690 AD
22		390		
	240		690	1300 AD
27		480		
	570		1170	820 AD
54		970		
	120		2130	150 BC
35		620		
	65		2760	770 BC

Notes [a] time interval represented at 33 mm/590-a event assuming no loss of sediment
[b] years before 1988
[c] as discussed in the text

PROBABILITY OF THE NEXT EVENT

From the mean interval between events (590 a), the standard deviation of the mean (≈ 170 a), and the time since the last event (≈ 300 a), it is possible to estimate the likelihood of the next great Cascadia earthquake. At present there is about a 5 % chance that the next earthquake should have already happened. For the future, the conditional probabilities are crudely 0.1 % in the next year, 5 % in the next 50 a, 10 % in the next 100 a, and 25 % in the next 200 a. These numbers need to be recomputed using a lognormal distribution model (following Nishenko and Buland, 1987), and a revised date for the last earthquake; however such revisions would be unlikely to change the above probabilities greatly.

CONCLUSIONS

Turbidites in the tributaries of the Cascadia Channel and at other places along the Oregon-Washington margin were deposited from turbidity currents probably triggered by 13 great Cascadia subduction zone earthquakes since the Mazama eruption. Earthquakes the order of magnitude 9.1 have occurred every 590 a on average. Analysis of the pelagic intervals deposited between the turbidites suggests that the earthquakes occurred quite regularly, with a standard deviation of 170 a or less on the event spacing, similar to the variability found for great earthquake cycles elsewhere.

The thickness of the topmost pelagic layer suggests the last earthquake was 300 ± 60 years ago, but this number may be a biased underestimate due to washout during the collecting process. It is, however, consistent with the youngest subsidence event on the Washington coast. The near-term risk of a great earthquake in the Pacific Northwest is appreciable, and rising.

Rhythmic triggering of turbidity currents by great earthquakes may be a much more common phenomenam than hitherto realized, and might be expected at continental margins such as Alaska, Japan, New Zealand, and Chile where great thrust earthquakes with a long return period are combined with a moderate supply of sediment to the edge of the

shelf. If sampled correctly, the turbidite record can provide a quick estimate of the paleoseismicity of a margin and so guide confirmation by onshore paleoseismology studies.

ACKNOWLEDGMENTS

This work would not have been possible without the meticulous work of G. B. Griggs, his contemporaries, and their supervisor La Verne Kulm. I thank Mitch Lyle and the College of Oceanography for their co-operation and for making the core logs available. D. Piper assisted with technical advice regarding the behaviour of turbidity currents, and B. Atwater pointed out the importance of the bias in the uncalibrated radiocarbon ages. I thank P.W. Basham, M.J. Berry, D.J.W. Piper, and G.C. Rogers for valuable critical comments on early versions of this manuscript.

REFERENCES

Adams, J.
1984: Active deformation of the Pacific Northwest continental margin, Tectonics, v. 3, p. 449-472.

Ando, M. and Balazs, E.I.
1979: Geodetic evidence for aseismic subduction of the Juan de Fuca plate; Journal of Geophysical Research, v. 84, p. 3032-3027.

Atwater, B.F.
1987a: Evidence for great Holocene earthquakes along the outer coast of Washington State, Science, v. 236, p. 942-944.
1987b: Subduction-earthquake telltales beneath coastal lowlands; in A.J. Crone, and E.M. Omdahl, Directions in Paleoseismology, U.S. Geological Survey, Open File Report 87-673, p. 157-162.
1988: Geologic studies for seismic zonation of the Puget lowland; in National Earthquake Hazard Reduction Program, Summaries of Technical Reports, v. XXV, U.S. Geological Survey, Open File Report 88-16, p. 120-134.

Atwater, B.F., Hull, A.G., and Bevis, K.A.
1987: Aperiodic Holocene recurrence of widespread, probably coseismic subsidence in southwestern Washington, EOS, v. 68, p. 1468.

Bacon, C.R.
1983: Eruptive history of Mount Mazama and Crater Lake Caldera, Cascade Range, U.S.A.; Journal of Volcanology and Geothermal Research, v. 18, p. 57-115.

Barnard, W.D.
1978: The Washington continental slope: Quaternary tectonics and sedimentation; Marine Geology, v. 27, p. 79-114.

Duncan, J.R.
1968: Late Pleistocene and postglacial sedimentation and stratigraphy of deep-sea environments off Oregon; Ph.D. thesis, Oregon State University, 222 p.

Fryxell, R.
1965: Mazama and Glacier Peak volcanic ash layers: relative ages; Science, v. 147, p. 1288-1290.

Griggs, G.B.
1969: Cascadia Channel: the anatomy of a deep-sea channel; Ph.D. thesis, Oregon State University, 183 p.

Griggs, G.B. and Kulm, L.D.
1970: Sedimentation in Cascadia deep-sea channel; Geological Society of America Bulletin, v. 81, p. 1361-1384.

Griggs, G.B., Carey, A.G., and Kulm, L.D.
1969: Deep-sea sedimentation and sediment-fauna interaction in Cascadia Channel and on Cascadia Abyssal Plain, Deep-Sea Research; v. 16, p. 157-170.

Heaton, T.H. and Hartzell, S.H.
1986: Source characteristics of hypothetical subduction earthquakes in the northwestern United States; Bulletin Seismological Society of America, v. 76, p. 675-708.
1987: Earthquake hazards on the Cascadia subduction zone; Science, v. 236, p. 162-168.

Heaton, T.H. and Kanamori, M.
1984: Seismic potential associated with subduction in the northwestern United States; Bulletin Seismological Society of America, v. 74, p. 933-941.

Heezen, B.C. and Ewing, M.
1952: Turbidity currents and submarine slumps, and the 1929 Grand Banks Earthquake, American Journal of Science, v. 250, p. 849-873.

Hull, A.G.
1987: Buried lowland soils from Willapa Bay, southwest Washington: further evidence for recurrence of large earthquakes during the last 5000 years; EOS, v. 68, p. 1468.

Moran, K. and Hurlbut, S.E.
1986: An analysis of potential slope instability due to wave loading on the Nova Scotian Shelf; Proceedings, 3rd Canadian Conference on Marine Geotechnical Engineering, St. John's, Newfoundland, p. 980-999.

Nelson, H.
1976: Late Pleistocene and Holocene depositional trends, processes, and history of Astoria Deep-sea Fan, northeast Pacific; Marine Geology, v. 20, p. 129-173.

Nelson, A.R., Personius, S.F., and Rhea, S.
—: Earthquake recurrence and Quaternary deformation in the Cascadia subduction zone, coastal Oregon, in National Earthquake Hazard Reduction Program, Summaries of Technical Reports, v. XXVI, U.S. Geological Survey, Open File Report, (in press).

Nishenko, S.P. and Buland, R.
1987: A generic recurrence interval distribution for earthquake forcasting; Bulletin Seismological Society of America, v. 77, p. 1382-1399.

Peterson C.D., Darienzo, M.E., and Parker, M.
1988: Coastal neotectonic field guide for Netarts Bay, Oregon; Oregon Geology, v. 50, p. 99-106 and 117.

Reilinger, R. and Adams, J.
1982: Geodetic evidence for active landward tilting of the Oregon and Washington coastal ranges; Geophysical Research Letters, v. 9, p. 401-403.

Riddihough, R.P. and Hyndman, R.D.
1976: Canada's active western margin — the case for subduction; Geoscience Canada, v. 3, p. 269-278.

Rogers, G.C.
1988: An assessment of the megathrust potential of the Cascadia subduction zone; Canadian Journal of Earth Sciences, v. 25, p. 844-852.

Sternberg, R.W.
1986: Transport and accumulation of river-derived sediment on the Washington Continental Shelf; Geological Society of London Journal, v. 143, p. 945-956.

Stuiver, M. and Reimer, P.J.
1986: A computer program for radiocarbon age calibration; ed. M. Struiver and Renee S. Kra, Radiocarbon, v. 28 no. 2B, p. 1022-1030.

Thorbjarnarson, K.W., Nittrouer, C.A., and DeMaster, D.J.
1986: Accumulation of modern sediment in Quinault Submarine Canyon; Marine Geology, v. 71, p. 107-124.

A Paleozoic-Mesozoic rift framework for seismic hazard assessment in eastern North America

P.W. Basham
Geophysics Division

Basham, P.W., A Paleozoic-Mesozoic rift framework for seismic hazard assessment in eastern North American; in Current Research, Part F, Geological Survey of Canada, Paper 89-1F, p. 45-50, 1989.

Abstract

Earthquake hazard estimates in eastern North America are accompanied by a large degree of uncertainty. The larger earthquakes ($M > 6$), which dominate the hazard estimates, appear confined to major rifts that surround or break the Precambrian craton (continental margin, St. Lawrence Valley, Mississippi embayment). Why do these features not appear to be uniformly active throughout their extent? Is it because our observation history is too short compared to repeat times that may be thousands of years? Or is it that in only some regions are the rift features favourably oriented with respect to the current stress regime? Elsewhere in eastern North America, smaller earthquakes ($M < 6$) are occurring in the Appalachian overthrust sheet (New Brunswick, Virginia), in lesser zones of weakness in the craton (Ohio, New York, western Quebec), or as crustal block motion in response to glacial unloading (eastern Arctic). For these, each new event is a surprise, as scientists had not previously clearly identified the potentially active feature.

Résumé

Les évaluations du péril séismique dans l'Est de l'Amérique du Nord sont sujettes à de grandes incertitudes. Les plus grands tremblements de terre ($M > 6$), qui dominent les estimés de péril, semblent être confinés dans les rifts majeurs qui entourent ou recoupent le craton précambrien (marge continentale, La vallée du Saint-Laurent, Le golfe du Mississippi). Du point de vue des sciences de la Terre, la question principale est d'établir pourquoi ces structures ne sont pas uniformément actives sur toute leur longueur. Est-ce simplement parce que notre période d'observation est trop courte lorsque comparée aux périodes de retour qui pourraient être de plusieurs milliers d'années? Ou est-ce parce que seules quelques régions sont orientées favorablement par rapport au système de contraintes actuel? Ailleurs dans l'Est de l'Amérique du Nord, des tremblements de terre plus faibles ($M < 6$), se produisent dans les nappes appalachiennes (Nouveau-Brunswick, Virginie), dans des zones de faiblesse de craton (Ohio, New-York, Ouest du Québec), ou comme mouvement de bloc montrant un mouvement différentiel suite au ratrait glaciaire (Est de l'Arctique). Pour ces derniers, tout nouvel événement représente un peu une surprise pour les sciences de la Terre; Les géoscientifiques n'avaient pas précédemment identifié le trait structural potentiellement actif.

INTRODUCTION

Figure 1 shows the fundamental data base that is the starting point for any discussion of seismic hazards in eastern North America. One does not need to be an earth scientist to see the gross geographical trends in these data. The earthquakes tend to surround what appears to be a stable region in the central continent. One does, however, have to be an excellent, perhaps clairvoyant, earth scientist to tell our decision-makers where the next damaging and likely fatal earthquake will occur in the next few decades.

The halo of larger earthquakes around the stable Precambrian craton of North America has a reasonably well-established basis in the large-scale geological structures that remain from the last two episodes of North Atlantic plate tectonics. These episodes tore and battered the craton from the east while the proto-Atlantic Ocean was opening and closing. At the present stage of opening, the Mid-Atlantic Ridge is producing compressional stresses that can reactivate these older geological structures.

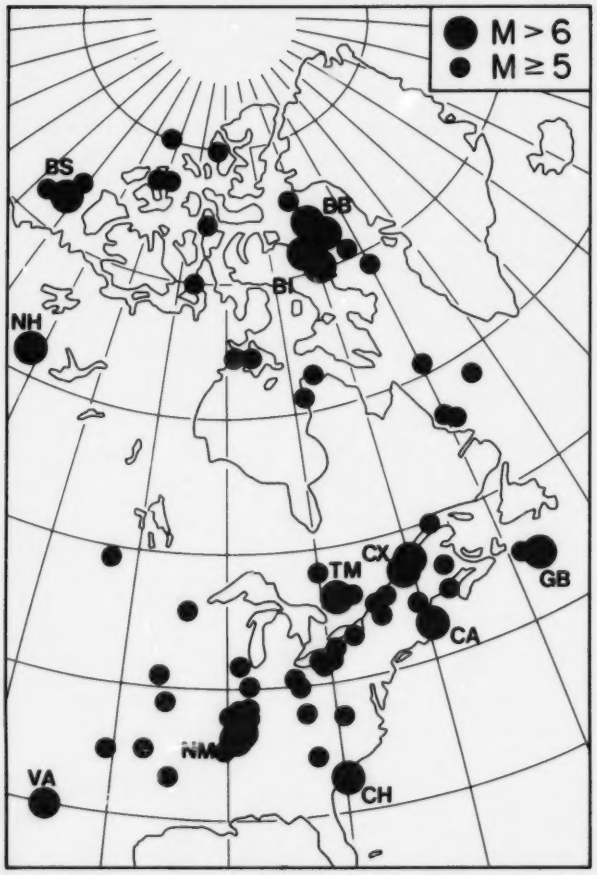

Figure 1. Historical earthquakes greater than magnitude 5 (small dots) and greater than magnitude 6 (large dots) in eastern North America. Earthquakes discussed in the text are identified as follows: NM, New Madrid; CH, Charleston; CX, Charlevoix; TM, Timiskaming; CA, Cape Ann; GB, Grand Banks; BB, Baffin Bay; BI, Baffin Island; BS, Beaufort Sea; NH, Nahanni; VA, Valentine, Texas.

The current stage of opening has produced reasonably uniform compression for tens of millions of years. Eastern North American society has observed and recorded the effects of the larger resultant earthquakes during only the last 300 years. Because so many of the larger historical earthquakes have been single events at their particular locations, we must assume that we have seen only a brief snapshot of the long-term earthquake potential. In the few locations where we have observed repetitive large earthquakes, the lack of surface geological evidence suggests that the causative faults have not been similarly active over thousands or tens of thousands of years; they may be currently active zones that have been turned on only in the very recent geological past.

Around and between the large ($M > 6$) earthquakes in Figure 1, almost at random, are numerous earthquakes of magnitude 5. The observational history for magnitude 5 earthquakes is not uniform throughout the map area. Some of the events in the eastern United States and southeastern Canada are known from written records in the eighteenth and nineteenth centuries; all of the events in uninhabited northern Canada date only from the time of reasonable global seismographic coverage in the 1930s. This probably accounts for the greater number of magnitude 5 earthquakes in the southeast than in northern Canada.

This is the observational framework within which we must estimate seismic hazards in eastern North America. In the following sections examples of some of the knowns and unknowns about the earthquake potential are elaborated upon, a conceptual model based on plate-tectonic rifting that can be used to address this potential is described, and a brief discussion of how this affects our immediate need of providing decision makers with defendable estimates of seismic hazards is summarized.

THE LARGE EARTHQUAKES OF EASTERN NORTH AMERICA

New Madrid

Although magnitude estimates for pre-instrumental earthquakes are uncertain, there is no question that the Mississippi Embayment in the Missouri-Arkansas-Kentucky-Tennesee border region experienced great (magnitude 8) earthquakes in the winter of 1811-1812. These events are unique for eastern North America and rare elsewhere; only two other similar-sized earthquakes are known to have occurred in similar tectonic environments, in 1604 on the southeast China coast and in 1819 in northwest India (Coppersmith et al., 1987).

Through mainly geophysical studies and accurate locations of recent lower-magnitude seismicity (Braile et al., 1986), the 1811-1812 earthquakes have been associated with the New Madrid rift complex, which formed as a failed arm of a triple junction during a late Precambrian continental break-up. There are at least two other similar Precambrian rift structures with similar origins in the southern United States, the Delaware aulacogen of west Texas and the Oklahoma aulacogen, but these have not experienced large earthquakes during historical times.

Charlevoix

The first earthquake in the historical earthquake catalogues of eastern North America (1534) occurred in the St. Lawrence Valley, probably in the Charlevoix zone. Six large earthquakes have subsequently occurred in this zone: in 1638 (location somewhat uncertain), 1663, 1791, 1860, 1870, and 1925, all with estimated magnitudes of 6 or greater; the 1663 and 1925 events were about magnitude 7. Present seismicity at Charlevoix has been shown (Anglin, 1984) to align on northeast-striking planes that dip to the southeast at depths between 5 and 25 km. When the hypocenters are projected to the surface, they are confined between Paleozoic rift faults that have been mapped on the north shore and a bathymetric feature near the river's south shore, which is assumed to be a river-bottom expression of a parallel rift fault. These faults are part of the system remaining from the penultimate breakup of the North American continent (of similar age to the New Madrid rift complex noted above). The faults have been mapped along the St. Lawrence Valley, with "failed arms" extending northwestward up the Ottawa River Valley and southward through Lake Champlain (Kumarapeli, 1985).

If earthquakes at Charlevoix had been occurring at the historical rates during recent geological time, we would expect to see surface geological deformation on the rift faults that would amount to kilometres over a million years. That we do not see such deformation implies that the earthquake activity must be recent at Charlevoix, and perhaps intermittent along the remaining rift system, possibly with a time constant of thousands to tens of thousands of years.

Other earthquakes, magnitude about 6 near Montreal in 1732, magnitude 6.2 near Temiskaming in 1935, magnitude 5.6 at Cornwall-Massena in 1944, and close to magnitude 5 in the Lower St. Lawrence, are indicators that this rift system is capable of producing significant earthquakes elsewhere along its extent.

All other historical earthquakes in eastern North America with magnitudes greater than 6 can be associated with the geological features that remain from the last stage of rifting of the continental mass. This rifting produced the present continental margin and various fault systems that extend toward the continent as remnants of an attenuated continental crust resulting from the "pull-apart" rifting of the continent. These earthquakes are described south to north.

Charleston

The 1886 Charleston, South Carolina earthquake, with an estimated magnitude of 6.5 to 7, is the largest known along the eastern United States seaboard. Extensive studies of this earthquake have included geological and geophysical investigations (Gohn, 1983), intensity distribution (Bollinger, 1977), and paleo-earthquakes (Obermeier et al., 1985; Talwani and Cox, 1985). In contrast to the Grand Banks earthquake discussed below, the Charleston earthquake occurred not at the edge of the continental margin but in a region of attenuated continental crust that underlies the southeastern coastal plain and continental shelf.

Many studies have been undertaken to test the hypothesis that the tectonic environment of the Charleston earthquake is unique. Although much has been learned, its significance in terms of earthquake hazards remains controversial; the characteristics of the source region remain largely unknown and the earthquake has not yet been associated with any clearly identified geological feature (Seeber and Armbruster, 1988). Paleoseismic evidence suggests that at least three prehistoric earthquakes have shaken the Charleston region within the past 7200 years, but earthquakes of different ages have also occurred elsewhere along the South Carolina coast (Obermeier et al., 1987).

Cape Ann

Because of its age, both the magnitude and the location of the 1755 Cape Ann earthquake are poorly known. An interpretation of contemporary accounts, including observations from ships at sea, suggest an epicenter about 100 km east of Cape Ann (Weston Geophysical Corporation, 1976). Macroseismic information would suggest a magnitude of about 6. If the location is reasonably accurate, this places the earthquake in the attenuated crust on the continental shelf.

Grand Banks

The large historical earthquakes appear to move farther offshore northward. The 1929, magnitude 7.2, Grand Banks earthquake occurred right at the edge of the continental shelf, and triggered a large submarine slump that slid down the continental slope. The slump in turn became a turbidity current that flowed a thousand kilometres onto the deep ocean floor. The sudden displacement of the water column by the slump produced a tsunami which washed ashore on the southern coast of Newfoundland, 12 m above high tide, devastating the fishing villages and causing the loss of 27 lives. This is the only locally-generated tsunami known to have been produced on the eastern coast of North America.

Although the available instrumental seismic data is too poor to establish a definitive mechanism, the epicentral trends suggest the earthquake may have ruptured westward along a fault about 70 km long (Adams, 1986), although it has also been suggested that much of the seismic energy release was produced by the slumping itself (Hasegawa and Kanamori, 1987). The former mechanism is preferred by the current author, as it appears that subsequent seismicity, including four magnitude 5 earthquakes since 1951, may be occurring in the 1929 rupture zone.

The seismic hazard model for the current National Building Code of Canada (Basham et al., 1982) assumes that 1929-sized earthquakes occur at this location approximately every 300 years. However, recent geophysical surveys and sediment sampling of the 1929 slump suggest that large slumps are very infrequent at this location and the triggering earthquakes may have return periods of the order of 10 000 years. That other such earthquakes may have occurred in the past is suggested by prehistoric submarine slumps that have been found elsewhere along the margin (Basham and Adams, 1983; Piper et al., 1985).

Baffin Bay

The magnitude 7.3, 1933 Baffin Bay earthquake is the largest earthquake known to have occurred in northeastern Canada. Magnitude 6 events have since occurred in Baffin Bay in 1945, 1947, and 1957. There is evidence for an extinct seafloor spreading centre in the deep central region of Baffin Bay, a remnant of the Tertiary separation of Greenland and Baffin Island, but the large earthquakes are not associated with it. The 1933 earthquake occurred on the landward side of the 2000 m bathymetric contour which delimits a thick sequence of sediments. It occurred at a depth of about 10 km and had a thrust mechanism.

A model has been developed (Sleep et al., in press) that suggests that the recent removal of surface loads by deglaciation is a major source of local stress, comparable in magnitude to and superimposed on the compressional stress in the North American plate due to Mid-Atlantic Ridge spreading. These stresses are likely reactivating the faults that remain from the rifting episode.

The northeastern Baffin continental margin is a more recent (about 60 million years) equivalent to the late Precambrian/Paleozoic (approximately 500 million years) rifting of the Precambrian craton discussed above (New Madrid, St. Lawrence), and might yield more information than the buried rifts in the south. Unfortunately, because of its remoteness it has been very little studied.

Beaufort Sea

The Arctic Ocean margin was produced by rifting in Cretaceous time when Alaska rotated anticlockwise away from Arctic Canada. The earthquakes are clustered in regions where the transitional crust (continent-ocean) is loaded by thick sequences of sediments. The most active cluster is in the Beaufort Sea beneath a thick sequence of sediments deposited by the Mackenzie River; it includes a magnitude 6.5 earthquake in 1920.

Although the 1920 Beaufort Sea earthquake was identified as "transitional" (Coppersmith et al., 1987), the geological history of the Arctic Ocean margin is similar (in style but not in age) to that of the other margins in eastern North America. The Nahanni and Valentine, Texas, earthquakes shown in Figure 1 are also in this category.

A CONCEPTUAL FRAMEWORK FOR THE LARGE EARTHQUAKES

Each of the large historical earthquakes in eastern North America described above has been spatially associated with some geological feature that remains from the Paleozoic (approximately 500 million year old) rifting of the Precambrian proto-continent, or the Mesozoic (less than 200 million year old) last stage of rifting that formed the present eastern and northern North American continental margin.

The original work that has made these correlations so apparent was the excellent study by Coppersmith et al. (1987) of the seismicity of "stable continental interiors" (SCI) worldwide. This study was undertaken as part of the Electric Power Research Institute (EPRI) seismic hazard program for the eastern United States, to provide a scientifically-supportable base for maximum earthquake assessments. These authors developed a working definition of SCI with the restriction that the defined regions be geologically and tectonically similar to North America east of the Cordilleran thrust and fold belt. For nine SCI regions worldwide they compiled information on historical earthquakes greater than 5 (or epicentral intensities greater than VIII for older events with no assigned magnitude). They found that 71 percent of the SCI seismicity was associated with imbedded continental rifts and continental passive margins (one-sided rifts). Further, all of the 17 SCI earthquakes of magnitude 7 or greater are strongly associated with the imbedded rifts or passive margins.

We have adopted this framework for the purposes of discussion of the large earthquake potential in eastern Canada (Adams, in press; Adams and Basham, in press). A further generalization of the concept is shown in Figure 2.

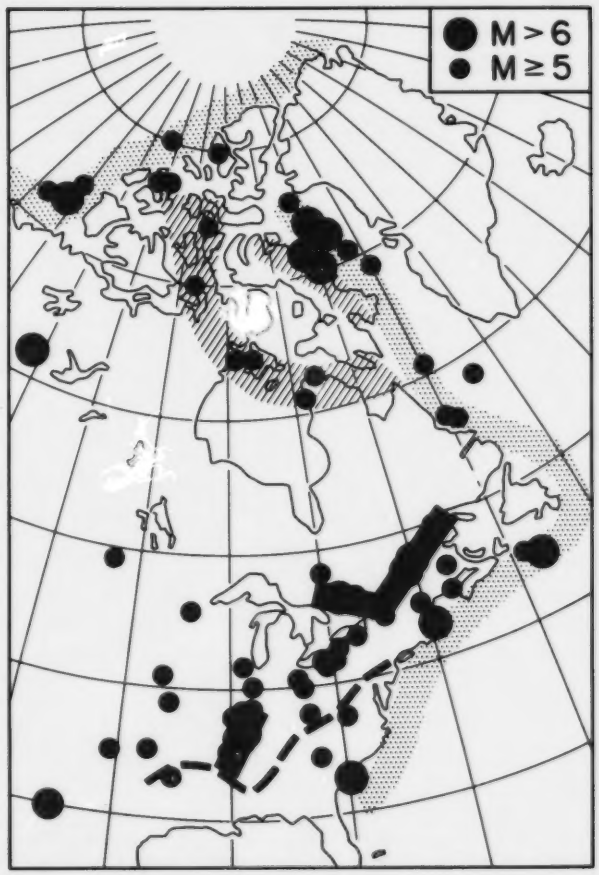

Figure 2. Schematic outline of Paleozoic rifting of the Precambrian craton (black); the buried edge of the craton in the southeastern United States (dashed line); Mesozoic rifting of the Arctic and Atlantic margins (stippled); and postglacial rebound reactivation of Paleozoic structures in the eastern Arctic (diagonal hash-marked), superimposed on the seismicity of Figure 1.

The schematic representation of the rifting of the passive margins (Fig. 2) is easy to draw; it can simply follow the continent-ocean transition, but it is intended to encompass adjacent regions of attenuated continental crust such as occur under the southeastern United States coastal plain. To refine this scheme, the inland boundary of the significant rift faults in the attenuated crust would have to be known. With this information, the band showing potential locations for large earthquakes would no doubt have variable width over its 10 000 km extent.

A complete schematic representation of the through-going Paleozoic rifts of the Precambrian craton is more difficult. The St. Lawrence system of rift faults is exposed on the Precambrian Canadian Shield. The more distinct faults can be spatially associated with the earthquakes only along the St. Lawrence and Ottawa river valleys (the sections shown in Fig. 2), but there is geological evidence that associated rifts may extend northeast toward the Labrador coast, south through Lake Champlain, and northwest into northern Ontario.

In the southeastern United States, equivalent features are buried beneath many kilometres of Phanerozoic sedimentary and overthrust Appalachian rocks, and are known only from remote sensing geophysical techniques. Only the New Madrid rift complex is shown in Figure 2. Perhaps it is best known because it has been most studied to find a source structure for the New Madrid earthquakes.

THE UBIQUITOUS MAGNITUDE 5 EARTHQUAKES

A number of magnitude 5-6 earthquakes has occurred at or near the locations of the large earthquakes discussed above: for example, southeastern Illinois 1968 and northeastern Arkansas 1976; Charlevoix 1939, 1952, 1979; Beaufort Sea 1975, 1987. Basham and Adams (1983) have argued that these could be considered long-delayed aftershocks of the larger historical earthquakes which caused a major perturbation to the ambient stress regime in a volume of the crust much larger than their rupture zones. Other magnitude 5 earthquakes are clearly displaced from the large earthquakes but covered by the rift framework of Figure 2 (recall the 71 percent of SCI seismicity noted above); for example, in the Lower St. Lawrence and at Cornwall-Massena on either end of the well-defined portion of the St. Lawrence rift; on the continental shelves of Labrador and the Arctic Ocean.

But there are numerous magnitude 5-6 earthquakes that cannot be accounted for by the rift framework of Figure 2. They occur in a wide variety of geological environments, that can be only briefly summarized here. From north to south, they occur:

1. beneath 10 km of sedimentary rocks in the Sverdrup Basin of the Arctic archipelago, perhaps on Cretaceous normal faults;
2. on shallow faults in Precambrian terrain on northeastern Baffin Island as a result of postglacial uplift and tilting of Baffin Island;
3. as a reactivation of Paleozoic structures near the Boothia Penninsula and northern Hudson Bay, suggestive of differential crustal block motion in response to postglacial uplift;
4. on extinct spreading ridges and fractures zones in the Labrador Sea;
5. as thrust faults in the Appalachian overthrust sheet in New Brunswick, and perhaps on the detachment surface between the overthrust sheet and the underlying Precambrian basement;
6. in an apparent zone of weakness in the Precambrian of western Quebec which may have been thermally stressed by a mantle hot spot 130 million years ago;
7. on an unknown structure beneath the Prairies near the Saskatchewan-North Dakota border;
8. in New Hampshire in a region where the earthquake potential may result from an intersection of faults and intrusive bodies;
9. Adirondacks on what may be old brittle fracture zones at relatively shallow depth in the Precambrian with some surface expression as lineaments, but little accumulated displacements;
10. in western New York state, possibly on the Clarendon-Linden fault, which offsets Paleozoic rocks at depth but whose surface expression is a gently dipping monocline;
11. beneath 2 km of flat-lying Paleozoic sediments in Ohio on what may be a Precambrian tectonic boundary known only from its aeromagnetic anomaly signature;
12. in the Precambrian basement of Virginia beneath the Appalachian detachment on what may be ancient rift faults near the edge of the craton.

When viewed as a whole, these magnitude 5 earthquakes are associated with a wide variety of geological features. It is not clear that we could estimate future locations of magnitude 5-6 earthquakes even if we knew the geological structure in some detail.

ISSUES CONFRONTING SEISMIC HAZARD ESTIMATES

It is clear that the description of eastern North American earthquakes in the previous two sections presents significant difficulty to those with responsibility for seismic hazard assessment. The larger earthquakes appear to be accommodated by the rifting framework model; but there is no conclusive evidence that these rifts should be considered uniformly active over their entire extent; certainly not in the next few decades. The smaller (magnitude 5) earthquakes occur in a large variety of geological environments; it appears that if we wait long enough we can expect to see one almost anywhere in eastern North America (although we may exclude much of the apparently stable central region).

A key problem in the hazard assessments is the relatively small number of large historical earthquakes for such a large

area. If we claim to know nothing about the geological controls on such earthquakes, for hazard estimates we could assume that in future they will occur at random. The hazard at moderate probabilities, such as used for building codes, would then be negligible at all locations and not protect against even a moderate nearby earthquake.

On the other hand, earth scientists are very uncomfortable with the suggestion that our (short) earthquake history will simply repeat itself during the next three centuries. Each of the four large earthquakes along, or adjacent to the eastern margin was an isolated event: Cape Ann, 1755; Charleston, 1886; Grand Banks, 1929; Baffin Bay, 1933. What grounds do we have for saying that the next one will occur in one of these locations?

While the New Madrid rift complex may have released its once-in-a-millenium seismic energy, the Charlevoix zone in the St. Lawrence Valley should be expected to continue its repetitive shocks. For the Charlevoix hazard model it would be prudent to expect at least one more; but the lack of geological deformation suggests that the activity has not persisted in the geological past and may turn off and start somewhere else along the rift system in the future.

The hazard models developed by the earth scientists must reflect these uncertainties. Recent examples of how uncertainties can be accommodated were the projects undertaken by the United States Nuclear Regulatory Commission and EPRI for seismic hazard estimates at sites of nuclear power stations in the eastern United States. These studies used "expert opinion" to incorporate a broad range of options into multiple earthquake-source-zone models of future earthquake potential. Each of the possible models is assigned a (judgemental) probability that it is the "correct" interpretation of the known earthquakes. The hazard calculation then appropriately weights each of these models in deriving the final "hazard curve" (seismic ground motion as a function of probability) for a particular site. The genuine uncertainty on a computed ground motion parameter can be a factor of 3 or more, and this must be recognized by the end user.

Existing hazard maps of eastern North America, computed at moderate probabilities for application to common structures (buildings, etc.), provide reasonable protection against large earthquakes in those few locations (New Madrid, Charleston, Charlevoix) where large earthquakes have occurred historically. They do not provide such protection at other locations; i.e. a large earthquake in a new location will likely seriously exceed the design loads of existing nearby structures. Until the earth scientists can learn much more about the earthquake potential in eastern North America, and change the hazard maps accordingly, this fact must also be recognized by the end user.

REFERENCES

Adams, J.
1986: Changing assessment of seismic hazard along the southeastern Canadian margin; Proceeding, Third Canadian Conference, Marine Geotechnical Engineering, St. John's, Newfoundland, p. 41-53.

—: Seismicity and seismotectonics of southeastern Canada; Proceedings of Conference on Earthquake Hazards and the Design of Constructed Facilities in the Eastern U.S., Annuals New York Academy of Sciences, (in press).

Adams, J. and Basham, P.W.
—: The seismicity and seismotectonics of eastern Canada; in Decade of North American Geology, v. CSMV-1, Neotectonics of North America, ed. E.R. Engdahl, D. Blackwell, D. Schwartz, and M. Zoback, Geological Society of America (in press).

Anglin, F.M.
1984: Seismicity and faulting in the Charlevoix zone of the St. Lawrence Valley; Bulletin Seismological Society of America, v. 74, p. 595-603.

Basham, P.W. and Adams, J.
1983: Earthquakes on the continental margin of eastern Canada: need future large events be confined to the locations of large historical events?; U.S. Geological Survey, Open File Report. 83-843, p. 456-467.

Basham, P.W., Weichert, D.H., Anglin, F.M., and Berry, M.J.
1982: New probabilistic strong seismic ground motion maps of Canada: a compilation of earthquake source zones, methods and results; Earth Physics Branch (Ottawa), Open File Report. 82-33, 205 p.

Bollinger, G.A.
1977: Reinterpretation of the intensity data for the 1886 Charleston, South Carolina, earthquake; U.S. Geological Survey, Professional Paper 1028, p. 27-32.

Braile, L.W., Hinze, W.J., Keller, G.R., E.G. Lidiak, and Sexton, J.L.
1986: Tectonic development of the New Madrid Complex, Mississippi Embayment, North America; Tectonophysics, v. 131, p. 1-21.

Coppersmith, K.J., Johnston, A.C., and Arabasz, W.J.
1987: Methods for assessing maximum earthquakes in the central and eastern United States; EPRI Research Project 2556-2, Working Report, Electric Power Research Institute, Palo Alto, California.

Gohn, G.S. (ed.)
1983: Studies related to the Charleston, South Carolina, earthquake of 1886 — tectonics and seismicity; U.S. Geological Survey, Professional Paper 1313.

Hasegawa, H.S. and Kanamori, H.
1987: Source mechanism of the magnitude 7.2 Grand Banks earthquake of November 1929: double couple or submarine landslide?; Bulletin Seismological Society of America, v. 77, p. 1984-2004.

Kumarapeli, P.S.
1985: Vestiges of Iapetan rifting in the west of the northern Appalachians; Geoscience Canada, v. 12, p. 55-59.

Obermeier, S.F., Gohn, G.S., Weems, R.E., Galinas, R.L., and Rubin, M.
1985: Geologic evidence for recurrent moderate to large earthquakes near Charleston; Science, v. 227, p. 408-411.

Obermeier, S.F., Weems, R.E., and Jackson, R.B.
1987: Earthquake-induced liquefaction features in the coastal South Carolina region; Proceeding, NCEER Symposium, Seismic Hazards, Ground Motions, Soil-Liquefaction and Engineering Practice in Eastern North America, National Center for Earthquake Engineering Research, State University, Buffalo, Technical Report NCEER-87-0025, p. 480-493.

Piper, D.J.W., Farre, J.A., and Shor, A.
1985: Late Quaternary slumps and debris flows on the Scotian Shelf; Bulletin, Geological Society of America, v. 96, p. 1508-1517.

Seeber, L. and Armbruster, J.G.
1988: Seismicity along the Atlantic seaboard of the U.S.: intraplate neotectonics and earthquake hazard; in The Atlantic Continental Margin, The Geology of North America, ed. R.E. Sheridan, and J.A. Grow, v. I-2,p. 565-582.

Sleep, N.H., Kroeger, G., and Stein, S.
—: Canadian passive margin stress field inferred from seismicity; Journal Geophysical Research (in press).

Talwani, P. and Cox, J.
1985: Paleoseismic evidence for recurrence of earthquakes near Charleston, South Carolina; Science, v. 229, p. 379-381.

Weston Geophysical Corporation
1976: Historical seismicity of New England; Report BE-SG7601, prepared for Boston Edison Company.

Aeromagnetic survey program of the Geological Survey of Canada, 1988-89

D.J. Teskey, E.E. Ready, P.E. Stone, B. Ellis, J. Tod, and R.A. Gibb
Geophysics Division

Teskey, D.J., Ready, E.E., Stone, P.E., Ellis, B., Tod, J., and Gibb, R.A., Aeromagnetic survey program of the Geological Survey of Canada, 1988-89; in Current Research, Part F, Geological Survey of Canada, Paper 89-1F, p. 51-53, 1989.

Abstract

During 1988-89 the GSC collected, processed or purchased 415 690 line kilometres of aeromagnetic total field, total field/gradiometer/VLF and time-domain electromagnetic/total field data. In addition to 'A' base programs (Prince Rupert, B.C., Yukon, Grand Banks), this work was carried out in support of Mineral Development Agreements with five provinces (British Columbia, Manitoba, Ontario, New Brunswick, Nova Scotia) and the Northwest Territories and the Gaspé Lower St. Lawrence Geoscience Program in Quebec, the Frontier Geoscience Program (Grand Banks and Yukon) and the Great Lakes International Multidisciplinary Program in Crustal Evolution (Lake Superior). Contracts were let to six airborne geophysical contractors, in addition to the Lake Superior survey, which was flown by the GSC's Queenair aircraft in 1987 and processed at the Geophysical Data Centre in 1988. One survey, flown to GSC specifications in the Canso Nova Scotia area was purchased from Seabright Resources Inc.

Résumé

En 1988-1989, la CGC a recueilli, traité et acheté 415 690 kilomètres linéaires de données et levés aéromagnétiques du champ total; du champ total, gradiométriques et à très base fréquence (VLF); et électromagnétiques temporisés par domaine et du champ total. Ce travail a été effectué dans le cadre non seulement de programmes de base « A » (Prince-Rupert (C.-B.), Yukon, Grands Bancs), mais aussi d'ententes sur l'exploitation minérale avec cinq provinces (Colombie-Britannique, Manitoba, Ontario, Nouveau-Brunswick, Nouvelle-Écosse) et du Programme géoscientifique des Territoires du Nord-Ouest et de Gaspé-Bas Saint-Laurent au Québec, du Programme géoscientifique des régions pionnières (Grands Bancs et Yukon) et du Great Lakes International Multidisciplinary Program in Crustal Evolution (lac Supérieur). Des contrats ont été adjugés à six entrepreneurs en géophysique aéroportée, en plus du levé du lac Supérieur qui a été réalisé par le Queenair de la CGC en 1987 et dont les données ont été traitées au Centre des données géophysiques en 1988. Les données d'un levé réalisé aux conditions de la CGC dans la région de Canso en Nouvelle-Écosse ont été achetées de la Seabright Resources Inc.

INTRODUCTION

During 1988-89 three detailed total field/gradiometer/VLF surveys and two regional surveys were initiated for a total of 104 694 km. Three total field/gradiometer/VLF and three regional surveys initiated in 1987-88 were completed for an additional 199 089 km. Total field/gradiometer/VLF survey data flown in the Cape Canso, Nova Scotia area by a private company were purchased. A time-domain EM magnetometer survey was flown and compiled in 1988, and a gradiometer/EM survey commenced in 1987 was completed in 1988. The survey parameters are given in Table 1 and the survey areas are shown in Figure 1.

Contractors involved in the current program are: Geoterrex Ltd., Ottawa; Kenting Earth Sciences International Ltd., Ottawa; Les Relevés Géophysiques Inc., Quebec City; Questor Surveys Ltd., Mississauga; Terraquest Ltd., Toronto; and Sander Geophysics Ltd., Kanata.

REGIONAL SURVEYS

The objective of the Prince Rupert, British Columbia survey is to help define lithologies and faults in the coastal range of the Cordillera. This area is adjacent to the Queen Charlotte Basin which is the subject of an intensive geological and geophysical investigation funded by the Frontier Geoscience Program (FGP) to evaluate mineral and hydrocarbon potential. The new aeromagnetic survey will complement this program and help to define the eastern margin of the basin and the major lithologies, structures and contacts in and adjacent to the basin.

The Northern Yukon survey, largely funded by FGP, will examine the structure of the Taiga foldbelt on the margin of the Cordillera and the structure of the basement under sedimentary cover to the north (Old Crow Basin, Dave Lord Uplift, Eagle Plain). This area is also under investigation for its hydrocarbon potential.

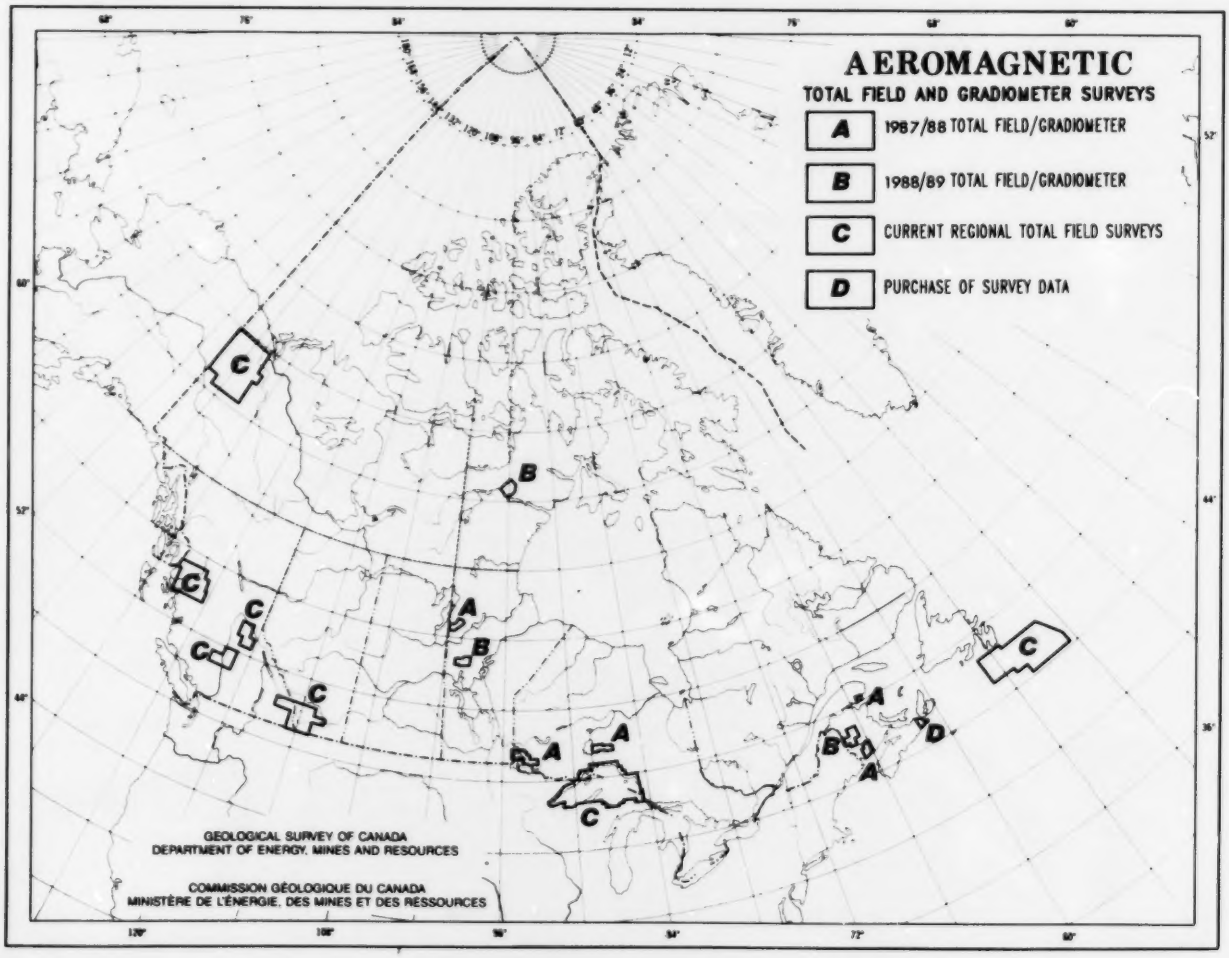

Figure 1. Locations of aeromagnetic total field, total field/gradiometer/VLF and EM/aeromagnetic total field surveys for 1987-88 and 1988-89.

Table 1. Aeromagnetic surveys.

Survey	Type	Km	Line Spacing	Altitude (m)
Ontario (Kenora – Ft. Francis) (1987-88)	Aeromagnetic Total Field Gradiometer VLF	21,288	300 m	150 Radar
Ontario (Geraldton–Beardmore) (1987-88)	Aeromagnetic Total Field Gradiometer VLF	16,725	200 m	150 Radar
New Brunswick (1987-88)	Aeromagnetic Total Field Gradiometer VLF	13,524	300 m	150 Radar
Gaspé (1987-88)	Aeromagnetic Total Field Gradiometer EM	2,900	200 m	50 Radar
Manitoba (1987-88)	Time Domain EM Aeromagnetics	4,907	200 m	120 Radar
Grand Banks (1987-88)	Regional Aeromagnetics	37,304	4 km	400 Radar
S.E. B.C./Alberta (1987-88)	Regional Aeromagnetics	53,548	Williams Lake 1km Lethbridge 1.5 km	Variable Altitudes Depending on Topography (by blocks)
Lake Superior (1987-88)	Regional Aeromagnetics	56,916	1.9 km	300 Radar
Northwest Territories (1988-89)	Aeromagnetic Total Field Gradiometer VLF	6,855	300 m	150 Radar
Manitoba (1988-89)	Aeromagnetic Total Field Gradiometer VLF	8,180	300 m	150 Radar
New Brunswick (1988-89)	Aeromagnetic Total Field Gradiometer VLF	10,322	300 m	150 Radar
Nova Scotia (1988-89) (purchase)	Aeromagnetic Total Field Gradiometer VLF	4,200	300 m	150 Radar
Yukon (1988-89)	Regional Aeromagnetics	57,639	2 km (southern portion) 3 km (northern portion)	9,000 Bar 7,000 Bar
British Columbia (1988-89)	Regional Aeromagnetics	21,636	2 km	9,500 Bar

The objectives of the 1987-88 regional surveys (southeastern British Columbia/Alberta, Lake Superior, Grand Banks) were outlined by Ready et al. (1988).

DETAILED SURVEYS

The detailed surveys, except that in Quebec, were funded under federal-provincial Mineral Development Agreements. The survey areas wereselected by the relevant provincial agencies in consultation with the Geological Survey of Canada to stimulate and improve the effectiveness of mineral exploration.

REFERENCES

Ready, E.E., Knappers, W.A., Stone, P.E., Teskey, D.J., and Gibb, R.A.

1988: Aeromagnetic Survey Program of the Geological Survey of Canada 1987-88; in Current Research, Part F, Geological Survey of Canada, Paper 88-1F, p. 63-66. 1988.

Preservation of paleontological types

D.C. McGregor
Institute of Sedimentary and Petroleum Geology, Ottawa

McGregor, D.C., Preservation of paleontological types; in Current Research, Part F, Geological Survey of Canada, Paper 89-1F, p. 55-59, 1989.

Abstract

Type specimens are the international keystones of biological systematics, and are therefore fundamental to biostratigraphy. The Canadian National Type Collection of Invertebrate and Plant Fossils is curated and managed by the Geological Survey of Canada. It is maintained according to strict guidelines based in part on the international codes of botanical and zoological nomenclature. The basic guidelines apply to all kinds of fossils, although certain additional measures are necessary for the preservation of palynological type specimens. All paleontologists and scientific institutions concerned with paleontology should promote scrupulous preservation of type specimens.

Résumé

Les spécimens de types sont les clés internationales de la systématique en biologie et sont donc fondamentaux en biostratigraphie. La Collection nationale de types d'invertébrés et de fossiles de plantes du Canada est gérée par la Commission géologique du Canada. Elle est administrée selon des directives rigoureuses basées en partie sur les codes internationaux de nomenclature botanique et zoologique. Les directives de base s'appliquent à tous les genres de fossiles, même si certaines mesures de conservation supplémentaires s'imposent dans le cas de spécimens de types de nature palynologique. Tous les paléontologues et toutes les institutions scientifiques oeuvrant en paléontoloie devrait favoriser la conservation selon des règles rigoureuses des spécimens de types.

INTRODUCTION

The National Type Collection of Invertebrate and Plant Fossils is curated and managed by the Geological Survey of Canada (GSC), as an integral part of its scientific program. The collection is the property of the GSC and is held in trust by the GSC for the international scientific community. It comprises specimens designated as types by GSC scientific staff, by outside workers studying specimens that are the property of the GSC, and by others who elect to submit their type specimens to the GSC for inclusion in the National Collection. It is housed in Ottawa, and parts are on term loan to GSC offices in Calgary, Alberta, and Dartmouth, Nova Scotia. It is maintained by a curator in Ottawa and, under his/her direction, by designated others in Calgary and Dartmouth. They maintain the collection according to exacting guidelines to ensure its permanent preservation and its availability for study by qualified scientists.

One of the aims of this paper is to describe the rationale and methods of the GSC for preserving the national paleontological type collection. A second objective is to suggest recommendations that may help to increase awareness amongst paleontologists and heads of Canadian scientific institutions, that type specimens provide stability for paleontological systematics, and are therefore fundamental to biostratigraphy. It is hoped that stating these details will serve to encourage a continued high standard of curation of the National Type Collection beyond the term of the present curator, as well as to remind paleontologists and appropriate institutions outside the Survey, in Canada and elsewhere, that they share responsibility for the scrupulous preservation of type specimens of fossils.

Acknowledgments

I thank R.K. Herd, T.E. Bolton, Curator of the National Type Collection of Invertebrate and Plant Fossils, and A.E.H. Pedder, J. Utting and other staff paleontologists of the Geological Survey for suggestions that improved the manuscript.

THE IMPORTANCE OF TYPE SPECIMENS

The International Code of Botanical Nomenclature (Voss et al., 1983) contains the following statement in its preamble:

"Botany requires a precise and simple system of nomenclature used by botanists in all countries, dealing on the one hand with the terms which denote the ranks of taxonomic groups or units, and on the other hand with the scientific names which are applied to the individual taxonomic groups of plants. The purpose of giving a name to a taxonomic group is not to indicate its characters or history, but to supply a means of referring to it and to indicate its taxonomic rank... The rules and recommendations apply to all organisms treated as plants... whether fossil or non-fossil."

Type specimens are fundamental to the system of nomenclature that is used almost universally by botanists and zoologists, including paleontologists. The types are the name-bearers, the specimens with which formal names of plants and animals are permanently associated. They do not limit the range of features that taxa may include (see Schopf, 1960), but they stand with the validly published diagnoses of the taxa in representing international "anchoring points" for biological systematics. Owen (1964, p. 288) has called type specimens "The greatest treasures in museums of zoology, botany and geology...".

Loss of, or failure to preserve type specimens should be regarded as a scientific disaster and a neglect of responsibility to future generations of scientists. Many, probably most, paleontologists engaged in systematics share this view. Nevertheless, some workers who may be enthusiastic in principle about preserving types may be apathetic in practice. The existence of some apathy is shown by the fact that the Geological Survey of Canada has had perennial difficulty extracting GSC-designated type collections from delinquent authors, and from some institutions that apparently lack curatorial facilities. Wherever paleontological type specimens are housed, they should be preserved at all costs, as they are vital to the maintenance of exacting standards in paleontology and biostratigraphy.

Preservation of type specimens of fossils should be the common concern of the whole geological community. Responsibility for preservation of type specimens rests not only with administrators and officially designated curators, but also with the authors of paleontological taxa and with all researchers who subsequently study the specimens.

GUIDELINES FROM THE INTERNATIONAL CODES OF BOTANICAL AND ZOOLOGICAL NOMENCLATURE (ICBN AND ICZN)

Both the ICBN and ICZN contain rules and recommendations concerning the rationale for, and the importance of, type specimens. They represent the internationally agreed standards on which the application of the type concept rests. It seems appropriate to quote the relevant provisions of the codes here, as the guidelines and recommendations that follow are based on them. The codes apply to all organisms, whether fossil or non-fossil.

From the ICBN (Voss et al., 1983)

Principle II: "The application of names of taxonomic groups is determined by means of nomenclatural types."

Article 7.2: "A nomenclatural type (*typus*) is that element to which the name of a taxon is permanently attached...".

Recommendation 7A: "It is strongly recommended that the material on which the name of a taxon is based, especially the holotype, be deposited in a permanent, responsible institution and that it be scrupulously conserved."

Article 9.5: "Type specimens of names of taxa must be preserved permanently...".

Article 37.1: "Publication on or after 1 Jan. 1958 of the name of a new taxon of the rank of family or below is valid only when the nomenclatural type is indicated...".

Recommendation 37B.1: "When the type of a new taxon is a specimen, the place where it is permanently conserved should be indicated."

Guide for the determination of types, T.1: "The choice [of nomenclatural type] made by the original author, if definitely expressed at the time of the original publication of the name of the taxon, is final."

From the ICZN (Ride et al., 1985)

Article 45(c): "The application of each species-group name is determined by reference to the name-bearing type... of its nominal taxon."

Article 61(a): "The name-bearing type provides the objective standard of reference by which the application of the name it bears is determined...".

Article 72(g): "Holotypes, syntypes, lectotypes, and neotypes are the bearers of the scientific names of all animal taxa. They are the international standards of reference that provide objectivity in zoological nomenclature. They are held in trust for science by all zoologists and by persons responsible for their safe keeping."

Recommendation 72D: "An author who designates a holotype or lectotype should deposit it in a museum or similar institution where it will be safely preserved and will be accessible for purposes of research; syntypes should also be deposited."

Recommendation 72E: "Holotypes, syntypes, lectotypes, and neotypes should be labelled in a way that will unmistakably denote their status."

Recommedation 72F: "An author who designates a holotype, lectotype, neotype, or syntypes should publish all information that appears on the labels accompanying the specimens, so as to facilitate the future recognition of specimens."

Recommendation 72G: "Every institution in which name-bearing types are deposited should:

1. ensure that all are clearly marked so that they will be unmistakably recognized as name-bearing types;
2. take all necessary steps for their safe preservation;
3. make them accessible for study;
4. publish lists of name-bearing types in its possession or custody; and
5. so far as possible, communicate information concerning name-bearing types when requested."

Article 73(a): "A holotype is the single specimen upon which a new nominal species-group taxon is based in the original publication...".

Recommendation 73A: "An author who establishes a new nominal species-group taxon should clearly designate its holotype."

Article 75(d): "A neotype is validly designated only when it is published with the following particulars:...

(6) a statement that the neotype is, or immediately upon publication has become, the property of a recognized scientific or educational institution, citied by name...".

Appendix A. 7. "Editors and others responsible for the publication of zoological papers should avoid publishing any paper that seems to them to contain a breach of the above principles."

GUIDELINES AND RECOMMENDATIONS FOR DESIGNATION AND PRESERVATION OF TYPES IN THE NATIONAL COLLECTION

The terminology applied to specimens in the National Collection includes both "primary types" (e.g., holotypes, paratypes), officially regulated by the ICBN and the ICZN, and "secondary types" (e.g., topotypes, figured specimens), not regulated by these codes. Type terms are not all defined in the same way in the ICBN and the ICZN, as the two codes were developed independently of one another. Authors of new taxa should refer to the definitions of terms in the appropriate code when instituting new types.

Publication

1. Each primary and secondary type specimen has a unique number in the GSC type catalogue. This number should appear in the appropriate plate legend of the paper in which the specimen is illustrated.
2. Authors must indicate unambiguously in their manuscripts the repository, specimen number, collector, geographic and geological provenance, and precise location on the rock specimen, microscope slide or other preparation, of each type specimen.
3. It is the author's responsibility to ensure that the information pertaining to the type specimens is consistent throughout the manuscript, and that it corresponds to the information on the specimen label.
4. A manuscript in which type specimens are described or figured should be accepted for publication only after the author has certified in writing to the editor that the types are preserved.

Depositing Specimens in a Repository

1. All type specimens that are entrusted to the care of the Geological Survey, whether studied at GSC offices or elsewhere, must ultimately be housed permanently in the National Type Collection. Centralization of the collection facilitates consistency and continuity of curation.
2. An author of a manuscript containing type or figured specimens that are to be incorporated in the National Type Collection must, as soon as the manuscript has been accepted for publication, send the specimens and accompanying data to the curator of the National Col-

lection, unless written permission has been obtained from the curator to retain the specimens. At the discretion of the curator, specimens may be borrowed for a specified interval of time if the borrower agrees to exercise the care required to preserve the integrity of the specimens.

3. As soon as the paper is published, the author should send a reprint or copies of relevant pages to the curator, to be deposited with the specimens.

Curation

1. The National Type Collection of Invertebrate and Plant Fossils is under the care of an officially designated paleontologist/curator at all times.

2. The curator, or his/her designate, is responsible for obtaining and maintaining detailed and up-to-date records, maintaining and repairing specimens, implementing the policy of the institution on lending and access, and making determined and persistent efforts to obtain collections from delinquent authors or borrowers.

3. The curator may, at his/her discretion, grant permission for additional preparation of certain type specimens, if such preparation seems likely to result in significant new information relevant to the taxonomy or understanding of the specimen. Such preparation should not be permitted if it entails the destruction of the specimen.

4. Type collections should be kept separate from general and reference collections, in a secure room.

5. The author of a paper in which type specimens destined for the National Type Collection are described or figured, is responsible for labelling and marking the location of all types. A label must be affixed to the rock specimen, microscopic slide, or other preparation, indicating the type number, the kind of type it is, and (space permitting) the binomial name, locality (stated, or by number), and reference to the publication in which the specimen is described or figured.

6. For microscopic specimens, the author should provide a master list keying type numbers to specimens or slide numbers and names of taxa and, if appropriate, England Finder coordinates or alternative designations of their position on the slide or other preparation. A copy of this list should be filed with the specimens.

Accessibility

Type specimens may be made available for loan to accredited workers for systematic studies, for limited periods of time and under stringent conditions, at the discretion of the curator. Normally, however, workers are encouraged to visit the institution to examine the specimens on the premises. Access to types is by appointment with the curator or a designated alternative. In all considerations regarding accessibility, the safety of the specimens is foremost.

Special recommendations pertaining to palynological types

The National Type Collection contains a large number of palynological specimens. They differ from most other fossils in their small size and in the methods required to isolate and preserve them. Permanent conservation of these microfossils requires special techniques.

The preparations on some of the older palynological slides in the National Type Collection have started to deteriorate; older methods of preparation were unable to reach the standard of permanency now attainable for such preparations. In addition, slides submitted by some recent authors do not comply with the most up-to-date standards of laboratory preparation and labelling. If such preparations are submitted to the national collection they are accepted, of course, but may require relabelling and more than average ongoing care to minimize their deterioration.

The following recommendations set out the standard of curation now preferred for palynological specimens in the National Type Collection.

1. Each specimen should be preserved in a "permanent" mount such as elvacite, bioplastic, or glycerin jelly ringed with paraffin wax. Hoyer's solution, silicone oil, or glycerin jelly sealed with "Cutex", for example, are not permanent. The nature of the mounting medium and the date of preparation should be indicated on the slide.

2. Preferably, type specimens are to be preserved as single-specimen mounts.

3. If the specimens are in strew mounts, their position in the mount should be indicated precisely, preferably by more than one indicator. Appropriate ways of recording their location are by means of "England Finder" grid co-ordinates; by an indelible mark around the specimen on the upper and/or lower surface of the slide; and by the x-and y- co-ordinates of a microscope stage keyed to the co-ordinates of a corner of the cover glass. The latter method is less convenient and may require awkward conversion of noncompatible stage scales (Traverse, 1958).

4. Each slide should bear a label showing the type and locality numbers and, space permitting, the name and author of each type specimen, and reference to the publication in which the specimen was first described and illustrated. Each slide also should bear an identifying inscription (e.g., the type number) by a diamond-scriber, so that the specimen may be identified if the label should become detached.

5. Slides should be stored individually (not stacked), flat, ideally in fire-resistant cabinets, in a location free from dust, and protected from flooding, mechanical damage, and excessive heat, cold, and humidity. An air conditioned room is recommended.

6. Preferably, palynological types mounted on stubs or slides suitable for study under a scanning electron microscope (SEM) should not be designated as primary types. If specimens mounted in this way must be types,

they should be covered with a protective cap and stored to protect them from excessive jarring, which might dislodge them from their support. Alternatively, with care these specimens can be removed from the stub or slide after SEM study and be mounted on standard microscope slides in a soluble mounting medium (e.g., glycerin jelly sealed with paraffin). The slides can then be stored in the same way as the rest of the type collection (Paris, 1978). Besides greater permanency, the latter procedure has the advantages that the specimen can be viewed by standard light microscopy, with little loss of optical quality if the SEM coating is thin or has been removed, and can be remounted for further study with the SEM.

7. Type slides should be inspected periodically for evidence of damage or deterioration. Any necessary repairs should be made or supervised by a palynologist designated by the curator. Thorough inspection of the palynological type collection at least once a year is recommended.

8. Maceration residues should be kept, as they are a potential source of neotypes and topotypes.

Additional recommendations

1. Those institutions with stated policies regarding curation of type collections of fossils should make their policies known to the paleontological community.

2. Editors should accept taxonomic papers for publication only if full documentation of the geological and geographic provenance of each new type specimen (or reference to such documentation published elsewhere), and its permanent repository, are included in the manuscript.

3. University staff and research students should ensure that type specimens are, as soon as possible after work on them has been completed, lodged along with the requisite documentation in a reputable institution that has an ongoing policy of adequate type curation.

4. University courses in biology and paleontology should contain instruction in curatorial techniques and the significance of the use of types in taxonomy and nomenclature.

5. Field geologists share responsibility for recording fully the provenance of the fossils they collect. They should include this geographic and biostratigraphic information in their reports.

6. Scientific societies concerned with paleontology, such as the Geological Association of Canada, the Canadian Society of Petroleum Geologists, and the Canadian Association of Palynologists, as well as those outside Canada, should promote preservation of type specimens. Promotion may be attained internationally, for example through the agency of the International Geological Correlation Project, the International Palaeontological Association, and the International Federation of Palynological Societies.

7. For Canada, the Paleontology Task Force of the National Inventory Program has recommended compilation of a central computerized file on the location and contents of all type collections in Canada. It would be appropriate for this file also to include a listing of type specimens that have been lost, or for which there is insufficient information.

REFERENCES

Bassett, M.G. (ed.)
1979: Curation of palaeontological collections; Palaeontological Association, Special Papers in Palaeontology, no. 22, p. 1-279.

Collinson, M.E.
1987: Special problems in the conservation of palaeobotanical material; Geological Curator, v. 4, no. 7, p. 439-445.

Owen, D.E.
1964: Care of type specimens; Museums Journal, v. 63, p. 288-291.

Paris, F.
1978: Apports du microscope electronique?a balayage dans l'?etude des chitinozoaires opaques; Annales des Mines de Belgique, v. 1978, no. 2, p. 193-202.

Ride, W.D.L., Sabrosky, C.W., Bernardi, G., and Melville, R.V. (eds.)
1985: International code of zoological nomenclature, third edition, adopted by the General Assembly of the International Union of Biological Sciences; International Trust for Zoological Nomenclature, London, p. 1-338.

Schopf, J.M.
1960: Emphasis on holotype (?); Science, v. 131, p. 1043.

Traverse, A.
1958: Locating plant microfossils on mixed slides; Micropaleontology, v. 4, no. 2, p. 207-208.

Voss, E.G., Burdet, H.M., Chaloner, W.G., Demoulin V., Hiepko, P., McNeill, J., Meikle, R.D., Nicolson, D.H., Rollins, R.C., Silva, P.C., and Greuter, W. (eds.)
1983: International Code of Botanical Nomenclature adopted by the Thirteenth International Botanical Congress, Sydney, August 1981; Regnum vegetabile, v. 111, Bohn, Scheltema and Holkema, Utrecht, p. 1-472.

Shallow seismic reflections using SV waves

K.G. Neave[1] and S.E. Pullan
Terrain Sciences Division

Neave, K.G. and Pullan, S.E., Shallow seismic reflections using SV waves; in Current Research, Part F, Geological Survey of Canada, Paper 89-1F, p. 61-64, 1989.

Abstract

A shallow seismic reflection survey using vertically polarized shear waves was carried out in northern Ontario. The success of this survey in mapping the bedrock topography and overburden stratigraphy suggests that this technique may have potential for future use in engineering and groundwater studies.

Résumé

Un levé de sismique-réflexion peu profond utilisant des ondes de cisaillement verticalement polarisées a été effectué dans le nord ontarien. Le succès de ce levé pour la cartographie de la roche en place et la stratigraphie de couverture suggère que cette technique pourrait avoir des applications prometteuses en géologie appliquée et en hydrologie des eaux souterraines.

[1] Northern Seismic, R.R. #1, Echo Bay, Ontario, POS 1CO.

INTRODUCTION

Shallow seismic reflection techniques have been developed for various engineering purposes, including determining depth to bedrock and delineating stratigraphy within the overburden (Hunter et al., 1984, in press). These techniques have used compressional wave (P-wave) reflections exclusively. The success of P-wave shallow reflection surveys is critically dependent on the ability of the ground to transmit high frequency energy — a factor that limits the applicability of the technique, particularly in areas where the surface materials are dry and coarse grained. Because shear waves are transmitted through the soil framework and are not as sensitive as P-waves to the presence of interstitial water, shallow shear wave reflection techniques may be successful in areas where compressional wave reflection techniques fail.

Some shallow horizontally polarized shear wave (SH-wave) reflection and refraction surveys have been reported by Stümpel et al. (1984). Hasbrouck (1987) has been successful in outlining old mines and concealed near surface features using a hammer source and both SV- (vertically polarized shear) and SH-waves. Suyama et al. (1987) have used SH surveys for delineating sediments in Japan. The present report demonstrates the potential of using SV reflections for mapping the bedrock surface and overburden stratigraphy in Canadian Shield terrain. The data presented here were recorded using simple equipment and field procedures, and it is suggested that this technique can provide an additional seismic tool for engineering and groundwater studies.

EQUIPMENT AND FIELD METHODS

A home-built single channel system was used for recording the data. It consists of a preamplifier with an analog low-pass filter, and an analog-to-digital converter for input to an Apple II+ microcomputer. Since shear wave energy is concentrated in the low frequency range (<60 Hz), there is not the requirement for high sampling rates needed to record compressional waves. Several attempts have been made to record S-waves at high frequencies, but the energy levels are so low at high frequencies that P-wave reverberations prevent interpretation.

The source for the S-wave survey was a hammer striking a triangular wooden block. A 3 kg hammer provided enough energy to produce reflections from 50 m below surface. A timing trigger for the microcomputer recorder was generated by a contact closure between the hammer and the block. The head of the hammer was wired for 5 V, and the wooden block was wrapped in aluminum foil or aluminum screening, which was grounded. When the hammer hit the block, the voltage drop in the hammer circuit signaled the start time for recording the trace. Three hammer blows were stacked to improve the signal-to-noise ratio.

Because S-waves are polarized perpendicular to the direction of ray propagation, the source must be designed so as to excite a horizontal motion. For this survey, the hammer struck a face of the wooden block that was approximately 45° to the vertical to impart a combination of horizontal motion plus some normal force necessary for coupling to the ground. The geophone (Hall-Sears, 14 Hz) was placed at approximately 30° from horizontal to pick up the largest amplitude signal (Fig. 1).

The survey was conducted just east of Sault Ste. Marie, Ontario in terrain that is typical of much of the Canadian Shield. The overburden consists of lacustrine clay; the bedrock is Precambrian quartzite. A layer of coarse morainic material, several metres thick, commonly occurs between the clay and the bedrock. A strong velocity contrast exists at the top of the bedrock, and a large amplitude reflector is therefore expected from this interface.

The depth to the water table, which has proved to be a critical factor in shallow P-wave reflection surveys, does not appear to affect the propagation of S-wave energy. The clay in this particular study area is under-saturated down to the maximum depth of frost penetration (approximately 2 m), and, as a result, there have been reverberations on the P-wave records from energy trapped between the free surface and the large velocity contrast at the water table. The low-velocity layer above the water table also introduces static errors in P-wave studies. There is no requirement in S-wave surveys to measure and correct for these static problems, so that processing and displaying shear wave records is simpler in this regard.

Two types of records were collected in this study. The first was an expanding spread where the detector was advanced along the survey line while the source remained stationary. These records were analyzed to determine an average velocity down to the reflecting horizon. The second was a profile mode wherein the source and detector were advanced along the survey line with a common spacing of 12 m. These records were then plotted side by side to produce a representation of the subsurface structure.

The records were plotted on a Tektronix flat-bed plotter, using software designed for processing and displaying P-wave data. An automatic gain control was applied to the common offset records, but otherwise the data are presented here as recorded.

RESULTS

The expanding spread record is shown in Figure 2. This record illustrates a number of important features of the SV surveys. First, there is little evidence of P-waves to interfere

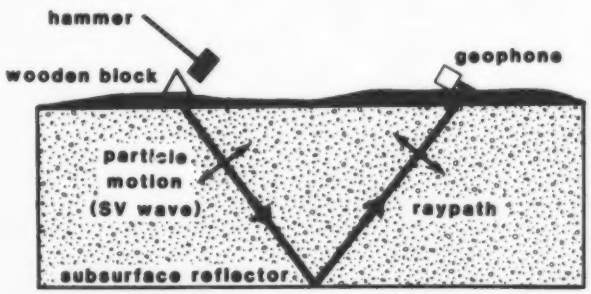

Figure 1. Source and geophone configuration for SV survey.

with the arrival of S-waves. P-waves are characterized by much higher velocities (approximately 1500 m/s in water-saturated unconsolidated materials), and so would arrive early on the record. The trace at 12 m offset distance has some high frequency energy between 0.03 and 0.09 s, which is the largest P-wave signal on the record. The P-waves do not constitute any interference problem for the interpretation of S-wave reflections. Even the surface waves (Rayleigh waves) suffer higher attenuation rates and fail to interfere with the S-reflectors.

The bedrock reflection is visible at a time of approximately 0.3 s. It is the largest signal on the record at wide angles, and therefore it can be identified and interpreted without any difficulty. A T^2-X^2 plot provides an estimate of the average velocity to the reflector of 120 m/s, and a depth for the reflector of 18 m. (This record was shot just off the shallow end of the section shown in Figure 3, where the bedrock was flat-lying, allowing an accurate determination of velocity to be made).

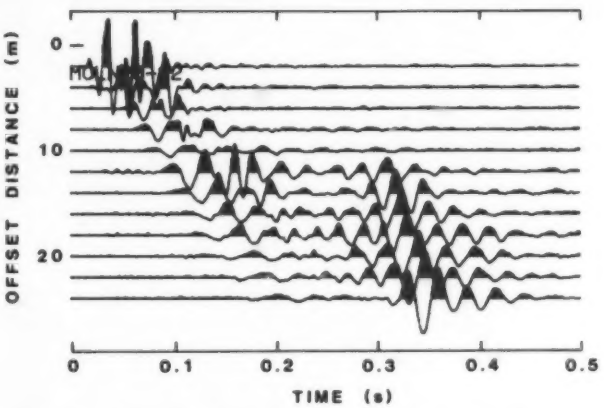

Figure 2. Expanding spread record for velocity determination. The bedrock reflector arrives at approximately 0.3 s. It is the largest signal on the record for the last six traces.

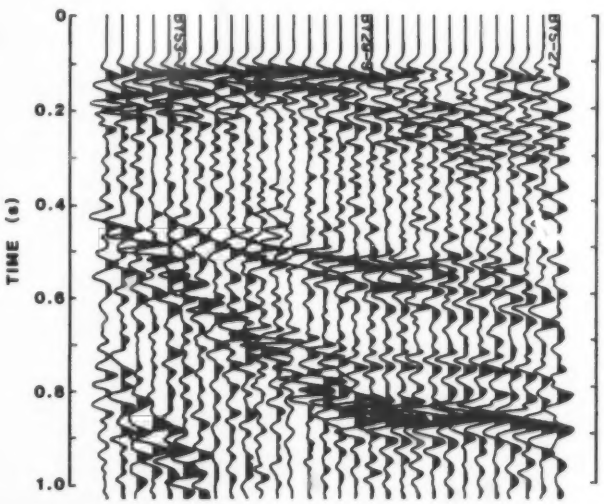

Figure 3. Common offset profile with 12 m separation between source and receiver and 6 m spacing between shots. The bedrock reflection can be seen on every trace. Several reflectors within the overburden are apparent.

On the common offset profile (Fig. 3), the bedrock reflector can be seen rising from 0.85 s at the right of the section, to 0.4 s at the left. The large amplitude event dropping off from 0.7 s on the far left is the first multiple from bedrock, and not a deeper reflection.

Two reflecting horizons can be seen above the bedrock in this figure. These represent boundaries in the depositional history of the clay. No coherent reflections are apparent in the first 0.2 s of the record, because of interference with surface waves and the shallow S-wave reverberations.

An interpretative section is shown in Figure 4, with a depth scale that has been calculated using an average velocity of 120 m/s in the overburden. The reflectors within the overburden may indicate changes in lithology (even quite subtle changes; for example, an increase in silt/clay ratio) or boundaries between depositional stages. The bedrock surface varies between 25 and 50 m-below surface. The section also shows the draping of the overburden reflectors over the bedrock slope and the probable locations of the old beaches where the reflectors meet the bedrock.

DISCUSSION AND CONCLUSIONS

The results of this survey have demonstrated the utility of the SV reflection technique in outlining bedrock and determining overburden characteristics for this particular terrain: clay over Precambrian bedrock. Other tests, not reported here, suggest that overburden consisting of sand and gravel underlain by Paleozoic bedrock is also a possible operating terrain for this method of surveying. In comparison with the P-wave reflection technique, the SV technique

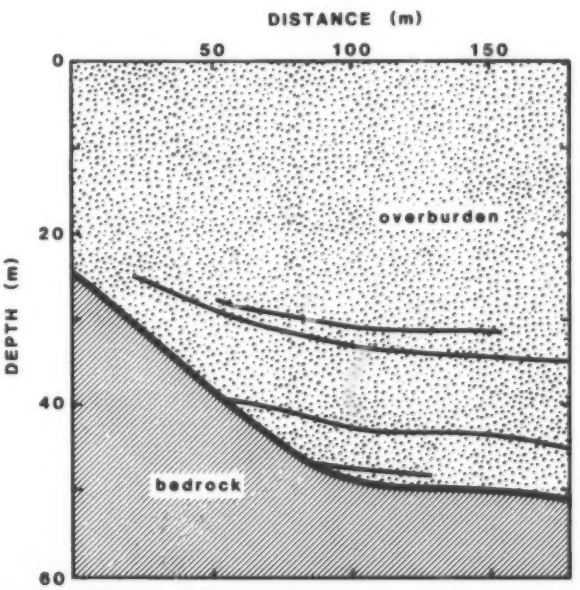

Figure 4. An interpretation of the common offset profile of Figure 3.

has the advantages of requiring less energy input and encountering fewer problems with shallow reverberations and static corrections. The one complication in S-wave surveys that is not found when using P-waves is the polarization geometry of the source and receiver. Both techniques are limited to bedrock depths greater than 20 m because of the direct wave interference.

REFERENCES

Hasbrouck, W.P.
1987: Hammer-impact, shear-wave studies; in Shear Wave Exploration, ed. S.H. Danbom and S.N. Domenico; Society of Exploration Geophysicists, Tulsa, p. 97-121.

Hunter, J.A., Pullan, S.E., Burns, R.A., Gagné, R.M., and Good, R.L.
1984: Shallow seismic reflection mapping of the overburden-bedrock interface with the engineering seismograph — some simple techniques; Geophysics, v. 49, no. 8, p. 1381-1385.
—: Applications of a shallow seismic reflection method to groundwater and engineering studies; in Proceedings of Exploration 87, Toronto, Canada (in press).

Stümpel, H.S., Kahler, S., Meissner, R., and Milkereit, B.
1984: The use of seismic shear waves and compressional waves for lithological problems of shallow sediments; Geophysical Prospecting, v. 32, p. 662-675.

Suyama, K., Imai, T., Ohtomo, H., Ohta, K., and Takahashi, T.
1987: Delineation of structures in alluvium and diluvium using SH-wave reflection and VSP methods; in Shear Wave Exploration, ed. S.H. Danbom and S.N. Domenico, Society of Exploration Geophysicists, Tulsa, p. 165-179.

AUTHOR INDEX

Adams, J. 37
Basham, P.W. 45
Boyd, J.B. 5
Boyle, D.R. 23
Broome, J. 1
Drysdale, J.A. 31
Ellis, B. 51
Gibb, R.A. 5, 51
Gregoire, D.C. 23
Hall, G.E.M. 17, 27
Horner, R.B. 31
Jonasson, I.R. 9
Lamontagne, M. 31
Larocque, A.C.L. 9
LeCheminant, G.M. 9
McGregor, D.C. 55
Neave, K.G. 61
Pullan, S.E. 61
Ready, E.E. 51
Stone, P.E. 51
Teskey, D.J. 51
Tod, J. 51
Turner, C. 1
Vaive, J.E. 17,27

Geological Survey of Canada, Paper 88-1, Current research
below, that can be purchased separately:

Recherches en cours, une publication de la Commission géologique du Canada
publiée en huit parties, dont les numéros d'exemplaires suivants peuvent être achetés séparément :

Part A, Abstracts
Partie A, Résumés

Part B, Eastern and Atlantic Canada
Partie B, Est et région atlantique du Canada

Part C, Canadian Shield
Partie C, Bouclier canadien

Part D, Interior Plains and Arctic Canada
Partie D, Plaines intérieures et région arctique du Canada

Part E, Cordillera and Pacific Margin
Partie E, Cordillère et marge du Pacifique

Part F, National and general programs
Partie F, Programmes nationaux et généraux

Part G, Frontier Geoscience Program, Arctic Canada
Partie G, Programme géoscientifique des régions pionnières, région arctique du Canada

Part H, Frontier Geoscience Program, Queen Charlotte Islands, offshe Canada
Partie H, Programme géoscientifique des régions pionnières, îles de la Reine-Charlotte,
Colombie-Britannique